Cyclic bordism and rack spaces

by

Jean Alison Flower

Submitted for the degree of Ph.D.

University of Warwick
Mathematics department

March, 1995

Contents

Figures

Acknowledgements

I would like to thank my supervisor, Dr. Brian Sanderson for his guidance and encouragement throughout my time at Warwick. Thanks also to Dr. Lickorish and Dr. Barden at Pembroke for inspiring me to do research in the first place. Thanks to my parents for their support and to all past and present residents of 147 Hearsall Lane. This thesis was partially funded by EPSRC (formerly SERC).

Declaration

I declare that the work contained in this thesis is entirely my own, except where otherwise stated.

Summary

This thesis falls into two parts, the first explores a cyclic version of bordism and the second studies the homotopy groups of rack spaces.

In chapters 2-5 we begin by reviewing some theory of cyclic homology but we present it in a topological framework. Then cyclic bordism is introduced as a parallel theory. In particular we prove the equivalence of cyclic and equivariant theories. This enables us to reduce the question of representation of cyclic homology by cyclic bordism to that of representation of ordinary homology by bordism. Finally, we state a fixed point theorem of periodic bordism.

In chapters 6-10 we study rack spaces, or the classifying spaces of racks. The homotopy groups of rack spaces are invariants of the rack up to rack isomorphism, and give invariants of semiframed non-split (irreducible) links in the three-sphere. We describe methods for calculating the second homotopy group in chapter 7 and in the next chapter we apply one of the methods to find generators for the second homotopy of a class of racks, the finite Alexander quotients. Chapter 9 discusses topological racks. The classifying spaces of racks with a non-discrete topology have a cell structure and, although it fails to be a CW cell structure, it can be used to calculate homotopy groups. The third homotopy group of a rack space is seen to be in one-to-one correspondence with bordism classes of framed labelled immersed surfaces in the three-sphere. We finish in chapter 10 by simplifying such surfaces within bordism to calculate the third homotopy group of the trivial rack and the cyclic racks, $\pi_3(\mathbb{B}(C_n)) \cong \mathbb{Z}_2$.

Chapter 1. Introduction

The study of cyclic cohomology and homology began as a theory of associative algebras over the complex numbers when, in 1981, A.Connes discovered an action of the cyclic group on the Hochschild complex. Cyclic cohomology was the result of factoring by this action. The most important basic property of cyclic (co)homology is the existence of a periodicity operator (which I shall call the shift map) and a resulting long exact sequence. This work is covered in [C1].

In [LQ], the authors extended the definition of cyclic (co)homology to a theory of associative algebras over any commutative ground ring. This definition focuses on a double complex, the Loday-Quillen double complex. Their work shed light on some proofs of Connes in [C2]. In this paper Connes defines the cyclic category and introduces the B-b double complex, giving rise to a definition of the cyclic cohomology of a cyclic chain complex.

The singular chain groups of a topological space with a circle action form a cyclic chain complex, and this allows us to define the cyclic homology of such a space. In chapter 1, I will review some fundamental theory from cyclic homology, including proofs, all based in this topological framework.

The aim of this work is to provide a cyclic bordism theory and compare it to cyclic homology in the same way that we can compare bordism with homology in the non-cyclic setting. This includes questions of representing cyclic homology classes by cyclic bordism classes.

An important theorem of cyclic homology was given in [JDSJ1], showing an equivalence between cyclic and equivariant homology. We show in chapter 5 that cyclic bordism is equivalent to equivariant bordism. This result reduces the question of representation of cyclic homology with cyclic bordism to the representation of homology with bordism.

Racks (and quandles) have been studied since the 1950's in various guises ([DJ], [SM], [EB], [K]). In [N], Neuwirth shows that an unoriented knot in S^3 has a complete invariant given by algebra (the knot group with a peripheral subgroup, all its conjugates and a meridian). Then in [DJ], Joyce shows that the unordered pair of the knot quandle and its reverse determines and is determined by Neuwirth's algebraic invariant, thus the knot quandle also classifies unoriented knots. The paper [FR] covers the groundwork of this subject and gives new results on racks classifying semiframed codimension 2 embedded manifolds, and rack presentations. Rack spaces (also called classifying spaces) are introduced in [FRS] and the algebra of racks is explored in [HR].

In this thesis we begin by presenting definitions and examples of racks. In the seventh chapter we describe two methods of calculation of the second homotopy group of a rack, and apply these methods to some simple racks. The next chapter finds the second homotopy group of a broad class of racks, the Alexander quotients. Next we adapt the method of calculation to topological racks.

In chapter 10 we move on to the third homotopy group of racks. Elements of the third homotopy group correspond to bordism classes of immersed framed labelled surfaces in S^3. By simplifying surface representations we find that the third homotopy group of the trivial rack is the group with two elements. This amounts to a geometric proof to show that $\pi_4(S^2) \cong \mathbb{Z}_2$. Finally, the calculation is improved to show that the third homotopy group of any cyclic rack is $\mathbb{Z}_2$.

Chapter 2. Cyclic homology

In this chapter we give definitions of the cyclic homology of a space with a circle action, following the algebra definitions in [C1], [C2] and [LQ]. See also [L] for a good review of cyclic homology.

The first section introduces the cyclic category, [C1], which has the same objects as the simplicial category, with additional morphisms of a cyclic nature. The singular chain groups of an S^1-space form a cyclic set, and in 2.2, the cyclic morphisms are used to construct the Loday-Quillen double complex, [LQ]. The cyclic homology of a circle-space is defined to be the total homology of this double complex.

Alternate columns of the Loday-Quillen double complex are acyclic, and after removing these in 2.3 we get the Connes B-b double complex [C2]. Cyclic homology can be defined equivalently as the total homology of the Connes double complex. A fundamental property of cyclic homology is the existence of a shift map, or periodicity operator [C1] and in 2.4 we state and prove the exactness of the shift long exact sequence.

In 2.5 we calculate an example, the cyclic homology of a point, and see that after factoring by degeneracies in 2.6, this calculation is considerably simplified.

2.1 The cyclic category and cyclic sets. [C2]

The **cyclic category** has objects indexed by $\mathbb{Z}_{\geq 0}$; $[n] = \{0, ..., n\}$ and morphisms generated by

$$\delta_i : [n] \longrightarrow [n+1]; \quad j \mapsto \begin{cases} j & j < i \\ j+1 & j \geq i \end{cases} \quad 0 \leq i \leq n+1$$

$$\sigma_i : [n] \longrightarrow [n-1]; \quad j \mapsto \begin{cases} j & j \leq i \\ j-1 & j > i \end{cases} \quad 0 \leq i \leq n-1$$

$$\tau : [n] \longrightarrow [n]; \quad j \mapsto \begin{cases} j-1 & j > 0 \\ n & j = 0 \end{cases}$$

The relations between these morphisms are

$$\delta_i \delta_j = \delta_j \delta_{i-1} \text{ if } i > j$$

$$\sigma_i \sigma_j = \sigma_j \sigma_{i+1} \text{ if } i \geq j$$

$$\sigma_i \delta_j = \begin{cases} \delta_j \sigma_{i-1} & i > j \\ 1 & i = j \text{ or } i = j+1 \\ \delta_{j-1} \sigma_i & i < j-1 \end{cases}$$

$$\tau \delta_i = \begin{cases} \delta_{i-1} \tau & i \neq 0 \\ \delta_{n+1} & i = 0 \end{cases}$$

$$\tau \sigma_i = \begin{cases} \sigma_{i-1} \tau & i \neq 0 \\ \sigma_{n-1} \tau^2 & i = 0 \end{cases}$$

and

$$\tau^{n+1} = 1$$

A **cyclic set** is a contravariant functor from the cyclic category to the category of sets. Denoting the image of $[n]$ by X^n; the images of δ_i, σ_i, τ by d_i, s_i, t we have

$$d_i: X^{n+1} \longrightarrow X^n$$

$$s_i: X^{n-1} \longrightarrow X^n$$

$$t: X^n \longrightarrow X^n$$

satisfying the opposites of the relations in the cyclic category, for example $d_j d_i = d_{i-1} d_j$ if $i > j$. An example of a cyclic set is given by $X^n = S_n(Y)$ where Y is a topological space and $S_n(Y)$ is the space of continuous maps from a canonical n-dimensional simplex to the space Y. The maps d_i are induced from face maps f_i taking the n-simplex to the $n+1$-simplex in $n+1$ ways. So if the canonical n-simplex is taken to have coordinates $(t_0, t_1, ..., t_n)$ with $0 \leq t_i \leq 1$ and $t_0 + ... + t_n = 1$ then the i^{th} face map f_i is given by inserting a zero in the i^{th} coordinate, and

$$d_i = (f_i)^*$$

Similarly

$$s_i = (g_i)^*$$

where the g_i are degeneracy maps on simplexes (adding adjacent coordinates together in Δ). The map $t: S_n(Y) \longrightarrow S_n(Y)$ is *not* induced from a map from the Δ^n to itself, and it is only defined when Y has a circle action. Regarding S^1 as $[0,1]$ with 0 and 1 identified and given $\rho \in S_n(Y)$, define the singular simplex

$$\begin{array}{rccc} t(\rho): & \Delta^n & \longrightarrow & Y \\ & (t_0, ..., t_n) & \mapsto & t_0.\rho(t_1, .., t_n, t_0) \end{array}$$

To see that this is a cyclic set, we need to check the relations, for example

$$d_i(t(\rho)) = t(d_{i-1}(\rho))$$

when $i > 0$.

$$d_i(t(\rho))(t_0, ..., t_n) = t(\rho)(t_0, .., t_{i-1}, 0, t_i, .., t_n) = t_0 \rho(t_1, ., t_{i-1}, 0, t_i, .., t_n, t_0)$$

$$t(d_{i-1}(\rho))(t_0, ..., t_n) = t_o d_{i-1}(\rho)(t_1, ..., t_n, t_o) = t_0 \rho(t_1, ., t_{i-1}, 0, t_i, .., t_n, t_0)$$

Also check

$$t^{n+1}(\rho) = \rho \quad \text{for all } \rho \in S_n(Y)$$

since

$$t^{n+1}(\rho)(t_0, ..., t_n) = t_0 t^n(\rho)(t_1, .., t_n, t_o)$$

$$= (t_0 + t_1 + .. + t_j) t^{n-j}(\rho)(t_{j+1}, ., t_n, t_0, ., t_j)$$

$$= (t_0 + ... + t_n) \rho(t_0, ..., t_n) = \rho(t_o, ..., t_n)$$

because in the canonical simplex $t_0 + ... + t_n = 1$ and 1 and 0 are identified as the unit of the circle. The other relations may be checked similarly.

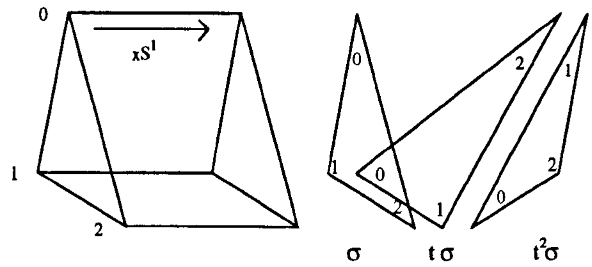

Figure 2.1.1 The cyclic operator t.

2.2 The Loday-Quillen double complex. [LQ]

Given X, a topological space with circle action, define

$$\begin{array}{rccc} \hat{t}\colon & S_n(X) & \longrightarrow & S_n(X) \\ & \rho & \mapsto & (-1)^n t(\rho) \end{array}$$

Lemma (a) If $N = 1 + \hat{t} + \ldots + \hat{t}^n \colon S_n(X) \longrightarrow S_n(X)$ then the composite maps $N(1-\hat{t})$ and $(1-\hat{t})N$ on $S_n(X)$ are both the zero map.

(b) the following diagrams commute

$$\begin{array}{cccccc} & S_n(X) & \xrightarrow{N} & S_n(X) & \\ \sum_{j=0}^{n}(-1)^j d_j & \downarrow & & \downarrow & \sum_{j=0}^{n-1}(-1)^j d_j \\ & S_{n-1}(X) & \xrightarrow{N} & S_{n-1}(X) & \end{array}$$

$$\begin{array}{cccccc} & S_n(X) & \xrightarrow{1-\hat{t}} & S_n(X) & \\ \sum_{j=0}^{n-1}(-1)^j d_j & \downarrow & & \downarrow & \sum_{j=0}^{n}(-1)^j d_j \\ & S_{n-1}(X) & \xrightarrow{1-\hat{t}} & S_{n-1}(X) & \end{array}$$

Proof (a) Both are equal to $1 - ((-1)^n)^{n+1} t^{n+1} = 1 - (+1)1 = 0$

(b) Introduce some notation

$$b = \sum_{j=0}^{n}(-1)^j d_j, \text{ and } b' = \sum_{j=0}^{n-1}(-1)^j d_j \colon S_n(X) \longrightarrow S_{n-1}(X)$$

Then

$$Nb = \sum_{j=0}^{n-1}\sum_{i=0}^{n}(-1)^{(n-1)j}(-1)^i t^j d_i$$

$$= \sum_{j+i\leq n}(-1)^{nj+j+i} d_{i+j} t^j + \sum_{j+i>n}(-1)^{nj+j+i} d_{j-n+1} t^{j+1}$$

$$= \sum_{j+i\leq n}(-1)^{nj+j+i} d_{i+j} t^j + \sum_{k+l>n}(-1)^{nk+l+n+k} d_{k+l-n} t^k$$

$$= \sum_{q\leq p}(-1)^{nq+p} d_p t^q + \sum_{p<q}(-1)^{nq+p} d_p t^q = b'N$$

and

$$\begin{aligned}
b(1-\hat{t}) &= \sum_{j=0}^{n}(-1)^j d_j(1-\hat{t}) \\
&= \sum_{j=0}^{n}(-1)^j d_j - \sum_{j=0}^{n}(-1)^j d_j\hat{t} \\
&= \sum_{j=0}^{n}(-1)^j d_j + \sum_{j=0}^{n}(-1)^{j+n+1} d_j t \\
&= \sum_{j=0}^{n}(-1)^j d_j + \sum_{j=1}^{n}(-1)^{j+n+1} t d_{j-1} + (-1)^{n+1} d_n \\
&= \sum_{j=0}^{n-1}(-1)^j d_j + \sum_{j=0}^{n-1}(-1)^{j-n} t d_j \\
&= (1-\hat{t})b'
\end{aligned}$$

□

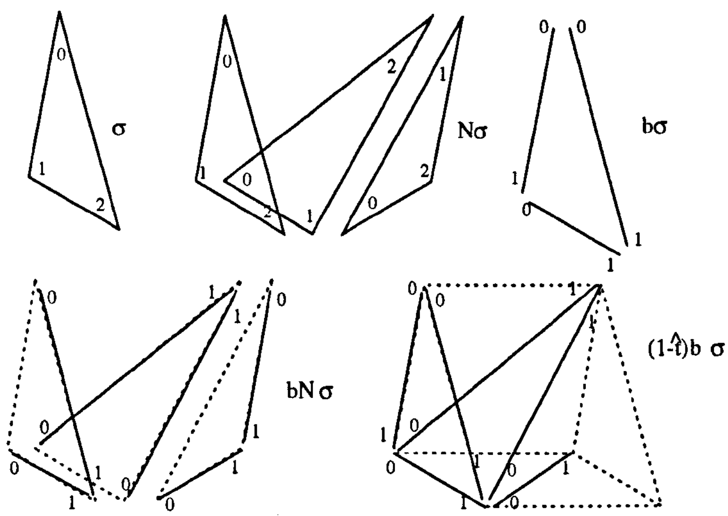

Figure 2.2.1 Commutativity of the Loday-Quillen double complex.

The following diagram commutes

$$\begin{array}{ccccccc}
 & \vdots & & \vdots & & \vdots \\
\cdots & S_n(X) & \xrightarrow{N} & S_n(X) & \xrightarrow{1-\hat{t}} & S_n(X) \\
 & b\downarrow & & b'\downarrow & & b\downarrow \\
\cdots & S_{n-1}(X) & \xrightarrow{N} & S_{n-1}(X) & \xrightarrow{1-\hat{t}} & S_{n-1}(X) \\
 & b\downarrow & & b'\downarrow & & b\downarrow \\
\cdots & S_{n-2}(X) & \xrightarrow{N} & S_{n-2}(X) & \xrightarrow{1-\hat{t}} & S_{n-2}(X) \\
 & \vdots & & \vdots & & \vdots
\end{array}$$

Lemma The rows and columns of this diagram are chain complexes.

Proof We already know the rows are chain complexes, and we have

$$
\begin{aligned}
bb &= \sum_{k=0}^{n-1}(-1)^k d_k \sum_{j=0}^{n}(-1)^j d_j \\
&= \sum_{k=0}^{n-1}\sum_{j=0}^{n}(-1)^{k+j} d_k d_j \\
&= \sum_{n-1\geq k\geq j\geq 0}(-1)^{k+j} d_k d_j + \sum_{0\leq k<j\leq n}(-1)^{k+j} d_k d_j \\
&= \sum_{n-1\geq k\geq j\geq 0}(-1)^{k+j} d_k d_j + \sum_{0\leq k<j\leq n}(-1)^{k+j} d_{j-1} d_k \\
&= \sum_{n-1\geq k\geq j\geq 0}(-1)^{k+j} d_k d_j + \sum_{0\leq k\leq p\leq n-1}(-1)^{k+p+1} d_p d_k \\
&= 0
\end{aligned}
$$

and

$$
\begin{aligned}
b'b' &= \sum_{k<j=1}^{n-1}(-1)^{j+k} d_{j-1} d_k + \sum_{0\leq k<j\leq n}(-1)^{j+k} d_j d_k \\
&= 0
\end{aligned}
$$

by the same argument. □

The Loday-Quillen double complex is obtained by negating the maps b'.

$$
\begin{array}{ccccccc}
 & \vdots & & \vdots & & \vdots \\
\cdots & S_n(X) & \xrightarrow{N} & S_n(X) & \xrightarrow{1-\hat{t}} & S_n(X) \\
 & b\downarrow & & -b'\downarrow & & b\downarrow \\
\cdots & S_{n-1}(X) & \xrightarrow{N} & S_{n-1}(X) & \xrightarrow{1-\hat{t}} & S_{n-1}(X) \\
 & b\downarrow & & -b'\downarrow & & b\downarrow \\
\cdots & S_{n-2}(X) & \xrightarrow{N} & S_{n-2}(X) & \xrightarrow{1-\hat{t}} & S_{n-2}(X) \\
 & \vdots & & \vdots & & \vdots
\end{array}
$$

Commutativity of the previous diagram ensures that this diagram anti-commutes, that is, it is a double complex. The **cyclic homology of the space** X is defined to be the total homology of this double complex. $HC_n(X)$ has cycle representatives from the sum $S_n(X) \oplus S_{n-1}(X) \oplus .. \oplus S_0(X)$.

Lemma Alternate columns of the Loday-Quillen complex

$$\cdots S_n(X) \xrightarrow{b'} S_{n-1}(X) \xrightarrow{b'} S_{n-2}(X) \cdots$$

are acyclic.

Proof The contracting chain homotopy is given by $s: S_n(X) \longrightarrow S_{n+1}(X)$ where $s = ts_n$ because

$$\begin{aligned} b's = b'ts_n &= \sum_{j=0}^{n}(-1)^j d_j ts_n \\ &= d_0 ts_n + \sum_{j=1}^{n}(-1)^j t d_{j-1} s_n \\ &= d_{n+1} s_n + \sum_{j=1}^{n}(-1)^j s_{n+1} d_{j-1} \\ &= 1 - \sum_{j=0}^{n}(-1)^j t s_{n+1} d_j = 1 - ts_{n+1}b' = 1 - sb' \end{aligned}$$

□

2.3 The Connes double complex. [C2]

The Connes B-b double complex is obtained by contracting these acyclic columns from the Loday-Quillen double complex. Define a composite map

$$B = (1 - \hat{t})ts_{n-1}N: S_{n-1}(X) \longrightarrow S_n(X)$$

check that

$$\begin{aligned} Bb = (1-\hat{t})ts_{n-1}Nb &= (1-\hat{t})ts_{n-1}b'N \\ &= (1-\hat{t})(1-b'ts_n)N \\ &= -b(1-\hat{t})ts_nN = -bB \end{aligned}$$

and

$$BB = (1-\hat{t})ts_nN(1-\hat{t})ts_{n-1}N = 0$$

The Connes B-b double complex is

$$\begin{array}{ccccc} & \vdots & & \vdots \\ \cdots & S_n(X) & \xrightarrow{B} & S_{n+1}(X) \\ & b\downarrow & & b\downarrow \\ \cdots & S_{n-1}(X) & \xrightarrow{B} & S_n(X) \\ & \vdots & & \vdots \end{array}$$

where

$$B = (1 - (-1)^n t)ts_{n-1}\sum_{j=0}^{n-1}(-1)^{(n-1)j}t^j$$

on $S_{n-1}(X)$. The cyclic homology of the S^1-space X can be defined as the total homology of this double complex.

Theorem The total homology of the Loday-Quillen double complex is equal to that of the Connes double complex.

Proof Define a map α from the Connes double complex to the Loday-Quillen double complex. Elements of the chain groups of total homology are elements of a direct sum. This means that they are finite sums of elements of the groups. In this case, the sums would be finite even in a direct product, because of the convention $S_n(X)$ is zero whenever the index n is negative.

Define

$$\alpha(..., x_{n-2}, x_n) = (..., x_{n-2}, sNx_{n-2}, x_n)$$

The subscripts have $x_j \in S_j(X)$.

First show that α is a chain map. Use ∂ for the boundary operator in each complex.

$$\partial\alpha(.., x_{n-2}, x_n) = \partial(..., x_{n-2}, sNx_{n-2}, x_n)$$

$$= (.., ((1-\hat{t})sNx_{n-4} + bx_{n-2}), (Nx_{n-2} - b'sNx_{n-2}), ((1-\hat{t})sNx_{n-2} + bx_n))$$

$$\alpha\partial(.., x_{n-2}, x_n) = \alpha(.., (Bx_{n-4} + bx_{n-2}), (Bx_{n-2} + bx_n))$$

$$= (.., (Bx_{n-4} + bx_{n-2}), (sNBx_{n-4} + sNbx_{n-2}), (Bx_{n-2} + bx_n))$$

Check that

$$Nx_{n-2r} - b'sNx_{n-2r} = (1 - b's)Nx_{n-2r} = sb'Nx_{n-2r} = sNbx_{n-2r}$$

$$= sN(1-\hat{t})sNx_{n-2r-2} + sNbx_{n-2r} = sNBx_{n-2r-2} + sNbx_{n-2r}$$

and

$$((1-\hat{t})sNx_{n-2r} + bx_{n-2r+2}) = (Bx_{n-2r} + bx_{n-2r+2})$$

This completes the proof that α is a chain map. Next show that α is injective. Take a cycle of the Connes complex

$$(..., (By_{n-3} + by_{n-1}), (By_{n-1} + by_{n+1}))$$

It maps to

$$(.., (By_{n-3} + by_{n-1}), (sNBy_{n-3} + sNby_{n-1}), (By_{n-1} + by_{n+1}))$$

$NB = 0$ and subtracting $\partial(y_{n+1})$ we see that this is homologous to

$$(.., (By_{n-3} + by_{n-1}), sNby_{n-1}, By_{n-1})$$

Now subtract $\partial(sNy_{n-1})$

$$(.., (By_{n-3} + by_{n-1}), (sNby_{n-1} + b'sNy_{n-1}), (By_{n-1} - (1-\hat{t})sNy_{n-1}))$$

$$= (.., (By_{n-3} + by_{n-1}), (sb' + b's)Ny_{n-1})$$

$$= (.., (By_{n-3} + by_{n-1}), Ny_{n-1})$$

Now subtract $\partial(y_{n-1})$

$$= (.., By_{n-3})$$

Continue cancelling the finite number of non-zero terms in y and the chain in shown to be homologous to zero.

Finally, show that α is surjective. Take a cycle in the Loday-Quillen double complex, $..,x_{n-1},x_n$. Take r minimal with x_r non-zero. If $n-r$ is odd then we have $b'x_r = 0$, so $x+r = b'sx_r$. We can add $\partial(sx_r) = (-b'sx_r,(1-\hat{t})sx_r,0,..)$ to cancel the lowest degree term.

We may assume that $n-r$ is even so $bx_r = 0$. Subtract $\alpha(x_r)$ from the cycle, eliminating the lowest degree term again. Continuing in this way we construct a cycle in the Connes complex mapping to $(x_r,..,x_{n-1},x_n)$. α is surjective. □

2.4 The shift exact sequence. [C1]

Theorem If X is a space with a circle action then the sequence

$$HC_{n-1}(X) \longrightarrow H_n(X) \longrightarrow HC_n(X) \longrightarrow HC_{n-2}(X) \longrightarrow H_{n-1}(X)$$

is exact, where the maps are

$$\begin{array}{ccc} H_n(X) & \longrightarrow & HC_n(X) \\ \rho^n & \mapsto & (0,..,0,\rho^n) \end{array}$$

$$\begin{array}{ccc} HC_n(X) & \longrightarrow & HC_{n-2}(X) \\ (..,\rho^{n-2},\rho^n) & \mapsto & (...,\rho^{n-2}) \end{array}$$

$$\begin{array}{ccc} HC_{n-2}(X) & \longrightarrow & H_{n-1}(X) \\ (...,\rho^{n-2}) & \longrightarrow & B(\rho^{n-2}) \end{array}$$

called inclusion, shift and B respectively.

Proof

(i) Exactness at $HC_n(X)$.

The composite map is

$$\rho^n \mapsto (0,...,0,\rho^n) \mapsto (0,...,0)$$

Take $(...,\rho^{n-2},\rho^n) \in HC_n(X)$ mapping to zero in $HC_{n-2}(X)$

$$(..,\rho^{n-4},\rho^{n-2}) = (..,B(x^{n-5}) + b(x^{n-3}), B(x^{n-3}) + b(x^{n-1}))$$

for some chain $(..,x^{n-3},x^{n-1}) \in .. \oplus S_{n-3}(X) \oplus S_{n-1}(X)$. Using equivalence in $HC_n(X)$

$$\begin{aligned} &(..,\rho^{n-4},\rho^{n-2},\rho^n) \\ &= (..,\rho^{n-4} - Bx^{n-5} - bx^{n-3},\rho^{n-2} - Bx^{n-3} - bx^{n-1},\rho^n - Bx^{n-1}) \\ &= (0,..,0,\rho^n - Bx^{n-1}) \end{aligned}$$

which lies in the image of the inclusion map.

(ii) Exactness at $HC_{n-2}(X)$.

The composite map is

$$(..,\rho^{n-2},\rho^n) \mapsto (..,\rho^{n-2}) \mapsto B\rho^{n-2}$$

and $B\rho^{n-2} = -b\rho^n = 0$ in homology.

Take $(.., \rho^{n-2}) \mapsto B\rho^{n-2} = 0$ so $B\rho^{n-2} = by^n$ for some $y^n \in S_n(X)$. Then $(.., \rho^{n-2}, -y)$ represents an element of $HC_n(X)$ mapping to $(.., \rho^{n-2})$ under the shift map.

(iii) Exactness at $H_n(X)$.

The composite map is

$$(.., \rho^{n-3}, \rho^{n-1}) \mapsto B\rho^{n-1} \mapsto (0, .., 0, B\rho^{n-1})$$

and equivalence in $HC_n(X)$ gives

$$(0, .., 0, B\rho^{n-1}) = (.., B\rho^{n-3} - b\rho^{n-1}, B\rho^{n-1} - B\rho^{n-1})$$

which is zero because $(.., \rho^{n-1})$ is a cycle in $HC_{n-1}(X)$.

Take $\rho^n \mapsto (0, .., 0, \rho^n) = 0$.

$$(0, .., 0, \rho^n) = (.., Bx^{n-3} + bx^{n-1}, Bx^{n-1} + bx^{n+1})$$

giving, in $H_n(X), \rho^n = \rho^n - bx^{n+1} = Bx^{n-1}$ and $(.., x^{n-3}, x^{n-1})$ represents an element of $HC_{n-1}(X)$ which maps to ρ^n. □

2.5 An example. Calculate $HC_*(*)$.

Identify the chain groups $S_n(*)$ with the integers $\mathbb{Z}$. The maps $b: S_n(*) \longrightarrow S_{n-1}(*)$ and $B: S_n(*) \longrightarrow S_{n+1}(*)$ are

$$b: S_n(*) \longrightarrow S_{n-1}(*); 1 \mapsto \begin{cases} 1 & \text{n even} \\ 0 & \text{n odd} \end{cases}$$

$$B: S_n(*) \longrightarrow S_{n+1}(*); 1 \mapsto \begin{cases} 2(n+1) & \text{n even} \\ 0 & \text{n odd} \end{cases}$$

So the differential in Connes double complex is

$$\begin{array}{ccc} S_0 \oplus S_2 \oplus ... \oplus S_{2n} & \longrightarrow & S_1 \oplus S_3 \oplus ... \oplus S_{2n-1} \\ (z_0, z_2, ..., z_{2n}) & \mapsto & (2z_0 + z_2, 6z_2 + z_4, ..., 2(2n-1)z_{2n-2} + z_{2n}) \end{array}$$

The alternate differential maps are all zero, so the homology is alternately the kernel of this map and the cokernel of this map. The set of equations

$$\begin{aligned} 2z_0 + z_2 &= r_0 \\ 6z_2 + z_4 &= r_2 \\ &\vdots \\ 2(2n-1)z_{2n-2} + z_{2n} &= r_{2n-2} \end{aligned}$$

have solutions for all choices of $(r_0, .., r_{2n-2})$ (just put $z_0 = 0$ for example and the other values follow). So the cokernel is zero. The kernel is isomorphic to $\mathbb{Z}$, so $HC_*(*)$ has a single generator of degree 2.

$$HC_*(*) \cong H_*(\mathbb{C}P^\infty)$$

The exact sequence here is

$$\begin{array}{ccccccccccc} ... \rightarrow & H_{2n} & \rightarrow & HC_{2n} & \rightarrow & HC_{2n-2} & \rightarrow & H_{2n-1} & \rightarrow & ... \\ ... \rightarrow & 0 & \rightarrow & \mathbb{Z} & \cong & \mathbb{Z} & \rightarrow & 0 & \rightarrow & ... \end{array}$$

$$\begin{array}{ccccccccccc} \ldots\rightarrow & H_{2n-1} & \rightarrow & HC_{2n-1} & \rightarrow & HC_{2n-3} & \rightarrow & H_{2n-2} & \rightarrow & \ldots \\ \ldots\rightarrow & 0 & \rightarrow & 0 & \rightarrow & 0 & \rightarrow & 0 & \rightarrow & \ldots \end{array}$$

2.6 Normalisation in Cyclic Homology.

We can modify Connes' double complex further.

Theorem The homology of

$$\begin{array}{ccc} \widehat{S_n}(X) & \longrightarrow & \widehat{S_{n+1}}(X) \\ \downarrow & & \downarrow \\ \widehat{S_{n-1}}(X) & \longrightarrow & \widehat{S_n}(X) \end{array}$$

is equal to cyclic homology; that of

$$\begin{array}{ccc} S_n(X) & \longrightarrow & S_{n+1}(X) \\ \downarrow & & \downarrow \\ S_{n-1}(X) & \longrightarrow & S_n(X) \end{array}$$

where the hat denotes non-degenerate singular simplexes.

Before proving this, I'll introduce some notation.

If $\rho\colon \Delta^n \longrightarrow X$ is a singular simplex, denote it by

$$\begin{pmatrix} 0 \\ 1 \\ \vdots \\ n \end{pmatrix}_\rho$$

Usually I will omit the ρ on the bracket. The bracket symbol can be used to define singular simplexes; any map $\pi\colon \{0,..,m\} \longrightarrow \{0,..,n\}$ determines an m-simplex by

$$\begin{pmatrix} \pi^{-1}(0) \\ \vdots \\ \pi^{-1}(n) \end{pmatrix} : (t_0,..,t_m) \mapsto \rho\Big(\sum_{i\in\pi^{-1}(0)} t_i, .., \sum_{i\in\pi^{-1}(n)} t_i \Big)$$

For example

$$d_i(\rho) = \begin{pmatrix} 0 \\ 1 \\ \vdots \\ i-1 \\ \\ i \\ \vdots \\ n-1 \end{pmatrix}$$

(there is a gap here between the $i-1$ and the i)

$$\partial \begin{pmatrix} 0 \\ 1 \\ 2 \\ 3 \end{pmatrix} = \begin{pmatrix} \\ 0 \\ 1 \\ 2 \end{pmatrix} - \begin{pmatrix} 0 \\ \\ 1 \\ 2 \end{pmatrix} + \begin{pmatrix} 0 \\ 1 \\ \\ 2 \end{pmatrix} - \begin{pmatrix} 0 \\ 1 \\ 2 \\ \\ \end{pmatrix}$$

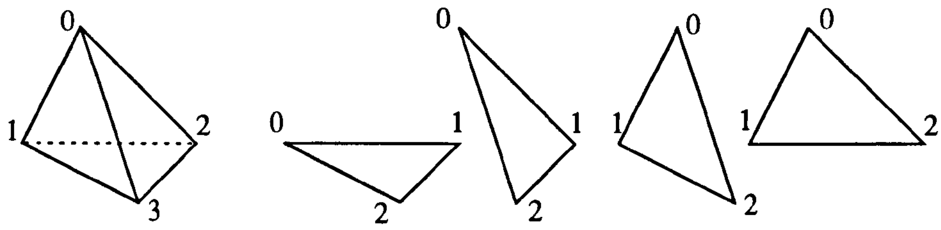

Figure 2.6.1 The boundary of a 3-simplex.

If the image space has a circle action (or in fact an action of the reals will do) then brackets with multiple columns can be used. Take a map π from $\{0,..,m\}$ to $\{0,..,n,n+1,..,2n+1\}$.

$$\begin{pmatrix} \pi^{-1}(0) & \pi^{-1}(n+1) \\ \vdots & \vdots \\ \pi^{-1}(n) & \pi^{-1}(2n+1) \end{pmatrix}$$

represents the singular m-simplex

$$(t_0,..,t_m) \mapsto \Big(\sum_{j=0}^{n} \sum_{i\in\pi^{-1}(n+1+j)} t_i\Big)\rho\Big(\sum_{k\in\pi^{-1}(0)\cup\pi^{-1}(n+1)} t_k, ..., \sum_{k\in\pi^{-1}(n)\cup\pi^{-1}(2n+1)} t_k\Big)$$

For example,

$$\rho = \begin{pmatrix} 0 \\ \vdots \\ n \end{pmatrix} \quad \text{has} \quad t(\rho) = \begin{pmatrix} 1 & \\ 2 & \\ \vdots & \\ n & \\ & 0 \end{pmatrix} \quad \text{and} \quad t^j(\rho) = \begin{pmatrix} j & \\ \vdots & \\ n & \\ & 0 \\ & \vdots \\ & j-1 \end{pmatrix}$$

The number of entries in the second column is the number of times t has been applied.

$$s_n\rho = \begin{pmatrix} 0 \\ 1 \\ \vdots \\ n-1 \\ n, n+1 \end{pmatrix} \quad ts_n\rho = \begin{pmatrix} 1 & \\ \vdots & \\ n & \\ n+1 & 0 \end{pmatrix} \quad ts_nt^j\rho = \begin{pmatrix} j+1 & \\ \vdots & \\ n+1 & 0 \\ & 1 \\ & \vdots \\ & j \end{pmatrix}$$

$$B(\rho) = \begin{pmatrix} 1 & \\ 2 & \\ \vdots & \\ n & \\ n+1 & 0 \end{pmatrix} \pm \begin{pmatrix} 2 & \\ \vdots & \\ n & \\ n+1 & 0 \\ & 1 \end{pmatrix} \pm \begin{pmatrix} 3 & \\ \vdots & \\ n+1 & 0 \\ & 1 \\ & 2 \end{pmatrix}, ..$$

$$..,\pm\begin{pmatrix} n & \\ n+1 & 0 \\ & 1 \\ & \vdots \\ & n-1 \end{pmatrix} \pm \begin{pmatrix} n+1 & 0 \\ & 2 \\ & \vdots \\ & n-1 \\ & n \end{pmatrix} \pm \begin{pmatrix} 2 & \\ 3 & \\ \vdots & \\ n+1 & \\ & 0,1 \end{pmatrix} \pm \begin{pmatrix} 3 & \\ \vdots & \\ n+1 & \\ & 0,1 \\ & 2 \end{pmatrix},..$$

$$..,\pm\begin{pmatrix} n & \\ n+1 & \\ & 0,1 \\ & \vdots \\ & n-1 \end{pmatrix} \pm \begin{pmatrix} n+1 & \\ & 0,1 \\ & 2 \\ & \vdots \\ & n \end{pmatrix} \pm \begin{pmatrix} 0,1 \\ 2 \\ 3 \\ \vdots \\ n+1 \end{pmatrix}$$

The signs here are as in the defining equation of B;

$$B = (1-(-1)^{n+1}t)ts_n\sum_{j=0}^{n}(-1)^{nj}t^j$$

$$B\begin{pmatrix} 0 \\ 1 \\ 2 \end{pmatrix} = \begin{pmatrix} 1 & \\ 2 & \\ 3 & 0 \end{pmatrix} + \begin{pmatrix} 2 & \\ 3 & 0 \\ & 1 \end{pmatrix} + \begin{pmatrix} 3 & 0 \\ & 1 \\ & 2 \end{pmatrix} - \begin{pmatrix} 2 & \\ 3 & \\ & 0,1 \end{pmatrix} - \begin{pmatrix} 3 & \\ & 0,1 \\ & 2 \end{pmatrix} - \begin{pmatrix} 0,1 \\ 2 \\ 3 \end{pmatrix}$$

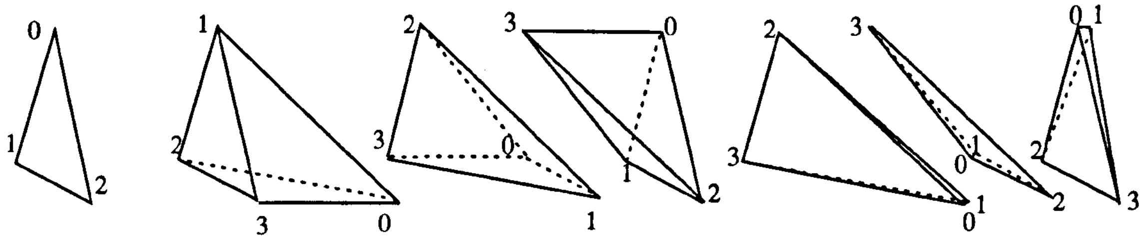

Figure 2.6.2 The map B on a 2-simplex.

A simplex is degenerate if $j, j+1$ occurs for some j in this bracket notation. It can be seen from the above expansion that $t^2 s_n t j \rho$ is degenerate for any ρ and any j. Also if ρ is degenerate then every term in $B(\rho)$ is degenerate (two rows are identified) so $B(\rho)$ is degenerate. If $Deg_n(X)$ denotes the subgroup of degenerate simplexes in $S_n(X)$ then we have a well-defined map

$$B\colon Deg_n(X) \longrightarrow Deg_{n+1}(X)$$

and since the chain group is free, a well-defined map on the quotient.

$$B\colon \widehat{S_n}(X) \longrightarrow \widehat{S_{n+1}}(X)$$

Lemma The chain complex

$$\cdots \longrightarrow Deg_n(X) \longrightarrow Deg_{n-1}(X) \longrightarrow \cdots$$

where the map is the boundary map on singular simplexes, is acyclic.

Proof Any degenerate simplex can be written $s_i(\sigma)$ for some i, σ and choose i minimal. Then, define a map

$$\begin{array}{rccc} s\colon & Deg_n(X) & \longrightarrow & Deg_{n+1}(X) \\ & s_i(\sigma) & \mapsto & (-1)^i s_i s_i(\sigma) \end{array}$$

$$sb(\rho) = s\Big(\sum_{i=0}^{n}(-1)^i d_i\rho\Big)$$

$$= s\Big(\sum_{i=0}^{n}(-1)^i d_i s_j\sigma\Big)$$

$$= s\Big(\sum_{i<j}(-1)^i s_{j-1}d_i\sigma + \sum_{i\geq j}(-1)^i s_j d_{i-1}\sigma\Big)$$

$$= \sum_{i<j}(-1)^{i+j-1} s_{j-1}s_{j-1}d_i\sigma + \sum_{i\geq j}(-1)^{i+j} s_j s_j d_{i-1}\sigma$$

$$bs(\rho) = \sum_{i=0}^{n+1}(-1)^{i+j} d_i s_j s_j\sigma$$

$$= \sum_{i<j}(-1)^{i+j} s_{j-1}d_i s_j\sigma + \sum_{i>j+1}(-1)^{i+j} s_j d_{i-1}s_j\sigma$$

$$= \sum_{i<j}(-1)^{i+j} s_{j-1}s_{j-1}d_i\sigma + \sum_{i-1>j+1}(-1)^{i+j} s_j s_j d_{i-2}\sigma + s_j\sigma$$

$$sb\rho + bs\rho = \rho$$

$$sb + bs = 1$$

□

Using the bracket notation, the degenerate simplex has

$$s\rho = s\begin{pmatrix} 0 \\ \vdots \\ i, i+1 \\ \vdots \\ n \end{pmatrix} = \begin{pmatrix} 0 \\ \vdots \\ i, i+1, i+2 \\ \vdots \\ n+1 \end{pmatrix}$$

The terms in the expansion of $b\rho$ are (with appropriate signs)

$$\begin{pmatrix} \\ 0 \\ 1 \\ \vdots \\ i-2 \\ i-1, i \\ i+1 \\ \vdots \\ n-2 \\ n-1 \end{pmatrix}\begin{pmatrix} 0 \\ \\ 1 \\ \vdots \\ i-2 \\ i-1, i \\ i+1 \\ \vdots \\ n-2 \\ n-1 \end{pmatrix}, \ldots$$

$$\ldots,\begin{pmatrix}0\\1\\\vdots\\i-2\\ \\i-1,i\\i+1\\\vdots\\n-2\\n-1\end{pmatrix}\begin{pmatrix}0\\1\\\vdots\\i-2\\i-1\\i\\i+1\\\vdots\\n-2\\n-1\end{pmatrix}\begin{pmatrix}0\\1\\\vdots\\i-2\\i-1\\i\\i+1\\\vdots\\n-2\\n-1\end{pmatrix}\begin{pmatrix}0\\1\\\vdots\\i-2\\i-1\\i,i+1\\ \\i+2\\\vdots\\n-1\end{pmatrix},\ldots,\begin{pmatrix}0\\1\\\vdots\\i-1\\i,i+1\\i+2\\\vdots\\n-2\\n-1\end{pmatrix}$$

The terms in $bs\rho$ are (with signs)

$$\begin{pmatrix} \\0\\1\\\vdots\\i-2\\i-1,i,i+1\\i+2\\\vdots\\n-1\\n\end{pmatrix}\begin{pmatrix}0\\ \\1\\\vdots\\i-2\\i-1,i,i+1\\i+2\\\vdots\\n-1\\n\end{pmatrix},\ldots$$

$$\ldots,\begin{pmatrix}0\\1\\\vdots\\i-2\\ \\i-1,i,i+1\\i+2\\\vdots\\n-1\\n\end{pmatrix}\begin{pmatrix}0\\1\\\vdots\\i-2\\i-1\\i,i+1\\i+2\\\vdots\\n-1\\n\end{pmatrix}\begin{pmatrix}0\\1\\\vdots\\i-2\\i-1\\i,i+1\\i+2\\\vdots\\n-1\\n\end{pmatrix}\begin{pmatrix}0\\1\\\vdots\\i-2\\i-1\\i,i+1\\i+2\\\vdots\\n-1\\n\end{pmatrix}\begin{pmatrix}0\\1\\\vdots\\i-1\\i,i+1,i+2\\ \\i+3\\\vdots\\n-1\\n\end{pmatrix},\ldots$$

$$\ldots,\begin{pmatrix}0\\1\\\vdots\\i-1\\i,i+1,i+2\\i+3\\\vdots\\n-1\\n\end{pmatrix}$$

so it is easily seen that $bs\rho$ consists of $sb\rho$ and ρ. (the signs need to be checked).

Lemma If a double complex has acyclic columns then it's acyclic.

Proof Take a cycle in the double complex

$$\begin{array}{ccccccc} & & \vdots & & \vdots & & \vdots \\ \cdots & \longrightarrow & E_2^{r+2} & \longrightarrow & E_1^{r+2} & \longrightarrow & E_0^{r+2} \\ & & \downarrow & & \downarrow & & \downarrow \\ \cdots & \longrightarrow & E_2^{r+1} & \longrightarrow & E_1^{r+1} & \longrightarrow & E_0^{r+1} \\ & & \downarrow & & \downarrow & & \downarrow \\ \cdots & \longrightarrow & E_2^{r} & \longrightarrow & E_1^{r} & \longrightarrow & E_0^{r} \\ & & \vdots & & \vdots & & \vdots \end{array}$$

Let the vertical maps be α and the horizontal ones β. Take $(x_0, x_1, x_2, ..) \in E_0^r \oplus E_1^{r+1} \oplus E_2^{r+2} \oplus ...$ a representative chain. An element of the direct *sum* is a *finite* sum of group elements, only finitely many of the x_i are non-zero. Then $\alpha(x_0) = 0$ and the columns are acyclic so x_0 is the boundary of y; subtract $(\alpha + \beta)(y)$ from the representative chain, eventually giving zero. (See proof that Connes' and the Loday-Quillen complex are equivalent in 2.3). □

Theorem The homology of Connes' double complex remains unchanged after normalisation of the chain groups $S_n(X)$.

Proof Denote the total complex by $... \longrightarrow K_n \longrightarrow K_{n-1} \longrightarrow ...$ and the acyclic subcomplex by $... \longrightarrow L_n \longrightarrow L_{n-1} \longrightarrow ...$. The following diagram has exact rows

$$\begin{array}{ccccccccc} & & \vdots & & \vdots & & \vdots & & \\ 0 & \longrightarrow & L_n & \longrightarrow & K_n & \longrightarrow & K_n/L_n & \longrightarrow & 0 \\ & & \downarrow & & \downarrow & & \downarrow & & \\ 0 & \longrightarrow & L_{n-1} & \longrightarrow & K_{n-1} & \longrightarrow & K_{n-1}/L_{n-1} & \longrightarrow & 0 \\ & & \vdots & & \vdots & & \vdots & & \end{array}$$

The resulting long exact sequence has

$$.. \longrightarrow H_{n+1}^{K/L} \longrightarrow H_n^L \longrightarrow H_n^K \longrightarrow H_n^{K/L} \longrightarrow H_{n-1}^L \longrightarrow ...$$

So $H_*^L = 0$ implies the isomorphism

$$H_*^K \cong H_*^{K/L}$$

□

Example Calculate $HC_*(*)$.

For all $n > 0$, $S_n(*) = Deg_n(*)$ so using the normalised double complex, we'll just get non-zero terms when we have $S_0(*)$.

$$\begin{array}{ccccc} \downarrow & & \downarrow & & \downarrow \\ \mathbb{Z} & \longrightarrow & 0 & \longrightarrow & 0 \\ & & \downarrow & & \downarrow \\ & & \mathbb{Z} & \longrightarrow & 0 \\ & & & & \downarrow \\ & & & & \mathbb{Z} \end{array}$$

The homology of this double complex is alternating $\mathbb{Z}$ and 0, and as before

$$HC_j(*) \cong H_j(\mathbb{C}P^\infty)$$

for all indices j.

In fact, if X is an S^1-space with trivial S^1-action then $\rho \in S_n(X)$ has

$$B(\rho) \in Deg_{n+1}(X)$$

so regarding the maps B as 0, we get

$$HC_n(X) = H_n(X) \oplus H_{n-2}(X) \oplus \ldots \oplus H_\epsilon(X)$$

where ϵ takes values 0 or 1 according to the parity of n.

Chapter 3. Equivariant homology

We are going to compare cyclic homology and equivariant homology. The space ES^1 is introduced and described in terms of the join construction (2.1) and as the realisation of a simplicial space (2.2). In the following sections, we decribe the isomorphism in [JDSJ1] from cyclic to equivariant homology.

Equivariant homology is defined to be

$$H_*^{S^1}(X) = H_*(ES^1 \times_{S^1} X)$$

The space $ES^1 \times_{S^1} X$ is the Borel construction on X and uses the classifying space of S^1.

Classifying spaces

If G is a topological group and EG is a contractible space upon which G acts freely and continuously then the orbit space BG is called the classifying space of the group G. The spaces BG and EG are defined up to homotopy equivalence.

3.1 The join model for ES^1.

In [M], Milnor expressed EG in terms of the join construction. The join of two spaces A and B, written $A * B$, is the product $I \times A \times B$ after identifications

$$(0, a, b_1) \sim (0, a, b_2)$$

$$(1, a_1, b) \sim (1, a_2, b)$$

If A and B have circle actions then $A * B$ has an action given by $(t, a, b)\theta = (t, a\theta, b\theta)$. The circle acts on itself, and an action is induced on $S^1 * S^1$, $(S^1 * S^1) * S^1$ and so on. Define $(S^1)^{*1} = S^1$ and $(S^1)^{*n+1} = (S^1)^{*n} * S^1$. There is a circle action on each $(S^1)^{*n}$, and there are inclusion maps $(S^1)^{*n-1} \longrightarrow (S^1)^{*n} * S^1$ induced from $A \longrightarrow A * B; a \mapsto (0, a, b)$. These inclusions are equivariant. Define

$$(S^1)^{*\infty} = \bigcup_{j \geq 1} (S^1)^{*j}$$

Proposition $(S^1)^{*\infty}$ is contractible with a free circle action.

Proof First note that the join of A and B is homotopy-equivalent to the suspension of the smash of A and B;

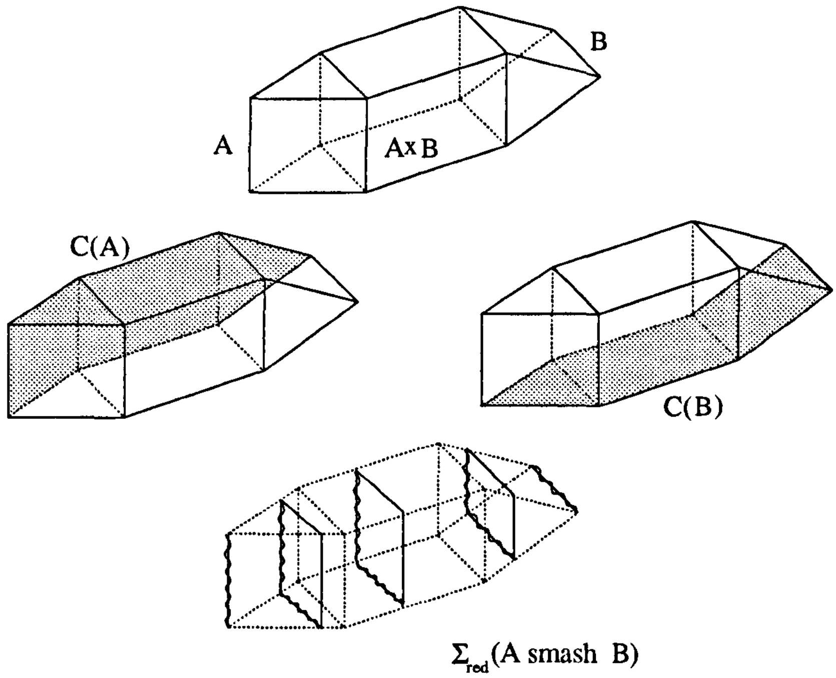

Figure 3.1.1 The join and the smash.

thus $(S^1)^{*\infty}$ is an infinite suspension, has trivial homotopy groups, and is homotopy equivalent to a point.

Take x in $(S^1)^{*\infty}$ and $\theta \in S^1$ with $x\theta = x$. We can write $x \in \bigcup_{j\geq 1}(S^1)^{*j}$. Take i minimal with $x \in (S^1)^{*i}$,

$$x = (t_{i-1}, (t_{i-2}, .., \theta_{i-1}), \theta_i)$$

$$x = x\theta = (t_{i-1}, (t_{i-2}, .., \theta_{i-1}) + \theta, \theta_i + \theta)$$

Minimality of i ensures that *either* t_{i-1} is non-zero, so $\theta_i = \theta_i + \theta$ *or* $i - 1 = 1$ and $t_1 = 0$ in which case $\theta_1 = \theta_1 + \theta$. Deduce that $\theta = 0$ and the action is free.□

Omitting brackets from the expression $x = (t_{i-1}, (t_{i-2}, .., \theta_{i-1}), \theta_i)$ and reordering the co-ordinates leaves us with

$$\bigcup_{r\geq 1}(S^1)^r \times I^{r-1}$$

under the join identifications

$$(\theta_1, \theta_2, \theta_3, .., \theta_r, 0, t_2, .., t_{r-1}) \sim (\theta_1, \theta_2 + \epsilon_2, \theta_3, .., \theta_r, 0, t_2, .., t_{r-1})$$

$$(\theta_1, \theta_2, \theta_3, .., \theta_r, 1, t_2, .., t_{r-1}) \sim (\theta_1 + \epsilon_1, \theta_2, \theta_3, .., \theta_r, 1, t_2, .., t_{r-1})$$

$$(\theta_1, \theta_2, \theta_3, .., \theta_r, t_1, 0, .., t_{r-1}) \sim (\theta_1, \theta_2, \theta_3 + \epsilon_3, .., \theta_r, t_1, 0, .., t_{r-1})$$

$$(\theta_1, \theta_2, \theta_3, .., \theta_r, t_1, 1, .., t_{r-1}) \sim (\theta_1 + \epsilon_1, \theta_2 + \epsilon_2, \theta_3, .., \theta_r, t_1, 1, .., t_{r-1})$$

$$\ldots$$

$$(\theta_1, \theta_2, \theta_3, .., \theta_r, t_1, t_2, .., 0) \sim (\theta_1, \theta_2, \theta_3 + \epsilon_3, .., \theta_r + \epsilon_r, t_1, t_2, .., 0)$$

$$(\theta_1,\theta_2,\theta_3,..,\theta_r,t_1,t_2,..,1)\sim(\theta_1+\epsilon_1,\theta_2+\epsilon_2,\theta_3+\epsilon_3,..,\theta_r,t_1,t_2,..,1)$$

and the inclusions identify

$$(\theta_1,\theta_2,..,\theta_r,t_1,t_2,..,t_{r-1})\sim(\theta_1,\theta_2,..,\theta_r,0,t_1,t_2,..,t_{r-1},0)$$

Now reparametrise the interval co-ordinates by letting

$$s_i=\begin{cases}(1-t_1)(1-t_2)..(1-t_{r-1}) & \text{i=1}\\ t_{i-1}(1-t_i)..(1-t_{r-1}) & 2\leq \text{i} \leq \text{r-1}\\ t_{r-1} & \text{i=r}\end{cases}$$

The sum of the s_i is 1 and we can re-express the space $(S^1)^{*\infty}$ as $\bigcup_{r\geq 1}(S^1)^r\times\Delta^{r-1}$ under the join identifications

$$(\theta_1,\theta_2,..,\theta_r,0,s_2,..,s_r)\sim(\theta_1+\epsilon_1,\theta_2,..,\theta_r,0,s_2,..,s_r)$$

$$(\theta_1,\theta_2,..,\theta_r,s_1,0,..,s_r)\sim(\theta_1,\theta_2+\epsilon_2,..,\theta_r,s_1,0,..,s_r)$$

$$\cdots$$

$$(\theta_1,\theta_2,..,\theta_r,s_1,s_2,..,0)\sim(\theta_1,\theta_2,..,\theta_r+\epsilon_r,s_1,s_2,..,0)$$

and the inclusion identifications

$$(\theta_1,\theta_2,..,\theta_r,s_1,s_2,..,s_r)\sim(\theta_1,\theta_2,..,\theta_r,0,s_1,s_2,..,s_r,0)$$

Finally, reparametrise the circle co-ordinates by letting

$$\phi_i=\begin{cases}\theta_1 & \text{i=1}\\ \theta_i-\theta_{i-1} & 2\leq\text{i}\leq\text{r}\end{cases}$$

and $(S^1)^{*\infty}$ becomes $\bigcup_{r\geq 1}(S^1)^r\times\Delta^{r-1}$ under the equivalences

$$(\phi_1,\phi_2,\phi_3,..,\phi_r,0,s_2,..,s_r)\sim(\phi_1+\epsilon,\phi_2,\phi_3,..,\phi_r,0,s_2,..,s_r)$$

$$(\phi_1,\phi_2,\phi_3,..,\phi_r,s_1,0,..,s_r)\sim(\phi_1-\epsilon_2,\phi_2+\epsilon_2,\phi_3,..,\phi_r,s_1,0,..,s_r)$$

$$\cdots$$

$$(\phi_1,\phi_2,..,\phi_r,s_1,s_2,..,0)\sim(\phi_1,\phi_2,..\phi_{r-1}-\epsilon_r,\phi_r+\epsilon_r,s_1,s_2,..,0)$$

$$(\phi_1,\phi_2,\phi_3,..,\phi_r,s_1,s_2,..,s_r)\sim(\phi_1,\phi_2,\phi_3,..,\phi_r,0,s_1,s_2,..,s_r,0)$$

The free group action is given by

$$(\phi_1,\phi_2,\phi_3,..,\phi_r,s_1,s_2,..,s_r)\alpha=(\phi_1,\phi_2,\phi_3,..,\phi_r+\alpha,s_1,s_2,..,s_r)$$

This is the model for ES^1 which will be used in the chapters on cyclic and equivariant bordism.

3.2 The simplicial realisation model for ES^1.

In [S1] G. Segal gives a semisimplicial space whose realisation is a model for the classifying space of a topological group as follows. Begin with a topological category $\mathcal{C}$, so the object set and morphism set have topologies with the structure maps continuous. Define **the nerve of the catgory** $N\mathcal{C}$ to be the semi-simplicial space whose vertices correspond to the objects of $\mathcal{C}$, the 1-simplexes correspond to the morphisms of $\mathcal{C}$, the 2-simplexes correspond to the commuting triangles and so on. $B\mathcal{C}$, **the classifying space of** $\mathcal{C}$, is the realisation of this semisimplicial space.

Given a topological group define the category $\mathcal{G}$ which has a single object and a morphism for each element of G. Then $B\mathcal{G} = BG$ is the classifying space of the group.

Further, the category $\overline{\mathcal{G}}$ has objects corresponding to group elements and morphisms in the product $G \times G$. This category has exactly one morphism between any given pair of objects, this morphism is an isomorphism, and the category is naturally equivalent to the category with a single object and a single morphism.

The n-simplexes of $B\overline{\mathcal{G}}$ are indexed by n-tuples of pairs which can compose;

$$(g_0,g_1),(g_1,g_2),..,(g_{n-2},g_{n-1}),(g_{n-1},g_n)$$

Identify such n-tuples of pairs with $n{+}1$-tuples of group elements $(g_0,g_1,..,g_{n-1},g_n)$ Then we have $B\overline{\mathcal{G}} = \bigcup_{n\geq 0} G^{n+1} \times \Delta^n$ subject to the following identifications

$$((g_0,g_1),(g_1,g_2),..,(g_{n-1},g_n),0,t_1,t_2,..,t_n) \sim ((g_1,g_2),..,(g_{n-1},g_n),t_1,t_2,..,t_n)$$

$$((g_0,g_1),(g_1,g_2),..,(g_{n-1},g_n),t_0,0,t_2,..,t_n) \sim ((g_0,g_1)(g_1,g_2),..,(g_{n-1},g_n),t_0,t_2,..,t_n)$$
$$= ((g_0,g_2),(g_2,g_3),..,(g_{n-1},g_n),t_0,t_2,..,t_n)$$

$$\dots$$

$$((g_0,g_1),..,(g_{n-2},g_{n-1}),(g_{n-1},g_n),t_0,t_1,..,0,t_n)$$
$$\sim ((g_0,g_1),..,(g_{n-2},g_{n-1})(g_{n-1},g_n),t_0,t_1,..,t_n)$$
$$= ((g_0,g_1),(g_1,g_2),..,(g_{n-2},g_n),t_0,t_1,..,t_n)$$
$$((g_0,g_1),..,(g_{n-2},g_{n-1}),(g_{n-1},g_n),t_0,t_1,..,t_{n-1},0)$$
$$\sim ((g_0,g_1),..,(g_{n-2},g_{n-1}),t_0,t_1,..,t_{n-1})$$

Removing the bracketing and repetition from these expresions leaves us with

$$(g_0,g_1,g_2,g_3,..,g_{n-1},g_n,0,t_1,t_2,..,t_n) \sim (g_1,g_2,g_3,..,g_{n-1},g_n,t_1,t_2,..,t_n)$$
$$(g_0,g_1,g_2,g_3,..,g_{n-1},g_n,t_0,0,t_2,..,t_n) \sim (g_0,g_2,g_3,..,g_{n-1},g_n,t_0,t_2,..,t_n)$$

$$\dots$$

$$(g_0,g_1,g_2,..,g_{n-2},g_{n-1},g_n,t_0,t_1,..,0,t_n) \sim (g_0,g_1,g_2,..,g_{n-2},g_n,t_0,t_1,..,t_n)$$
$$(g_0,g_1,g_2,..,g_{n-2},g_{n-1},g_n,t_0,t_1,..,t_{n-1},0) \sim (g_0,g_1,g_2,..,g_{n-2},g_{n-1},t_0,t_1,..,t_{n-1})$$

This space has a free group action given by acting on each of the group co-ordinates.

A natural transformation between functors T and S from $\mathcal{C}$ to $\mathcal{D}$ gives a homotopy between BT and BS from $B\mathcal{C}$ to $B\mathcal{D}$. The equivalence between the category $\overline{\mathcal{G}}$

and the category with a single object and a single morphism shows that $B\overline{\mathcal{G}}$ is contractible.

This is the model for ES^1 that will be used in this chapter.

3.3 Theorem. The cyclic homology of a space with a circle action is isomorphic to the equivariant homology of the space.

We will describe the isomporphism here, following the construction in [JDSJ1]. There is also a proof given in [L].

The map $HC_n(X) \longrightarrow H_n(ES^1 \times_{S^1} X)$

$HC_*(X)$ is the total homology of

$$\begin{array}{ccccc} & \vdots & & \vdots \\ \cdots & S_n(X) & \xrightarrow{B} & S_{n+1}(X) \\ & b\downarrow & & b\downarrow \\ \cdots & S_{n-1}(X) & \xrightarrow{B} & S_n(X) \\ & \vdots & & \vdots \end{array}$$

where

$$B\colon \begin{pmatrix} 0 \\ 1 \\ \cdots \\ n \end{pmatrix} \longrightarrow \begin{pmatrix} 1 & \\ 2 & \\ \vdots & \\ n & \\ n+1 & 0 \end{pmatrix} \pm \begin{pmatrix} 2 & \\ \vdots & \\ n & \\ n+1 & 0 \\ & 1 \end{pmatrix} \pm .. \pm \begin{pmatrix} n & \\ n+1 & 0 \\ & \vdots \\ & n-2 \\ & n-1 \end{pmatrix} \pm \begin{pmatrix} n+1 & 0 \\ & 1 \\ & \vdots \\ & n-1 \\ & n \end{pmatrix}$$

is the horizontal map and the vertical map is the singular boundary map.

3.4 The shuffle product.

There is a close link between the map B on singular simplexes and the shuffle product. Here we describe the shuffle product in some detail, and define a map J which is essentially the same as B, up to the permutation of vertices.

Given simplexes $\rho\colon \Delta^p \longrightarrow X$, $\sigma\colon \Delta^q \longrightarrow Y$ with vertices at $x_0, .., x_p$ and $y_0, .., y_q$ respectively, and a sequence of points in $X \times Y$ given by $(x_{i(0)}, y_{j(0)}).., (x_{i(n)}, y_{j(n)})$, we can construct an n-simplex in $X \times Y$ with these vertices. The image of $(t_0, .., t_n)$ is

$$(\rho(\sum_{k \text{ with } i(k)=0} t_k, .., \sum_{k \text{ with } i(k)=p} t_k), \sigma(\sum_{k \text{ with } j(k)=0} t_k, .., \sum_{k \text{ with } j(k)=q} t_k))$$

Call a sequence $(i(k), j(k))$ for $0 \leq k \leq n$ a p, q**-zig-zag** if $n = p + q$ and

$$i(0) = j(0) = 0,\ i(n) = p,\ j(n) = q$$

$$\text{and for all } k \text{ either } i(k+1) = i(k) \text{ and } j(k+1) = j(k) + 1$$

$$\text{or } i(k+1) = i(k) + 1 \text{ and } j(k+1) = j(k)$$

There is a one-to-one correspondence between $p,\ q$-zig-zags and $p,\ q$-**shuffles**. A $p,\ q$-shuffle is a permutation α of $\{1,..,p+q\}$ which has

$$\alpha(1) < .. < \alpha(p) \quad \text{and} \quad \alpha(p+1) < .. < \alpha(p+q)$$

Given a shuffle, we can define a zig-zag with $i(k)$ being the number of r between 1 and p with $\alpha(r) \leq k$ and $j(k)$ being the number of r between $p+1$ and $p+q$ with $\alpha(r) \leq k$.

Conversely, given a $p,\ q$-zig-zag, define $\alpha(r)$ to be the number of elements of $i^{-1}\{0,..,r\}$ if $1 \leq r \leq p$ and $\alpha(r)$ to be the number of elements of $j^{-1}\{0,..,r-p\}$ if $p+1 \leq r \leq p+q$. Then α is a shuffle and these two constructions are inverse.

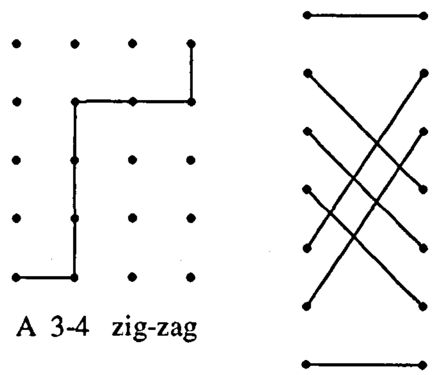

A 3-4 zig-zag

A 3-4 shuffle

Figure 3.4.1 A zig-zag and the corresponding shuffle.

The **shuffle product** of the simplexes ρ and σ is defined to be the chain

$$\theta(\rho,\sigma) = \sum_{\text{shuffles}} \text{sgn}(\alpha)(\rho(\sum_{0\leq r<\alpha(1)} t_r, \sum_{\alpha(1)\leq r<\alpha(2)} t_r, .., \sum_{\alpha(p)\leq r\leq p+q} t_r),$$

$$\sigma(\sum_{0\leq r<\alpha(p+1)} t_r, \sum_{\alpha(p+1)\leq r<\alpha(p+2)} t_r, .., \sum_{\alpha(p+q)\leq r\leq p+q} t_r))$$

$$= \sum_{\text{zig-zags}} \text{sgn}(i,j)(\rho(\sum_{r\in i^{-1}(0)} t_r, .., \sum_{r\in i^{-1}(p)} t_r), \sigma(\sum_{r\in j^{-1}(0)} t_r, .., \sum_{r\in j^{-1}(q)} t_r))$$

The signs ensure that common $n-1$-faces of the simplexes in these sums cancel. See also [G] for a definition of the shuffle map.

Take a space with a circle action $f: X \times S^1 \longrightarrow X$ and take z to be the generating cycle $t \mapsto e^{2\pi i t}$ in $S_1(S^1)$. Then we can use the shuffle product to define a map J

$$J: S_n(X) \longrightarrow S_{n+1}(X); \quad \rho \mapsto f_*\theta(\rho, z)$$

Using bracket notation, we have

$$J: \begin{pmatrix} 0 \\ 1 \\ \cdots \\ n \end{pmatrix} \longrightarrow \begin{pmatrix} 0 & 1 \\ & 2 \\ & \cdots \\ & n+1 \end{pmatrix} \pm \begin{pmatrix} 0 & \\ 1 & 2 \\ & 3 \\ & \cdots \\ & n+1 \end{pmatrix} \pm \ldots \pm \begin{pmatrix} 0 & \\ 1 & \\ \cdots & \\ n-1 & \\ n & n+1 \end{pmatrix}$$

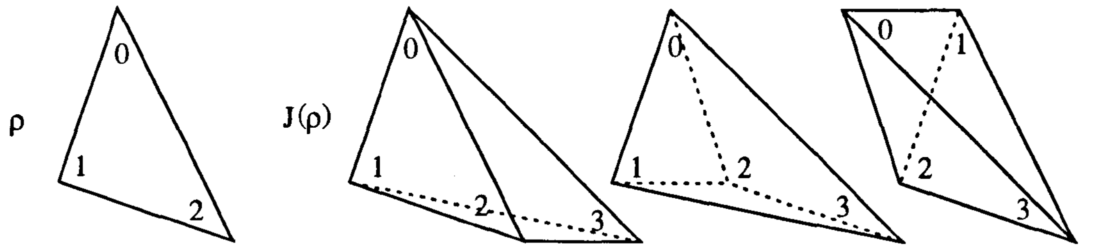

Figure 3.4.2 The map J.

3.5 Permutation of vertices.

The images of a cycle under the maps B and J are almost the same, differing only in the labelling of the vertices. Here I will show that if two chain maps differ by permutation of the vertices of simplexes then the maps are chain-homotopic.

Given a singular n-simplex ρ in X and a permutation α of $\{0,..,n\}$, define the simplex $\alpha_*(\rho)$

$$\alpha_*(\rho)(t_0,..,t_n) = \rho(t_{\alpha(0)},..,t_{\alpha(n)})$$

and define an $n+1$-chain $fill(\rho,\alpha) = \sum_{k=0}^{n} \pm\beta(\alpha,k,\rho)$

$$\beta(\alpha,k,\rho)(t_0,..,t_{n+1}) = \rho(t_{\gamma(0)},..,t_{\gamma(k)} + t_0, t_1,..,t_{n-k-1})$$

here $\gamma\colon \{0,..,k\} \longrightarrow \{n-k,..,n\}$ is an injective map defined using α; $\gamma(i) < \gamma(j)$ if and only if $\alpha(i) < \alpha(j)$.

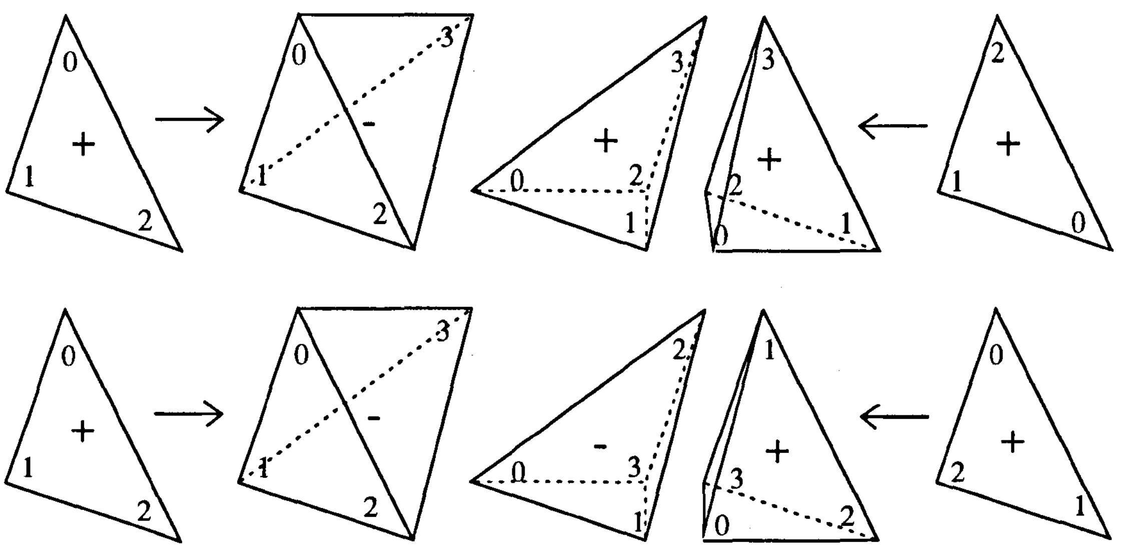

Figure 3.5.1 Filling between simplexes with permuted vertices.

This chain has boundary including both the simplexes ρ and $\alpha_*(\rho)$. Moreover, the rest of the boundary is the sum $\sum_{i=0}^{n} \pm fill(\partial_i\rho, \partial_i\alpha)$. Here $\partial_i\rho$ is the i^{th} face of ρ and $\partial_i\alpha$ is obtained from α by omitting i from the domain, omitting $\alpha(i)$ from the range and subtracting 1 from higher elements to recover a permutation of $\{0,..,n-1\}$.

We can apply this construction to a cycle. Given an n-cycle in X, and another n-cycle whose simpexes are all the same except for permutation of vertices, apply this construction 'fill' between all pairs of simplexes. Cancelling faces between simplexes in the cycles become cancelling n-chains. This shows, for example, that B and J are chain homotopic.

We can replace B by J in the definition of cyclic homology leaving $HC_*(X)$ unchanged up to isomorphism.

The shuffle product gives a map

$$S_1(S^1) \otimes .. \otimes S_1(S^1) \otimes S_i(X) \longrightarrow S_{r+i}((S^1)^r \times X)$$

where there are r copies of $S_1(S^1)$'s in the product in the domain. The shuffle product also induces a map

$$S_1(S^1) \otimes .. \otimes S_1(S^1) \otimes S_i(X) \longrightarrow S_1(S^1) \otimes .. \otimes S_1(S^1) \otimes S_{i+1}(X)$$

The number of $S_1(S^1)$ has reduced, we used the last $S_1(S^1)$ in the shuffle product with $S_i(X)$.

There is a boundary map

$$S_1(S^1) \otimes .. \otimes S_1(S^1) \otimes S_i(X) \longrightarrow S_1(S^1) \otimes .. \otimes S_1(S^1) \otimes S_{i-1}(X)$$

where the number of $S_1(S^1)$ remains the same (this corresponds to the bar construction in [JDSJ1]).

These three maps give commuting diagrams

$$\begin{array}{ccc} S_{i-1}(X) & \xrightarrow{J} & S_i(X) \\ \downarrow & & \downarrow \\ (S_1(S^1))^{\otimes r+1} \otimes S_{i-1}(X) & \xrightarrow{J} & (S_1(S^1))^{\otimes r} \otimes S_i(X) \\ \text{shuffle} \downarrow & & \text{shuffle} \downarrow \\ S_{r+i}((S^1)^{r+1} \times X) & \xrightarrow{\text{faces}} & S_{r+i}((S^1)^r \times X) \end{array}$$

$$\begin{array}{ccc} S_i(X) & \xrightarrow{\partial} & S_{i-1}(X) \\ \downarrow & & \downarrow \\ (S_1(S^1))^{\otimes r} \otimes S_i(X) & \xrightarrow{\text{bdry}} & (S_1(S^1))^{\otimes r} \otimes S_{i-1}(X) \\ \text{shuffle} \downarrow & & \text{shuffle} \downarrow \\ S_{r+i}((S^1)^r \times X) & \xrightarrow{\text{bdry}} & S_{r+i-1}((S^1)^r \times X) \end{array}$$

The maps $S_{r+i}((S^1)^{r+1} \times X) \xrightarrow{\text{faces}} S_{r+i}((S^1)^r \times X)$ are induced from the alternating sum of the attaching maps of the simplicial structure of $ES^1 \times_{S^1} X$

$$(S^1)^{r+1} \times X \xrightarrow{\text{faces}} (S^1)^r \times X$$

The maps $S_{r+i}((S^1)^r \times X) \xrightarrow{\text{bdry}} S_{r+i-1}((S^1)^r \times X)$ are the usual simplicial boundary maps.

The diagrams above commute and throw the cyclic homology J-b double complex onto the complex

$$
\begin{array}{ccccc}
 & \vdots & & \vdots \\
\cdots & S_{r+i+1}((S^1)^{r+1} \times X) & \xrightarrow{\text{faces}} & S_{r+i+1}((S^1)^{r} \times X) \\
 & \text{bdry} \downarrow & & \text{bdry} \downarrow \\
\cdots & S_{r+i}((S^1)^{r+1} \times X) & \xrightarrow{\text{faces}} & S_{r+i}((S^1)^{r} \times X) \\
 & \vdots & & \vdots
\end{array}
$$

Assume that X is a good enough space to ensure that the total homology of the double complex is equal to the homology of the realisation. This is a standard assumption [S2], [JDSJ1], [L].

The map between the double complexes induces an isomorphism in homology. The homology of the second double complex is the homology of the realisation of the simplicial space; the equivariant homology of X. □

Chapter 4. Cyclic bordism

In this chapter we will construct a cyclic bordism theory of spaces with a circle action. Cyclic bordism has a periodicity operator and the shift long exact sequence is proved in 4.2. In the later sections we discuss relative cyclic bordism, show the long exact sequence of a pair, define reduced cyclic bordism and prove excision.

4.1 Definitions. If M^n is an n-dimensional oriented manifold whose boundary ∂M has a circle action on it, then define

$$B(M^n) = (M^n \times S^1)/\sim$$

where $\sim$ is an identification

$$(x,\theta) \sim (\theta x, 0)$$

on points in $\partial M \times S^1$. Here we will identify S^1 with $\mathbb{R}/2\pi\mathbb{Z}$. This space is homeomorphic to, and can be defined as,

$$B(M^n) = (M^n \times S^1 \sqcup \partial M \times D^2)/\sim$$

where $\sim$ is an identification

$$(x,\theta) \sim (\theta x, 1e^{i\theta})$$

$1e^{i\theta} \in \partial D^2 \subset \mathbb{C}$

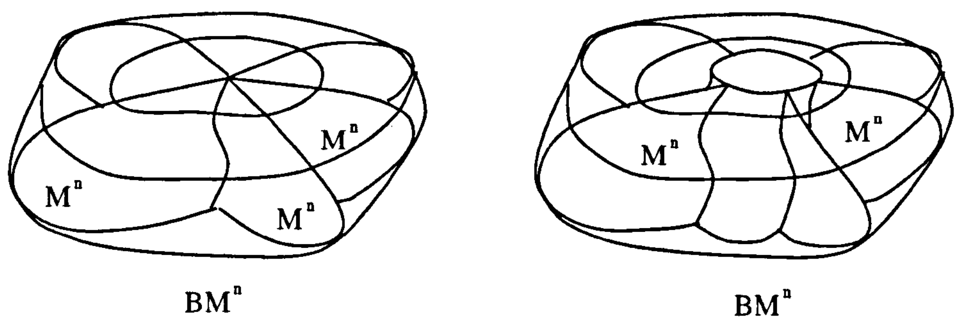

Figure 4.1.1 Definition of B.

If X is a space with a circle action, M^n is an n-manifold with a circle action on the boundary and f maps M^n to X with the restriction $\partial M^n \longrightarrow X$ equivariant, then there is a singular $n+1$-manifold in X ; $B(f): B(M^n) \longrightarrow X$; induced from the map

$$\begin{array}{ccc} M^n \times S^1 & \longrightarrow & X \\ (y,\theta) & \mapsto & \theta f(y) \end{array}$$

Check the identification;

$$\begin{array}{ccc} (x,\theta) & \mapsto & \theta f(x) \\ (\theta x, 0) & \mapsto & 0 f(\theta x) \end{array}$$

these images are equal because f is equivariant on ∂M. There is a natural circle action on $B(M)$ given by

$$\alpha(x,\theta) = (x, \alpha + \theta)$$

Check that this respects the identification;

$$\begin{aligned}\alpha(x,\theta) &= (x,\alpha+\theta) &= ((\alpha+\theta)x,0)\\ \alpha(\theta x,0) &= (\theta x,\alpha) &= ((\alpha+\theta)x,0)\end{aligned}$$

and the map $B(f)$ is equivariant with respect to these actions;

$$f(\alpha(x,\theta)) = f(x,\alpha+\theta) = f((\alpha+\theta)x,0)$$
$$= (\alpha+\theta)f(x) = \alpha(\theta f(x)) = \alpha f(x,\theta)$$

Define $\mathfrak{M}_n(X)$= the set of **closed singular oriented n-manifolds** in X.

Define **the oriented bordism group** $\Omega_n(X) = \mathfrak{M}_n(X)/\sim$ where the equivalence relation is generated by

$$(f_1\colon M_1 \longrightarrow X) \sim (f_2\colon M_2 \longrightarrow X) \iff$$
$$\text{there exists } (f\colon W \longrightarrow X), \partial W = N_1 \sqcup -N_2, N_1 \cong M_1, N_2 \cong M_2$$

where these oriented diffeomorphisms respect the maps $f_i, f|_{N_i}$ for i=1,2. See [BtD] and [CW].

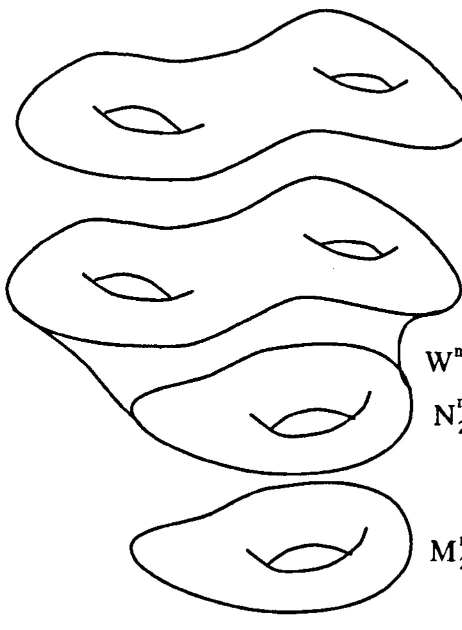

Figure 4.1.2 Definition of bordism.

Given a sequence of singular manifolds with an S^1-action on each boundary;

$$M^n, M^{n-2}, M^{n-4}, ..$$

call it an **admissible sequence** if there are equivariant orientation-preserving diffeomorphisms

$$\partial M^r \cong B(M^{r-2})$$

Then $\mathfrak{M}C_n(X)$ is defined to be the set of admissible sequences of singular manifolds in X. Finally, define the **oriented cyclic bordism group**

$$\Omega C_n(X) = \mathfrak{M}C_n(X)/\sim$$

where the equivalence relation has

$$(Q^n, Q^{n-2}, ...) \sim (P^n, P^{n-2}, ...) \iff$$
$$\text{there exists } (W^{n+1}, W^{n-1}, ...) \text{ such that}$$
$$\partial W^{i+1} \cong (Q^i \sqcup V^i \sqcup P^i)/\sim$$
$$\text{where } V^i = (W^{i-1} \times S^1)/\sim$$
$$(w, \theta) \sim (\theta w, 0) \text{ for all } w \in V^{i-2} \subseteq W^{i-1}$$

For low indices i, V^i is empty and the union $(Q^i \sqcup V^i \sqcup P^i)/\sim$ is disjoint. For higher dimensions, we have

$$\partial V^i \cong BQ^{i-2} \sqcup BP^{i-2}$$

and in $(Q^i \sqcup V^i \sqcup P^i)/\sim$,

$$\partial Q^i \sqcup \partial P^i \cong \partial V^i$$

Also require maps

$$f^{i+1}: W^{i+1} \longrightarrow X$$

restricting, up to diffeomorphism, to the given maps $Q^i, P^i \longrightarrow X$ and an equivariant map $V^i \longrightarrow X$ which is induced from the map $f^{i-1}: W^{i-1} \longrightarrow X$

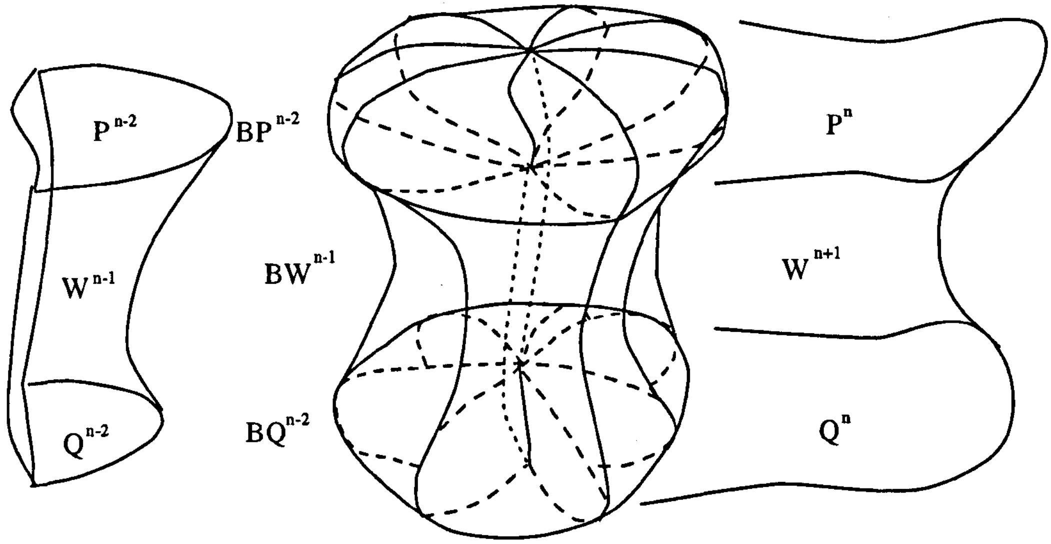

Figure 4.1.3 Cyclic bordism.

$\Omega_n(X)$ and $\Omega C_n(X)$ have a group structure by disjoint union.

Define unoriented theories similarly, giving the bordism group $\mathfrak{N}_n(X)$ and the cyclic bordism group $\mathfrak{N}C_n(X)$.

4.2 Theorem. There is an exact sequence, **the shift exact sequence**

$$...\Omega_n(X) \longrightarrow \Omega C_n(X) \longrightarrow \Omega C_{n-2}(X) \longrightarrow \Omega_{n-1}(X)...$$

where the maps are

$$[M^n] \longrightarrow [M^n, \phi, .., \phi]$$

$$[M^n, M^{n-2}, ..] \longrightarrow [M^{n-2}, ..]$$

$$[M^{n-2}, ..] \longrightarrow [BM^{n-2}]$$

called inclusion, shift and B respectively.

Proof First check that these maps are well-defined.

Inclusion is well-defined; if $[M^n] = [P^n]$ then there exists a W^{n+1} between them, and the existence of $[W^{n+1}, \phi, \phi, ..,]$ ensures that

$$[M^n, \phi, .., \phi] = [P^n, \phi, .., \phi]$$

The shift map is well-defined; if $[M^n, M^{n-2}, ..] = [P^n, P^{n-2}, ..]$ then there exists $[W^{n+1}, W^{n+1}, ..]$ with the appropriate diffeomorphisms. So $[W^{n-1}, ..]$ gives

$$[M^{n-2}, ..] = [P^{n-2}, ..]$$

B is well-defined; if $[M^{n-2}, ..] = [P^{n-2}, ..]$ then there exists $[W^{n-1}, ..]$ with the boundary of W^{n-1} being $M^{n-2} \sqcup P^{n-2}$ and an S^1-space; V^{n-2}; identified along common boundary components. Define

$$B(W^{n-1}) = W^{n-1} \times S^1 / \sim$$

where $\sim$ is generated by the relation $(x, \theta) \sim (\theta x, 0)$ between points in $V^{n-2} \times S^1$. $B(W^{n-1})$ is the required bordism between $B(M^{n-2})$ and $B(P^{n-2})$ in $\Omega C_{n-1}(X)$.

Now check exactness of the sequence. At $\Omega C_n(X)$ it's a complex because the composite map is

$$[M^n] \longrightarrow [M^n, \phi, \phi, ..] \longrightarrow [\phi, \phi, ..] = 0$$

Take $[M^n, M^{n-2}, ..]$ with $[M^{n-2}, ..] = 0$. So there exist $W^{n-1}, W^{n-3}, ..$ with $\partial W^{n-1} = M^{n-2} \sqcup V^{n-2}$. Let $P^n = M^n \sqcup B(W^{n-1})$ glued along $B(M^{n-2})$ then $P^n \times I, W^{n-1}, W^{n-3}, ..$ demonstrates $[M^n, M^{n-2}, ..] = [P^n, \phi, \phi, ..]$ so the kernel of the shift map is contained in the image of the inclusion.

At $\Omega C_{n-2}(X)$ it's a complex because the composite map is

$$[M^n, M^{n-2}, ..] \longrightarrow [M^{n-2}, M^{n-4}, ..] \longrightarrow [BM^{n-2}] = [\partial M^n] = 0$$

Take $[M^{n-2}, M^{n-4}, ..]$ with $[BM^{n-2}] = 0$ so $BM^{n-2} = \partial W^n$. The shift map takes $[W^n, M^{n-2}, ..] \longrightarrow [M^{n-2}, ..]$.

At $\Omega_n(X)$ it's a complex because the composite map is

$$[M^{n-1}, M^{n-3}, ..] \longrightarrow [BM^{n-1}] \longrightarrow [BM^{n-1}, \phi, \phi, ..] = 0$$

where the last equality is due to the bordism $BM^{n-1} \times I, M^{n-1}, M^{n-3}, \ldots$

Take $[M^n]$ with $[M^n, \phi, ..] = 0$. Then there exists $W^{n+1}, W^{n-1}, ..$ with $\partial W^{n+1} = M^n \sqcup V^n$ identified along their common boundary. M^n is closed, so this is a disjoint union and $[M^n] = [V^n] = [BW^{n-1}]$. Deduce that $[M^n]$ is in the image of B. □

4.3 Relative cyclic bordism.

In relative singular homology we include as representatives chains which fail to be cycles but whose boundaries lie in a smaller chain group. In relative bordism, include singular manifolds in X which are not closed but whose boundaries map to a subspace A are included.

In relative cyclic bordism, take a chain $M^n, M^{n-2}, ..$ and consider representatives whose boundaries $\partial M^n \cup B(M^{n-2}), ...$ fall in a subspace. More precisely, elements of $\Omega C_n(X, A)$ have representatives $M^n, V^{n-1}, M^{n-2}, V^{n-3}, ...$ subject to

$$\partial M^n \cong B(M^{n-2}) \cup V^{n-1}, \partial V^{n-1} \cong B(V^{n-3}), ...$$

$f: M^n \longrightarrow X$ restricting to $V^{n-1} \longrightarrow A$ and all restrictions to spaces of the form $B(-)$ equivariant. These unions are glued at $\partial B(M^{n-2}) \cong B(V^{n-3}) \cong \partial V^{n-1}$

Equivalence of representatives is given by the existence of $W^{n+1}, U^n, W^{n-1}, U^{n-2}, ...$ satisfying

$$\partial W^{n+1} \cong M_1^n \cup M_2^n \cup BW^{n-1} \cup U^n, ..$$

$$\partial U^n \cong V_1^{n-1} \cup V_2^{n-1} \cup BU^{n-2}, ..$$

These unions are glued at

$$\partial M_1^n \cong B(M_1^{n-2}) \cup V_1^{n-1}$$

$$\partial M_2^n \cong B(M_2^{n-2}) \cup V_2^{n-1}$$

$$\partial B(W^{n-1}) \cong B(M_1^{n-2}) \cup B(M_2^{n-2}) \cup B(U^{n-2})$$

$$\partial U^n \cong V_1^{n-1} \cup V_2^{n-1} \cup B(U^{n-2})...$$

and the final condition is that the spaces U^n map to A.

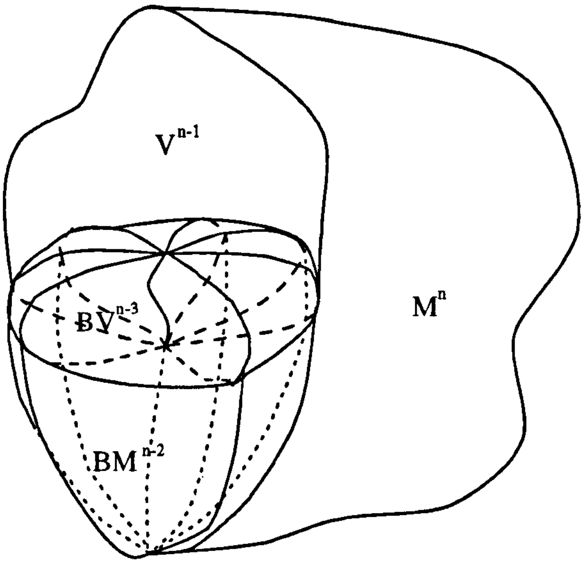

Figure 4.3.1 Relative cyclic bordism.

4.4 The long exact sequence of a pair.

Theorem If X is a space with a circle action and A is an invariant subspace then there is a long exact sequence

$$\Omega C_n(A) \longrightarrow \Omega C_n(X) \longrightarrow \Omega C_n(X,A) \longrightarrow \Omega C_{n-1}(A) \longrightarrow \Omega C_{n-1}(X)$$

Proof We have to check exactness in three cases:

(i) Exactness at

$$\Omega C_n(A) \longrightarrow \Omega C_n(X) \longrightarrow \Omega C_n(X,A)$$

There is a natural map $\Omega C_n(X) \longrightarrow \Omega C_n(X,A)$ giving a structure in which all the V^j are empty. The kernel of this map consists of those structures $M^n, M^{n-2},..$ in X which have an associated $W^{n+1}, U^n, W^{n-1}, U^{n-2},...$

satisfying $\partial W^{n+1} \cong M_1^n \cup BW^{n-1} \cup U^n, \partial U^n \cong BU^{n-2},...$

where these unions are glued at

$\partial M^n \cong B(M^{n-2}),\ \ \partial B(W^{n-1}) \cong B(M^{n-2}) \cup B(U^{n-2}),\ \ \partial U^n \cong B(U^{n-2})...$

The manifolds U must map into the subspace A of X.

If the element $M^n, M^{n-2},..$ came from $\Omega C_n(A)$, and so $f: M^n \longrightarrow A$, then the manifolds $U^n \cong M^n, W^{n+1} \cong M^n \times I$ will serve as a null-bordism in $\Omega C_n(X,A)$. Thus the composite $\Omega C_n(A) \longrightarrow \Omega C_n(X) \longrightarrow \Omega C_n(X,A)$ is the zero map.

Moreover, given an element in the kernel of $\Omega C_n(X) \longrightarrow \Omega C_n(X,A)$ use the structure provided, consider the W as a bordism in $\Omega C_n(X)$ between M^n and U^n. Then U^n is a manifold in A and M^n came from $\Omega C_n(X,A)$.

(ii) Exactness at

$$\Omega C_n(X) \longrightarrow \Omega C_n(X,A) \longrightarrow \Omega C_{n-1}(A)$$

where the last map takes a representative $M^n, V^{n-1}, M^{n-2}, V^{n-3},...$ to the representative $V^{n-1}, V^{n-3},...$

The composite is clearly the zero map, so it remains only to take a representative of an element of the kernel; $M^n, V^{n-1}, M^{n-2}, V^{n-3},...$ with nullbordism $U^n, U^{n-2},...$ for $V^{n-1}, V^{n-3},..$ in A.

Construct

$$M^n \cup U^n, M^{n-2} \cup U^{n-2},..$$

where the unions are glued along common part-boundaries $V^{n-1}, V^{n-3},....$ We get $\partial M^n \cup U^n \ \cong BM^{n-2} \cup BU^{n-2} \ \cong B(M^{n-2} \cup U^{n-2})$ This is a representative for the same element of $\Omega C_n(X,A)$ as

$$M^n, V^{n-1}, M^{n-2}, V^{n-3},...$$

the equivalence provided by

$$(M^n \cup U^n) \times I, W^n, (M^{n-2} \cup U^{n-2}) \times I, W^{n-2},...$$

Thus $M^n, V^{n-1}, M^{n-2}, V^{n-3}, ...$ is the image of $M^n \cup U^n, M^{n-2} \cup U^{n-2}, ..$; an element of $\Omega C_n(X)$.

(iii) Exactness at

$$\Omega C_n(X, A) \longrightarrow \Omega C_{n-1}(A) \longrightarrow \Omega C_{n-1}(X)$$

Take $M^n, V^{n-1}, M^{n-2}, V^{n-3}, ...$, it maps to $V^{n-1}, V^{n-3}, ..$ in A, and then the same expression, in X.

This last expression is equivalent to the empty manifold, because $M^n, M^{n-2}, ...$ forms a null-bordism in X.

Now take $V^{n-1}, V^{n-3}, ..$ in A which is zero in X; so there's a $M^n, M^{n-2}, ...$ with $\partial M^n \cong BM^{n-2} \cup V^{n-1}, ..$

confirming that

$$M^n, V^{n-1}, M^{n-2}, V^{n-3}, ...$$

may be considered as a representative of an element of $\Omega C_n(X, A)$. □

4.5 Reduced cyclic bordism and excision.

Define **reduced cyclic bordism** $\widetilde{\Omega C}_n(X) = ker[\Omega C_n(X) \longrightarrow \Omega C_n(*)]$ where $*$ is a point (with circle action). This is equivalent to the definition $\widetilde{\Omega C}_n(X) = \Omega C_n(X, *)$ where $*$ is a fixed point (an invariant subset) of X, if X has a fixed point, that is. The equivalence of these definitions is apparent in the splitting of the long exact sequence for the pair $(X, *)$.

Proposition $\Omega_n(X, Y) \cong \widetilde{\Omega}_n(X/Y)$.

This is proved using a homotopy equivalence $X \cup CY \longrightarrow X/Y$, and transversality to the copy of Y half-way up the cone; $Y^{1/2}$.

One map is $\Omega_n(X, Y) \longrightarrow \widetilde{\Omega}_n(X \cup CY)$ by doubling; a representative for an element of $\Omega_n(X, Y)$ is a manifold with boundary, $(M, \partial M)$. This maps to the bordism class of $M \cup_{\partial M} M$ where the boundaries are identified, and mapped to $Y^{1/2}$; collars of ∂M in M map to the two halves of the cone.

The inverse map is $\widetilde{\Omega}_n(X \cup CY) \longrightarrow \Omega_n(X, Y)$ and this is constructed by making the singular manifold transverse to $Y^{1/2}$ and removing the portion of M mapping into the top half of the cone. The composite maps can be seen to be the identity.

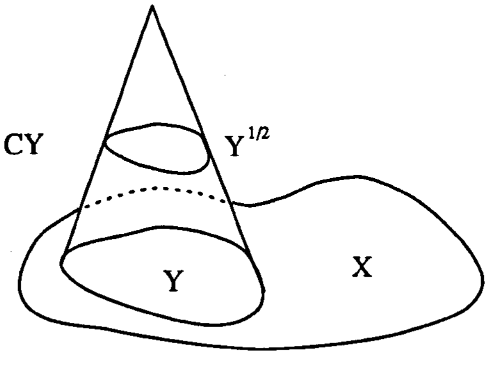

Figure 4.5.1 Excision in bordism.

Theorem Excision also holds in the cyclic case, $\Omega C_n(X,Y) \cong \tilde{\Omega} C_n(X/Y)$.

Proof Take a representative of an element of $\Omega C_n(X,Y)$

$$M^n, V^{n-1}, M^{n-2}, V^{n-3}, ..$$

and define

$$N^j = M^j \cup_{V^{j-1}} M^j$$

which has boundary

$$(\partial M^j - V^{j-1}) \cup_{\partial V^{j-1}} (\partial M^j - V^{j-1}) \cong B(M^{j-2}) \cup_{V^{n-3}} B(M^{j-2})$$
$$\cong B(M^{j-2} \cup_{V^{n-3}} M^{j-2}) \cong B(N^{j-2})$$

Using collars we map this doubled cyclic chain to $X \cup CY$.

Given a representative of an element of $\widetilde{\Omega C}_n(X/Y)$; $M^n, M^{n-2}, ..$ with null-bordism $W^{n+1}, W^{n-1}, ..$ in $\Omega C_n(*)$, we want to use the preimages of $Y^{1/2}$ and $X \cup Y^{\leq 1/2}$ in $M^n, M^{n-2}, ...$ We will use transversality to ensure that these are manifolds.

If M^n has ∂M^n mapping transversely to (X, A) then any homotopy necessary to make the map transverse on M^n can be chosen to leave the boundary fixed (because if a neighbourhood of $x \in \partial M$ maps transversely then immediately a neighbourhood of $x \in M$ maps transversely as well).

Also note that if $M^j \longrightarrow X \cup CY$ is transverse to $Y^{1/2}$ then the natural extension $BM^j \longrightarrow X \cup CY$ is transverse too. This is because, away from the spine, elements of the circle act as homeomorphisms, and at the spine, if a neighbourhood of $x \in M^n$ maps transversely then a neighbourhood of $x \in BM^n$ does too.

So now, we can assume in turn that $M^\epsilon, BM^\epsilon \cong \partial M^{\epsilon+2}, M^{\epsilon+2}, ...$ are transverse, giving preimages from $Y^{1/2}$ and $X \cup Y^{\leq 1/2}$ $V^{\epsilon-1}, V^{\epsilon+1}, ...$ and $U^\epsilon, U^{\epsilon+2}, ...$ ∂U^j is the preimage of $X \cup Y^{\leq 1/2}$ in $\partial M^j \cong BM^{j-2}$ with the preimage of $Y^{1/2}$ in M^j, so that's $BU^{j-2} \cup V^{j-1}$ and $U^n, V^{n-1}, U^{n-2}, V^{n-3}, ..$ has the structure of an element of the relative cyclic bordism group.

There are four checks that need to be made; each of these maps has to be well-defined under the equivalence of the domain group, and the composites each have to be the identity.

The map $\Omega C_n(X,Y) \longrightarrow \widetilde{\Omega C}_n(X/Y)$ is well-defined:

Take two equivalent representatives $M_1^n, V_1^{n-1}, ...M_2^n, V_2^{n-1}, ..$ with an equivalence given by

$$W^{n+1}, U^n, W^{n-1}, U^{n-2}, ...$$

satisfying

$$\partial W^{n+1} \cong M_1^n \cup M_2^n \cup BW^{n-1} \cup U^n, ..$$
$$\partial U^n \cong V_1^{n-1} \cup V_2^{n-1} \cup BU^{n-2}, ..$$

Glue the manifolds $W^j \cup W^j$ along the U^{j-1} part of their boundaries.

$$\partial(W^j \cup_{U^{j-1}} W^j)$$

$$\cong (M_1^{j-1} \cup M_2^{j-1} \cup BW^{j-2}) \cup_{\partial U^{j-1}} (M_1^{j-1} \cup M_2^{j-1} \cup BW^{j-2})$$
$$\cong (M_1^{j-1} \cup M_2^{j-1} \cup BW^{j-2}) \cup_{V_1^{j-2} \cup V_2^{j-2} \cup BU^{j-3}} (M_1^n \cup M_2^n \cup BW^{n-1})$$
$$\cong (M_1^{j-1} \cup_{V_1^{j-2}} M_1^{j-1}) \cup B(W^{j-2} \cup_{U^{j-3}} W^{j-2}) \cup (M_2^{j-1} \cup_{V_2^{j-2}} M_2^{j-1})$$

Thus the $W^j \cup_{U^{j-1}} W^j$ give an equivalence in $\widetilde{\Omega C}_n(X/Y)$ between the images of $M_1^n, V_1^{n-1}, ..$ and $M_2^n, V_2^{n-1}, ...$

The map $\widetilde{\Omega C}_n(X/Y) \longrightarrow \Omega C_n(X,Y)$ is well-defined:

Take two equivalent representatives $M_1^n, M_1^{n-2}, ..$ and $M_2^n, M_2^{n-2}, ...$ Let the equivalence be provided by $W^{n+1}, W^{n-1}, ...$ The images in $\Omega C_n(X,Y)$ are $N_1^n, V_1^{n-1}, ..$ and $N_2^n, V_2^{n-1}, ...$ Let K^{n+1} be the preimage of $X \cup Y^{\leq 1/2}$ in W^{n+1} and L^n be the preimage of $Y^{1/2}$ in $W^n + 1$. (We've taken the map on W^{n+1} transverse to $Y^{1/2}$; this is possible and within equivalence in $\Omega C_n(X,Y)$).

∂K^{n+1} is the union of the preimage of $X \cup Y^{\leq 1/2}$ in ∂W^{n+1} and the preimage of $Y^{1/2}$ in $W^n + 1$. This is $N_1^n \cup N_2^n \cup BK^{n-1} \cup L^n$, as required. ∂L^n is the preimage of $Y^{1/2}$ in $BW^{n-1} \cup M_1^n \cup M_2^n$ which is $BL^{n-2} \cup V_1^{n-1} \cup V_2^{n-1}$. Thus we have found an equivalence in $\Omega C_n(X,Y)$.

We can see that the composite $\Omega C_n(X,Y) \longrightarrow \widetilde{\Omega C}_n(X/Y) \longrightarrow \Omega C_n(X,Y)$ is the identity by observation that the maps in $\widetilde{\Omega C}_n(X/Y)$ are already transverse to $Y^{1/2}$.

The composite $\widetilde{\Omega C}_n(X/Y) \longrightarrow \Omega C_n(X,Y) \longrightarrow \widetilde{\Omega C}_n(X/Y)$ is the identity.

From $M^n, M^{n-2}, ..$ we get decompositions $M^j \cong N^j \cup_{V^{j-1}} (M^j - N^j)$ and the composite gives $N^n \cup_{V^{n-1}} N^n, ...$ Also, because $M^n \cong N^n \cup_{V^{n-1}} (M^n - N^n), ..$ is in the reduced group, there is a $W^{n+1}, ..$ as a null-bordism in $\Omega C(*)$. Consider

$$(N^n \times [-1,+1]) \cup ((M^n - N^n) \times [0,+1]) \cup (N^n \times [-1,0])$$

This has boundary $M^n \cup (N^n \cup_{V^{n-1}} N^n) \cup M^n$ where the first M^n maps are originally, and the second maps to the cone on Y, add a $M^n \times I$ to slide this map up to the point of the cone, and then add a W^{n+1} null-bordism at the point. This gives an equivalence between $M^n, M^{n-2}, ..$ and $N^n \cup_{V^{n-1}} N^n, ..$ in $\widetilde{\Omega C}_n(X/Y)$.□

Chapter 5. Equivariant bordism

The aim of this chapter is to provide a canonical isomorphism between cyclic bordism $\Omega C_n(X)$ and equivariant bordism $\Omega_n(ES^1 \times_{S^1} X)$, where X is a manifold with a circle action. This isomorphism will show that the shift long exact sequence of X is just the Gysin sequence of the bundle $ES^1 \times X \longrightarrow ES^1 \times_{S^1} X$.

5.1 A map from cyclic to equivariant bordism.

Recall the join model for ES^1; $\bigcup_{r=0}^{\infty}(S^1)^{r+1} \times \Delta^r$ under the equivalence relation generated by the following;

$$(\theta_1 - \epsilon, \theta_2, \theta_3, ., \theta_r, \theta_{r+1}, 0, t_1, t_2, ., t_{r-1}, t_r) \sim (\theta_1, \theta_2, \theta_3, ., \theta_r, \theta_{r+1}, 0, t_1, t_2, ., t_{r-1}, t_r)$$

$$(\theta_1 + \epsilon, \theta_2 - \epsilon, \theta_3, ., \theta_r, \theta_{r+1}, t_0, 0, t_2, ., t_{r-1}, t_r) \sim (\theta_1, \theta_2, \theta_3, ., \theta_r, \theta_{r+1}, t_0, 0, t_2, ., t_{r-1}, t_r)$$

$$(\theta_1, \theta_2 + \epsilon, \theta_3 - \epsilon, ., \theta_r, \theta_{r+1}, t_0, t_1, 0, ., t_{r-1}, t_r) \sim (\theta_1, \theta_2, \theta_3, ., \theta_r, \theta_{r+1}, t_0, t_1, 0, ., t_{r-1}, t_r)$$

$$\cdots$$

$$(\theta_1, \theta_2, \theta_3, ., \theta_r + \epsilon, \theta_{r+1} - \epsilon, t_0, t_1, t_2, ., t_{r-1}, 0) \sim (\theta_1, \theta_2, \theta_3, ., \theta_r, \theta_{r+1}, t_0, t_1, t_2, ., t_{r-1}, 0)$$

on $(S^1)^{r+1} \times \Delta^r$, and finally

$$(\theta_1, \theta_2, \theta_3, ., \theta_r + \theta_{r+1}, t_0, t_1, t_2, ., t_{r-1}) \sim (\theta_1, \theta_2, \theta_3, ., \theta_r, \theta_{r+1}, t_0, t_1, t_2, ., t_{r-1}, 0)$$

□

The free group action is given by

$$(\theta_1, \theta_2, \theta_3, ., \theta_r, t_0, t_1, t_2, ., t_{r-1})\alpha = (\theta_1, \theta_2, \theta_3, ., \theta_r + \alpha, t_0, t_1, t_2, ., t_{r-1})$$

Deduce the following model for $ES^1 \times_{S^1} X$;

$\bigcup_{r=0}^{\infty}(S^1)^r \times X \times \Delta^r$ under the equivalence relation generated by the following;

$$(\theta_1 - \epsilon, \theta_2, \theta_3, ..., \theta_r, x, 0, t_1, t_2, ..., t_{r-1}, t_r) \sim (\theta_1, \theta_2, \theta_3, ..., \theta_r, x, 0, t_1, t_2, ..., t_{r-1}, t_r)$$

$$(\theta_1 + \epsilon, \theta_2 - \epsilon, \theta_3, ..., \theta_r, x, t_0, 0, t_2, ..., t_{r-1}, t_r) \sim (\theta_1, \theta_2, \theta_3, ..., \theta_r, x, t_0, 0, t_2, ..., t_{r-1}, t_r)$$

$$(\theta_1, \theta_2 + \epsilon, \theta_3 - \epsilon, ..., \theta_r, x, t_0, t_1, 0, ..., t_{r-1}, t_r) \sim (\theta_1, \theta_2, \theta_3, ..., \theta_r, x, t_0, t_1, 0, ..., t_{r-1}, t_r)$$

$$\cdots$$

$$(\theta_1, \theta_2, \theta_3, ..., \theta_r + \epsilon, (-\epsilon)x, t_0, t_1, t_2, ..., t_{r-1}, 0) \sim (\theta_1, \theta_2, \theta_3, ..., \theta_r, x, t_0, t_1, t_2, ..., t_{r-1}, 0)$$

on $(S^1)^r \times X \times \Delta^r$, and

$$(\theta_1, \theta_2, \theta_3, ..., \theta_r x, t_0, t_1, t_2, ..., t_{r-1}) \sim (\theta_1, \theta_2, \theta_3, ..., \theta_r, x, t_0, t_1, t_2, ..., t_{r-1}, 0)$$

$ES^1 \times_{S^1} X$ has submanifolds L_1, L_2,...where

$$L_j = \{(\theta_1, \theta_2, ..., \theta_r, x, 0, 0, .., 0, t_j, .., t_r)\}$$

Each of these submanifolds is homeomorphic to another copy of $ES^1 \times_{S^1} X$ inside itself.

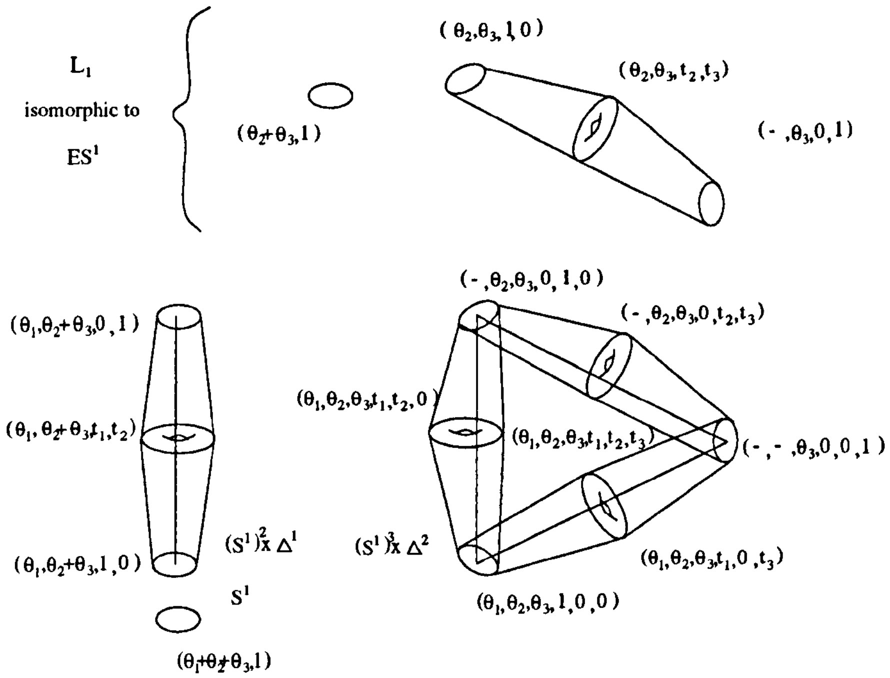

Figure 5.1.1 The manifold ES^1 and submanifold L_1.

First we have to construct a well-defined map from cyclic to equivariant bordism. An element of cyclic bordism is represented by a sequence of manifolds M^n, M^{n-2},.. all mapping into X. Given a map $M^{n-2j} \longrightarrow X$, we have

$$(S^1)^j \times M^{n-2j} \times \Delta^j \longrightarrow (S^1)^j \times X \times \Delta^j \longrightarrow ES^1 \times_{S^1} X$$

We will glue together the n-manifolds $(S^1)^j \times M^{n-2j} \times \Delta^j$ to give a closed n-manifold $\tilde{M}$ mapping into $ES^1 \times_{S^1} X$. The boundary of $(S^1)^j \times M^{n-2j} \times \Delta^j$ is made up of

$$(S^1)^j \times \partial M^{n-2j} \times \Delta^j$$

and $j+1$ copies of

$$(S^1)^j \times M^{n-2j} \times \Delta^{j-1}$$

First identify points in $(S^1)^{j+1} \times M^{n-2j-2} \times \Delta^j$ with points in $(S^1)^j \times BM^{n-2j-2} \times \Delta^j$, that is, points in $(S^1)^j \times \partial M^{n-2j} \times \Delta^j$.

Then, motivated by the equivalences in ES^1, identify points in each face by forgetting angles. More precisely, factor by the following relation on each $(S^1)^j \times M^{n-2j} \times \Delta^j$

$$(\theta_1, \theta_2, .., \theta_j, m, 0, t_1, .., t_j) \sim (\theta_1 + \alpha, \theta_2, .., \theta_j, m, 0, t_1, .., t_j)$$

$$(\theta_1, \theta_2, .., \theta_j, m, t_0, 0.., t_j) \sim (\theta_1 - \alpha, \theta_2 + \alpha, .., \theta_j, m, t_0, 0.., t_j)$$

$$(\theta_1, .., \theta_{j-1}, \theta_j, m, t_0, t_1, .., 0, t_j) \sim (\theta_1, .., \theta_{j-1} - \alpha, \theta_j + \alpha, m, t_0, t_1, .., 0, t_j)$$

and for points with $m = (\theta, \hat{m}) \in BM^{n-2j-2} = \partial M^{n-2j}$

$$(\theta_1, .., \theta_{j-1}, \theta_j, (\theta, \hat{m}), t_0, t_1, .., t_{j-1}, 0) \sim (\theta_1, .., \theta_{j-1}, \theta_j - \alpha, (\theta + \alpha, \hat{m}), t_0, t_1, .., t_{j-1}, 0)$$

After these identifications, the components $(S^1)^j \times M^{n-2j} \times \Delta^j$ are joined together by

$$(\theta_1, .., \theta_{j-1}, \theta_j, m, t_0, t_1, .., t_{j-1}, 0) \sim (\theta_1, .., \theta_{j-1}, (\theta_j, m), t_0, t_1, .., t_{j-1})$$

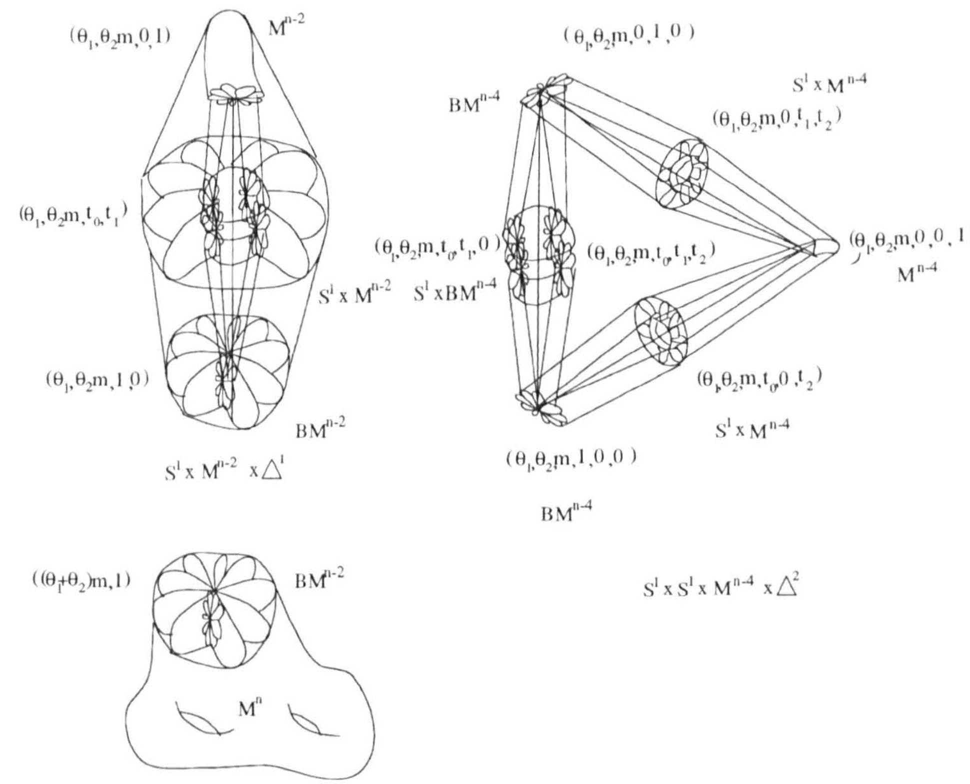

Figure 5.1.2 The construction of $\tilde{M}$.

Theorem Given representatives M^n, M^{n-2},.. of an element of cyclic bordism, the space $\tilde{M}$ constructed above is a manifold.

Proof Given a point in $\tilde{M}$, the neighbourhood of this point in $\tilde{M}$ is obtained from its neighbourhood in each $(S^1)^j \times M^{n-2j} \times \Delta^j$ after gluing by the relation

$$(\theta_1, .., \theta_{j-1}, \theta_j, m, t_0, t_1, .., t_{j-1}, 0) \sim (\theta_1, .., \theta_{j-1}, (\theta_j, m), t_0, t_1, .., t_{j-1})$$

Take a point in $(S^1)^j \times M^{n-2j} \times \Delta^j$. Write it as

$$(\theta_1, .., \theta_j, (\theta_{j+1}, (..(\theta_{k-1}, (\theta_k, m))..)), t_0, .., t_l, 0, .., 0)$$

Here m is in the interior of M^{n-2k}, so then

$$(\theta_k, m) \in BM^{n-2k} = \partial M^{n-2k+2} \subset M^{n-2k+2}$$

and

$$(\theta_{k-1}, (\theta_k, m)) \in BM^{n-2k+2} = \partial M^{n-2k+4} \subset M^{n-2k+4}$$

and so on. The neighbourhood of

$$(\theta_1, .., \theta_j, (\theta_{j+1}, (..(\theta_{k-1}, (\theta_k, m))..)), t_0, .., t_l, 0, .., 0)$$

in $(S^1)^j \times M^{n-2j} \times \Delta^j$ is a product of discs and possibly a cone on an annulus.

To justify this statement, I'll need to introduce some more notation; if a point m is in the boundary of a manifold, and h is in the interval $[0, 1)$ then $m + h$ is equal to m if $h = 0$ and otherwise is a point in the interior of the manifold, in a collar of the boundary. Consider the following maps of discs and $C(A)$ (the cone on an annulus) into $\tilde{M}$.

Take $j+1 \leq i \leq k-1$, if such exists. Map a disc to $(S^1)^j \times M^{n-2j} \times \triangle^j$ by

$$(h,\epsilon) \mapsto (\theta_1,..,\theta_j,(\theta_{j+1},(..(\theta_i+\epsilon,[(\theta_{i+1}-\epsilon,..(\theta_k,m)..)]+h))),t_0,..,t_l,0,..,0)$$

The cone on an annulus has points (ϵ,r,h) where $\epsilon \in S^1$ is forgotten if $r \in [0,1)$ and $h \in [0,1)$ are zero. If $l<j<k$ then we can map a cone on an annulus into $(S^1)^j \times M^{n-2j} \times \triangle^j$ by

$$(\epsilon,r,h) \mapsto (\theta_1,..,\theta_j,(\theta_{j+1},(..(\theta_{k-1}+\epsilon,[(\theta_k-\epsilon,m)+h])..)),t_0,..,t_l,0,..,r)$$

Take $l+1 \leq i \leq j-1$ then map a disc by

$$(h,\epsilon) \mapsto (\theta_1,..\theta_i+\epsilon,\theta_{i+1}-\epsilon,..,\theta_j,(\theta_{j+1},(..(\theta_{k-1},(\theta_k,m))..)),t_0,..,t_l,0,..,r,..,0)$$

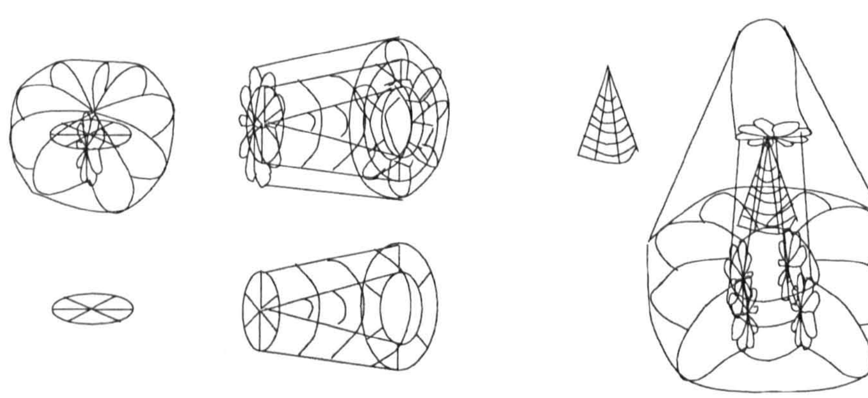

Figure 5.1.3 Disc and annulus-cone neighbourhoods in $\tilde{M}$.

There are two maps from the interval $[0,1)$ to consider; if $l=j$ (the last t_i is non-zero) then we can map the interval $[0,1)$ to $(S^1)^j \times M^{n-2j} \times \triangle^j$ by

$$h \mapsto (\theta_1,..,\theta_j,(\theta_{j+1},(..(\theta_{k-1},(\theta_k,m))..))+h,t_0,..,t_j)$$

If $k=j$ (the manifold point is in the interior of M^{n-2j}) then map the interval in by

$$r \mapsto (\theta_1,..,\theta_j,m,t_0,..,t_l,0,..,r)$$

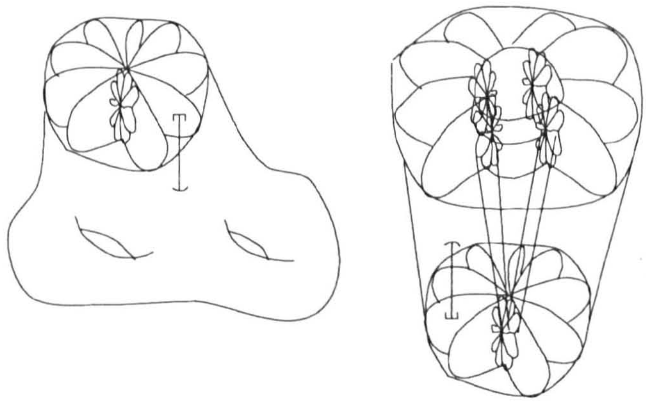

Figure 5.1.4 Interval neighbourhoods in $\tilde{M}$.

We can also map two higher-dimensional discs in; define a neighbourhood of m in M^{n-2k} by a map

$$D^{n-2k} \longrightarrow M^{n-2k}; x \mapsto m(x)$$

then we can map D^{n-2k} to $(S^1)^j \times M^{n-2j} \times \triangle^j$ by

$$x \mapsto (\theta_1, .., \theta_j, (\theta_{j+1}, (..(\theta_{k-1}, (\theta_k, m(x)))..)), t_0, .., t_l, 0, .., 0)$$

Finally, define a neighbourhood of $(\theta_1, .., \theta_l, t_0, .., t_l) \in (S^1)^l \times \triangle^l$;

$$y \mapsto (\theta_1(y), .., \theta_l(y), t_0(y), .., t_l(y))$$

Map D^{2l} to $(S^1)^j \times M^{n-2j} \times \triangle^j$ by

$$y \mapsto (\theta_1(y), .., \theta_l(y), \theta_{l+1} .., \theta_j, (\theta_{j+1}, (..(\theta_{k-1}, (\theta_k, m))..)), t_0(y), .., t_l(y), 0, .., 0)$$

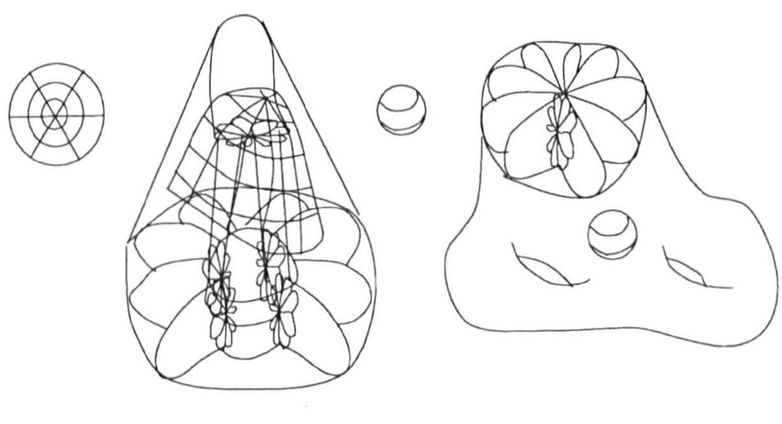

Figure 5.1.5 Higher-dimensional disc neighbourhoods in $\tilde{M}$.

The neighbourhood of a point in $(S^1)^j \times M^{n-2j} \times \Delta^j$ is a product of the above images. The identifications glue together the products to give an n-ball neighbourhood;

$$D^2 \times D^2 \times D^2 ... \times D^2 \times D^2 \times [0,1)$$
$$D^2 \times D^2 \times D^2 ... \times D^2 \times C(A)$$
$$D^2 \times D^2 \times D^2 ... \times C(A) \times D^2$$
$$...$$
$$D^2 \times D^2 \times C(A) ... \times D^2 \times D^2$$
$$D^2 \times C(A) \times D^2 ... \times D^2 \times D^2$$
$$C(A) \times D^2 \times D^2 ... \times D^2 \times D^2$$
$$[0,1) \times D^2 \times D^2 \times D^2 ... \times D^2 \times D^2$$

fit together to form D^{2k-2l}. □

The manifold $\tilde{M}$ has a natural map $\tilde{M} \longrightarrow ES^1 \times_{S^1} X$ because a representative of an element of $\Omega C_n(X)$ has not only the spaces M^{n-2j} but also maps of these spaces into X. Apply these maps to the co-ordinate m of $(\theta_1, .., \theta_r, m, t_0, .., t_r)$. This maps an element of $\tilde{M}$ to $ES^1 \times_{S^1} X$ and the process is well-defined after identification in $\tilde{M}$.

Theorem The map $[M^n, M^{n-2}, ..] \mapsto [\tilde{M}]$ is a well-defined map $\Omega C_n(X) \longrightarrow \Omega_n(ES^1 \times_{S^1} X)$.

Proof Given an equivalence $W^{n+1}, W^{n-1}, ..$ between $M_1^n, M_1^{n-2}, ..$ and $M_2^n, M_2^{n-2}, ..$, we can apply the same construction to get a manifold

$$\bigcup_{j=0}^{(n+1)/2} (S^1)^j \times W^{n-2j+1} \times \Delta^j$$

which has appropriate boundary. □

To see that the map $\Omega C_n(X) \longrightarrow \Omega_n(ES^1 \times_{S^1} X)$ is natural, consider its effect on the shift exact sequence.

5.2 The Gysin sequence.

In this section we will prove commutativity of the following diagram

$$\begin{array}{ccccccc} \Omega_n(X) & \longrightarrow & \Omega C_n(X) & \longrightarrow & \Omega C_{n-2}(X) & \longrightarrow & \Omega_{n-1}(X) \\ \downarrow & & \downarrow & & \downarrow & & \downarrow \\ \Omega_n(X) & \longrightarrow & \Omega_n(ES^1 \times_{S^1} X) & \longrightarrow & \Omega_{n-2}(ES^1 \times_{S^1} X) & \longrightarrow & \Omega_{n-1}(X) \end{array}$$

where the top long exact sequence is the shift long exact sequence introduced in 4.2, and the lower exact sequence is the Gysin exact sequence of the bundle $ES^1 \times X \longrightarrow ES^1 \times_{S^1} X$.

The Gysin sequence is proved using a long exact sequence of a pair, excision and the Thom isomorphism. These hold for oriented bordism groups and an oriented bundle. [BtD].

The first map in the Gysin exact sequence is induced from the inclusion of a copy of X in $ES^1 \times_{S^1} X$. The second map is given by making a manifold transverse to the codimension two submanifold L_1 of $ES^1 \times_{S^1} X$, and taking the preimage of L_1, giving a codimension 2 submanifold in the domain. The third map takes a singular manifold in $ES^1 \times_{S^1} X$ to the pullback over the total space $ES^1 \times X$ composed with a retraction of the total space to X.

Lemma The first square of the diagram commutes, that is, the first Gysin map is equal to the composite

$$\Omega_n(X) \longrightarrow \Omega C_n(X) \longrightarrow \Omega_n(ES^1 \times_{S^1} X)$$

Proof Take $[M^n] \in \Omega_n(X)$. Then $[M^m, \phi, ..] \in \Omega C_n(X)$ maps to $[\tilde{M}] = [M^n]$. The composite map leaves M^n mapping to some copy of X in $ES^1 \times_{S^1} X$. The Gysin map also does this, and if different copies of X are chosen, the maps are homotopic and so represent the same element of $\Omega_n(ES^1 \times_{S^1} X)$. □

Lemma The following composites are equal;

$$\Omega C_n(X) \longrightarrow \Omega_n(ES^1 \times_{S^1} X) \longrightarrow \Omega_{n-2}(ES^1 \times_{S^1} X)$$

and

$$\Omega C_n(X) \longrightarrow \Omega C_{n-2}(X) \longrightarrow \Omega_{n-2}(ES^1 \times_{S^1} X)$$

Proof The first map gives the manifold preimage of L_1 of the map $\tilde{M} \longrightarrow ES^1 \times_{S^1} X$. This map is already transverse to L_1 and the preimage of L_1 is $M^{n-2} \cup S^1 \times M^{n-4} \times \Delta^1$.... as required. □

Lemma The composite $\Omega C_n(X) \longrightarrow \Omega_n(ES^1 \times_{S^1} X) \longrightarrow \Omega_{n+1}(X)$ is equal to the map B in the ΩC shift exact sequence.

Proof Take $[M^n, M^{n-2}..]$ in $\Omega_n(X)$. It maps to $[\tilde{M}]$ in $\Omega_n(ES^1 \times_{S^1} X)$ The second map in the composite takes the pullback over $ES^1 \times X$ and maps it to X by collapsing ES^1 to a point. We want to show that this pullback is bordant to the singular manifold BM^n in X.

A point in $\tilde{M}$ can be expressed as

$$(\theta_1, .., \theta_k, m, t_o, .., t_k) \in (S^1)^k \times M^{n-2k} \times \Delta^k$$

where m lies in the interior of M^{n-2k}. The image in $ES^1 \times_{S^1} X$ is

$$(\theta_1, .., \theta_k, f(m), t_o, .., t_k)$$

and the preimage of this point in $ES^1 \times X$ consists of

$$(\theta_1, .., \theta_k, \alpha, -\alpha(f(m)), t_o, .., t_k)$$

Thus elements of the pullback are pairs

$$((\theta_1, .., \theta_k, m, t_o, .., t_k), (\theta_1, .., \theta_k, \alpha, -\alpha(f(m)), t_o, .., t_k))$$

Eliminate duplicated information in this expression by writing it as

$$(\theta_1, .., \theta_k, \alpha, m, t_o, .., t_k)$$

We need to show that the pullback is bordant to BM^n by presenting a manifold whose boundary is the disjoint union of these spaces. There is a surjective map from the pullback to BM^n, and the mapping cylinder provides the required bordism.

Map the pullback to BM^n by

$$(\theta_1, .., \theta_k, \alpha, m, t_o, .., t_k) \mapsto (-\alpha, m)$$

The preimage of a point $(-\alpha, m)$ in BM^n (with m in the interior of M^{n-2k}) consists of

$$(\theta_1, .., \theta_k, \alpha, m, t_o, .., t_k)$$

with identifications from $t_i = 0$,$0 \leq i \leq k-1$. For fixed α and m there are no identifications when t_k is zero. The preimage is in one-to-one correspondence with

$$(\theta_1, .., \theta_k, t_o, .., t_k) \in D^{2k}$$

Thus a point $(-\alpha, m)$ with m in the interior of M^{n-2k} has a cone on a $2k$-disc above it in the mapping cylinder.

There is a disc bundle around BM^{n-2k} in BM^{n-2k+2}. Above each point in the disc around $(-\alpha, m)$, there is a cone $C(D^{2k-2})$ in the mapping cylinder. Considering these disc bundles repeatedly we have constructed a neighbourhood out of

$$C(D^{2k}) \cup ([0,1) \times S^1 \times C(D^{2k-2}))$$
$$\cup([0,1) \times S^1 \times [0,1) \times S^1 \times C(D^{2k-4}))$$
$$\dots$$
$$\cup([0,1) \times S^1 \times ...[0,1) \times S^1 \times C(D^{2k-2r}))$$

To see how these are identified, take $(r, x) \in D^{2i-2}$, where $r \in [0,1]$ and $x \in S^{2i-3}$. There is a join map $g: S^1 \times I \times S^{2i-3} \longrightarrow S^{2i-1} \subset D^{2i}$ and

$$(0, \alpha, \lambda, (r, x)) \in [0,1] \times S^1 \times C(D^{2i-2})$$

is identified with

$$(\lambda, g(\alpha, r, x)) \in C(D^{2i})$$

These identifications join the cone neighbourhoods together to form a half-ball around $(-\alpha, m)$ in the base space BM^n.

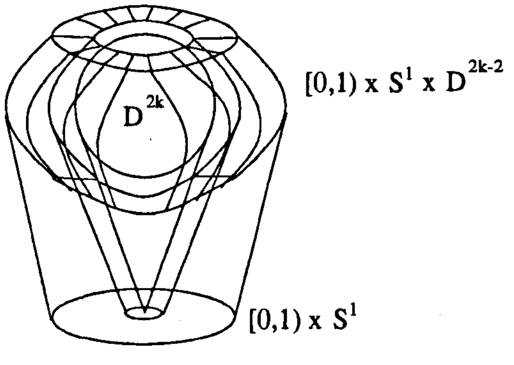

Figure 5.2.1 The half-ball neighbourhood in the mapping cylinder.

□

Next we will show that the map from cyclic bordism to equivariant bordism is an isomorphism by describing the inverse map.

5.3 A map from equivariant to cyclic bordism.

Recall the notation $L_i = \{(\theta_1, .., \theta_r, x, 0, .., 0, t_i, .., t_r)\}$ submanifolds of $ES^1 \times_{S^1} X$. So $L_0 = ES^1 \times_{S^1} X$. If f is a map from A to L_0, let $A_0 = A$ and make the map transverse to the submanifolds $..L_{i+1} \subset L_i \subset .. \subset L_0$, giving a submanifold sequence of preimages $..A_{i+1} \subset A_i \subset .. \subset A_0$ in A. $a_i \in A_i$ has $f(a_i) = (\theta_1, .., \theta_r, x, 0, .., 0, t_i, .., t_r)$. The identifications in the image space make information in $\theta_1, .., \theta_i$ redundant, and I'll write $f(a_i) = (.., \theta_{i+1}, .., \theta_r, x, 0, .., 0, t_j, .., t_r)$. The submanifold L_{i+1} in L_i has a normal disc bundle given by

$$(.., \theta_{i+1}, .., \theta_r, x, 0, .., 0, t_i, .., t_r) \mapsto (.., \theta_{i+2}, .., \theta_r, x, 0, .., 0, t_{i+1}, .., t_r)$$

where $0 \leq t_i \leq \epsilon$ for a fixed $0 < \epsilon < 1$. There is an induced normal disc bundle in A_i over A_{i+1}. Define ϵ_i so that, after homotopy, the map from the disc bundle D_i in A_i over A_{i+1} to the ϵ_i-disc bundle over L_{i+1} is a bundle map.

Define $Q_i = A_i \backslash D_i$; A_i with the open ϵ_i-bundle over A_{i+1} removed. The manifolds Q_i form an element of $\Omega C_n(X)$, that is, $\partial Q_i = B(Q_{i+1})$, but before we can prove this we need to make sense of the $B(Q_{i+1})$.

First notice that the image of Q_i in L_i is restricted to elements with t_i bounded away from zero. Letting t_i grow to 1 provides a retraction $L_i \backslash L_{i+1} \longrightarrow X$

$$(.., \theta_{i+1}, .., \theta_r, x, 0, .., 0, t_i, .., t_r) \mapsto (\theta_{i+1} + .. + \theta_r)x$$

So there are maps $Q_i \longrightarrow X$ given by the composite.

Points in the bundle over A_{i+1} are specified by their images in A_i and in L_{i+1}. Take $a \in A_{i+1}$, so $f(a) = (..\theta_{i+2}, .., \theta_r, x, 0, .., 0, t_{i+1}, .., t_r)$ and write the (unique) point in the ϵ_i-disc over a mapping to $(.., \theta_{i+1}, \theta_{i+2}, .., \theta_r, x, 0, .., 0, t_i, t_{i+1}, .., t_r)$ as

$$(a, (.., \theta_{i+1}, \theta_{i+2}, .., \theta_r, x, 0, .., 0, t_i, t_{i+1}, .., t_r))$$

The boundary of Q_i consists of points

$$(a, (.., \theta_{i+1}, \theta_{i+2}, .., \theta_r, x, 0, .., 0, \epsilon, t_{i+1}, .., t_r))$$

It has a circle action, on the θ_{i+1} co-ordinate, with respect to which the map to X is equivariant.

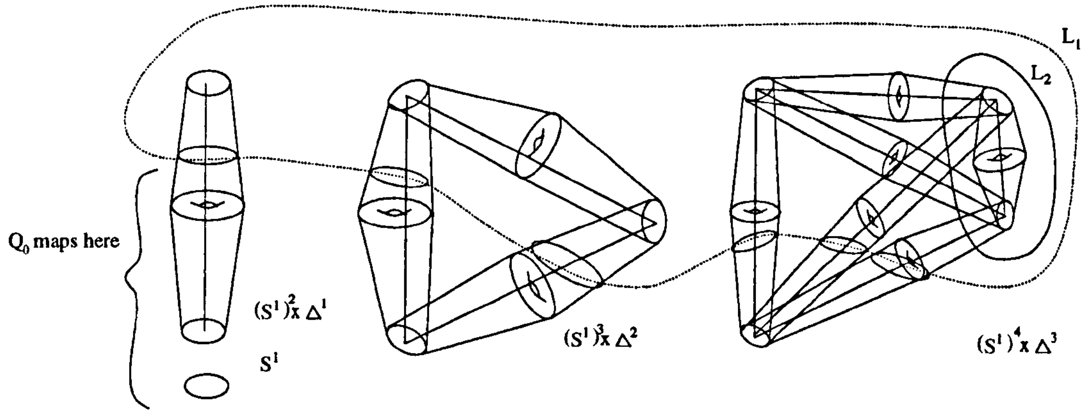

Figure 5.3.1 The preimages Q_i.

Theorem Given a map $A \longrightarrow ES^1 \times_{S^1} X$, the sequence $[Q_0, Q_1, ..]$ constructed above represents an element of $\Omega C_n(X)$.

Proof $BQ_i = \frac{(Q_i \times S^1)}{\sim}$ where $q \in \partial Q_i$ has $(q, \alpha) \sim (\epsilon q, \alpha - \epsilon)$. The homeomorphism $BQ_i \longrightarrow \partial Q_{i-1}$ takes

$$(q, \alpha) \mapsto (\hat{q}, (.., \alpha, \theta_{i+1}, .., \theta_r, x, 0, , 0, \epsilon, \hat{t_i}, .., \hat{t_r}))$$

where

$$f(q) = (.., \theta_{i+1}, .., \theta_r, x, 0, .., 0, t_i, t_{i+1}, .., t_r) \quad t_i \geq \epsilon$$

$$\hat{t_i} = \frac{t_i - \epsilon}{(1 - \epsilon)^2} \quad \hat{t_j} = \frac{t_j}{(1 - \epsilon)^2}$$

and $\hat{q}$ is equal to q unless q lies in the disc bundle over A_{i+1}, whose radius must lie between 1 and ϵ, in which case $\hat{q}$ is obtained by mapping the radii $[1, \epsilon]$ linearly to $[1, 0]$. This rescaling ensures that simplex co-ordinates always add up to 1, taking extremal values in the image if and only if they did in the domain. This map is welldefined, if $q \in \partial Q_i$ then $t_i = \epsilon$, $\hat{t_i} = 0$, $\hat{q} \in A_i$ and $\hat{\epsilon q} = \hat{q}$, so

$$(\hat{\epsilon q}, (.., \alpha - \epsilon, \theta_{i+1} - \epsilon, .., \theta_r, x, 0, .., 0, \epsilon, \hat{t_i}, .., \hat{t_r}))$$
$$= (\hat{q}, (.., \alpha, \theta_{i+1}, .., \theta_r, x, 0, , 0, \epsilon, \hat{t_i}, .., \hat{t_r}))$$

as required.

The inverse map is as follows; given $q \in \partial Q_{i-1}$ we have

$$f(q) = (.., \theta_i, .., \theta_r, x, 0, .., 0, \epsilon, t_i, .., t_r)$$

and an $a \in A_i$ with $f(a) = (.., \theta_{i+1}, .., \theta_r, x, 0, .., 0, \hat{t}_i, .., \hat{t}_r)$. If $t_i > 0$ then a can be pushed away from A_{i+1} giving an element of Q_{i+1}, by mapping $(0, 1] \longrightarrow (\epsilon, 1]$. The required element of BQ_i is represented by $(\theta_i, \hat{a})$. If $t_i = 0$ then the same procedure is carried out, once a value has been chosen for θ_i, t_i can be increased from zero to ϵ. Had a different value been chosen; $\theta_i + \alpha$; then θ_{i+1} would have been $\theta_{i+1} - \alpha$ and $\hat{a}$ would have been $-\alpha\hat{a}$. We would have got $(\theta_i + \alpha, -\alpha\hat{a})$. But this is identified with $(\theta_i, \hat{a})$ in BQ_i. □

5.4 Theorem. The maps between $\Omega C_n(X)$ and $\Omega_n(ES^1 \times_{S^1} X)$ defined in 5.1 and 5.3 are inverse isomorphisms.

Proof To prove that the composite from $\Omega C_n(X)$ to itself is the identity map, take $[M^n, M^{n-2}, ..] \in \Omega C_n(X)$ and construct the map $\tilde{M} \longrightarrow ES^1 \times_{S^1} X$ as in 5.3. Recall that $\tilde{M}$ consists of points $(\theta_1, .., \theta_k, m, t_0, .., t_k)$ where m lies in M^{n-2k}, under certain equivalences. To find the image of $[\tilde{M}]$ in $\Omega_n(ES^1 \times_{S^1} X)$, we need to make $\tilde{M} \longrightarrow ES^1 \times_{S^1} X$ transverse to the submanifolds L_i. But $\tilde{M}$ is already transverse to these manifolds because around

$$(..\theta_{i+1}, .., \theta_k, m, 0, .., 0, t_i, .., t_k) \in \tilde{M}$$

mapping to L_i, there is a disc

$$(r, \alpha) \mapsto (..\alpha, \theta_{i+1}, .., \theta_k, m, 0, .., 0, r, t_i, .., t_k) \in \tilde{M}$$

which maps onto the disc around

$$(..\theta_{i+1}, .., \theta_k, f(m), 0, .., 0, t_i, .., t_k) \in L_i \subset L_{i-1}$$

Define A_i to be the submanifold of $\tilde{M}$ mapping to L_i

$$A_i = \{(..\theta_{i+1}, .., \theta_k, m, 0, .., 0, t_i, .., t_k)\}$$

and

$$D_i = \{(..\theta_{i+1}, .., \theta_k, m, 0, .., 0, t_i, .., t_k) : t_i \in [0, \epsilon)\}$$

This is an open disc neighbourhood of A_{i+1} in A_i.

$$Q_i = \{(..\theta_{i+1}, .., \theta_k, m, 0, .., 0, t_i, .., t_k) : t_i \in [\epsilon, 1]\}$$

The boundary of Q_i has a circle action (on the θ_{i+1} co-ordinate) and we have

$$BQ_i \cong \partial Q_{i-1}$$

The image of $[\tilde{M}]$ in $\Omega C_n(X)$ is $[Q_0, Q_1, ..]$.

To show that $[Q_0, Q_1, ..] = [M^n, M^{n-2}, ..] \in \Omega C_n(X)$ we need sequences of manifolds W_i and V_i with

$$\partial V_i \cong (\partial M^{n-2i} \sqcup \partial Q_i) \cong (BM^{n-2i-2} \sqcup Q_{i+1})$$

$$\partial W_i \cong M^{n-2i} \cup V_i \cup Q_i$$

$$V_i \cong BW_{i+1}$$

Define

$$W_i = \{(..\theta_{i+1}, .., \theta_k, m, 0, .., 0, t_i, .., t_k, \lambda) : \lambda \in [\epsilon, 1], t_i \in [\lambda, 1]\} \subset \tilde{M} \times I$$

and

$$V_i = \{(..\theta_{i+1}, .., \theta_k, m, 0, .., 0, \lambda, t_{i+1}, , .., t_k, \lambda) : \lambda \in [\epsilon, 1], k > i\}$$

Then

$$\partial V_i = \{(..\theta_{i+1}, .., \theta_k, m, 0, .., 0, \epsilon, t_{i+1}, , .., t_k, \epsilon\}$$
$$\cup\{(..\theta_{i+1}, .., \theta_k, m, 0, .., 0, 1, 0, .., 0, 1)\}$$

$$\cong \partial Q_i \sqcup BM^{n-2i-2}$$

and

$$\partial W_i = \{(..\theta_{i+1},..,\theta_k,m,0,..,0,t_i,..,t_k,\epsilon) : t_i \in [\epsilon,1]\}$$
$$\cup\{(..\theta_{i+1},..,\theta_k,m,0,..,0,1,0,..,0,1)\}$$
$$\cup\{((..\theta_{i+1},..,\theta_k,m,0,..,0,\lambda,t_{i+1},..,t_k,\lambda) : \lambda \in [\epsilon,1]\}$$
$$\cong Q_i \cup M^{n-2i} \cup V_i$$

Finally,

$$BW_i = \{(..\theta_{i+1},..\theta_k,m,0,..,0,t_i,..,t_k,\lambda,\alpha)\}$$

with $\lambda \in [\epsilon,1]$ and $t_i \in [\lambda,1]$ with identifications on $V_i \times S^1$

$(..\theta_{i+1},..\theta_k,m,0,..,0,\lambda,t_{i+1},..,t_k,\lambda,\alpha) \sim (..\theta_{i+1}+\alpha,..\theta_k,m,0,..,0,\lambda,t_{i+1},..,t_k,\lambda,0)$

The required homeomorphism from BW_i to takes

$$(..\theta_{i+1},..\theta_k,m,0,..,0,t_i,..,t_k,\lambda,\alpha) \mapsto (..,\alpha,\theta_{i+1},..\theta_k,m,0,..,0,\lambda,\hat{t_i},..,\hat{t_k},\lambda)$$

The hats indicate scaling; $t_i \in [\lambda,1]$ is rescaled to $\hat{t_i} \in [0,1]$ and the other t_j are rescaled to ensure the sum of co-ordinates remains at 1.

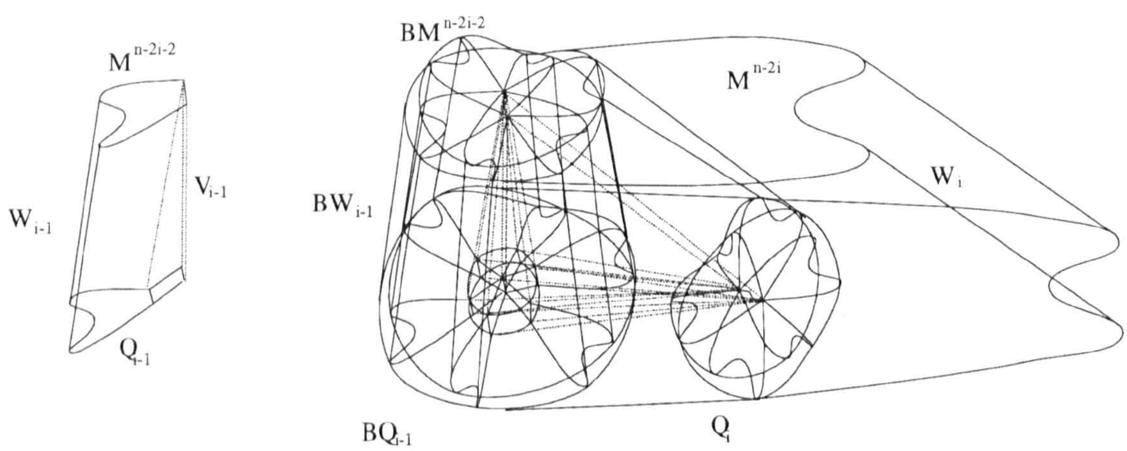

Figure 5.4.1 The composite on $\Omega C_n(X)$ is the identity.

This completes the proof that

$$\Omega C_n(X) \longrightarrow \Omega_n(ES^1 \times_{S^1} X) \longrightarrow \Omega C_n(X)$$

is the identity map.

Now consider the other composite, from $\Omega_n(ES^1 \times_{S^1} X)$ to itself. After homotopy, a map $f: A \longrightarrow ES^1 \times_{S^1} X$ is transverse to the L_i, with preimages A_i, discbundles D_i around A_{i+1} in A_i mapping by a bundle map to bundles around L_{i+1}. The complement $A_i \backslash D_i$ is called Q_i. Let $\phi_i: D_i \longrightarrow A_{i+1}$ be the bundle projection map.

Take a point $a \in A$ mapping to

$$(..\theta_{i+1},..,\theta_k,x,0,..,0,t_i,..,t_k)$$

Either $t_i \geq \epsilon_i$, in which case $a \in Q_i$ or $t_i \leq \epsilon_i$ and $\phi_i(a) \in A$ maps to

$$(..\theta_{i+2},..,\theta_k,x,0,..,0,\hat{t_{i+1}},..,\hat{t_k})$$

where the hats denote rescaling of simplex co-ordinates keeping the sum equal to 1; $\hat{t_j} = t_j/(1-t_i)$. For the rest of the proof I will supress such scaling moves.

Either $t_{i+1} \geq \epsilon_{i+1}$ and $\phi_i(a) \in Q_{i+1}$ or we can repeat this process, eventually finding a j with

$$\phi_j(\phi_{j-1}..\phi_{i-1}(\phi_i(a))..) \in Q_{j+1}$$

The boundary of Q_j is homeomorphic to BQ_{i+1} and so $(0,\phi_j(\phi_{j-1}..\phi_{i-1}(\phi_i(a))..))$ defines a point in Q_{i+1}.

The map $\Omega_n(ES^1 \times_{S^1} X) \longrightarrow \Omega C_n(X)$ takes the sequence $Q_0, Q_1,..$ to a manifold $\tilde{Q}$ mapping to X. Define a map ξ from A to $\tilde{Q}$ by

$$\xi(a) = (..\theta_{i+1},..,\theta_j,..,\theta_k,(0,(0,..(0,(\phi_j(\phi_{j-1}..\phi_{i-1}(\phi_i(a))..)))..)),0,..,0,t_i,..,t_k)$$

There are sufficient zeros in the expression $(0,(0,..(0,(\phi_j(\phi_{j-1}..\phi_{i-1}(\phi_i(a))..)))..))$ to turn $\phi_j(\phi_{j-1}..\phi_{i-1}(\phi_i(a))..) \in Q_{j+1}$ into an element of Q_k. This map is injective, well-defined (check where $t_i = \epsilon_i$) and is a homeomorphism from A to $\tilde{Q}$.

To show that A and $\tilde{Q}$ represent equal elements of $\Omega_n(ES^1 \times_{S^1} X)$, it is enough to show that after identifying the spaces with the above homeomorphism, the maps to $ES^1 \times_{S^1} X$ are homotopic. The map $\tilde{Q} \longrightarrow X$ has

$$\xi(a) \mapsto (..\theta_{i+1},..,\theta_j,..,\theta_k,f(0,(0,..(0,(\phi_j(\phi_{j-1}..\phi_{i-1}(\phi_i(a))..)))..)),0,..,0,t_i,..,t_k)$$

The maps f and

$$a \mapsto f(0,(0,..(0,(\phi_j(\phi_{j-1}..\phi_{i-1}(\phi_i(a))..)))..))$$

are homotopic, we have just collapsed some disc bundles in the second case. □

There is a map $\Omega_n(X) \longrightarrow H_n(X)$ using the fundamental cycle of an oriented manifold,

$$z_M \in S_n(M^n, \partial M^n)$$

The same construction gives a map from cyclic bordism to cyclic homology, and we get a commutative diagram

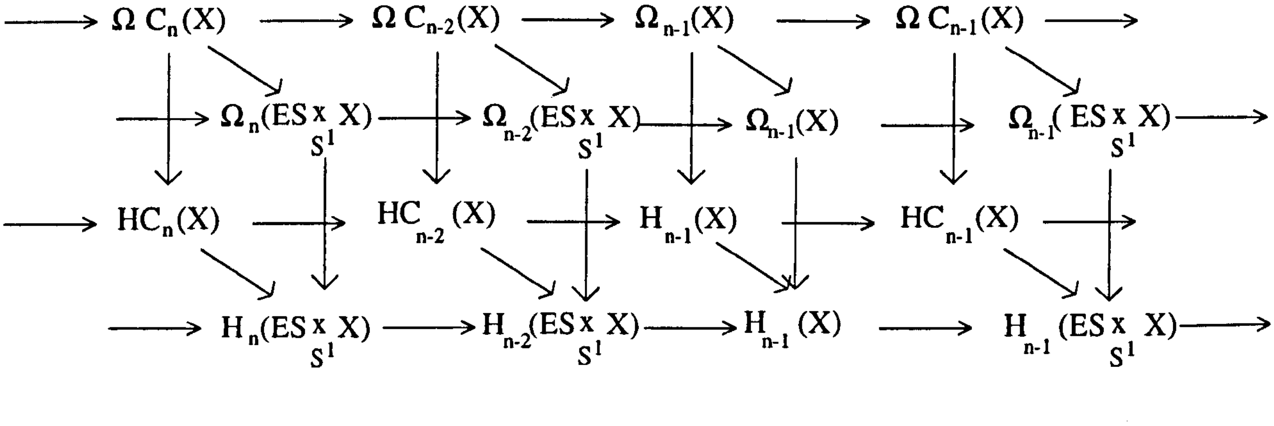

Figure 5.4.2 The shift and Gysin exact sequences.

in which all the diagonal maps are canonical isomorphisms.

The representation of a class in $HC_n(X)$ from $\Omega C_n(X)$ is equivalent to the representation of a class in $H_n(ES^1 \times_{S^1} X)$ from $\Omega_n(ES^1 \times_{S^1} X)$. The representation of ordinary homology by bordism is discussed in [T] and [BD].

5.5 Periodic theories.

In [JDSJ2], Jones showed a fixed point theorem for periodic homology, based on complex-valued de-Rham cohomology. Define completed periodic homology to be the inverse limit of the sequence

$$..HC_{*+2} \xrightarrow{shift} HC_* \xrightarrow{shift} HC_{*-2}...$$

Theorem If X is a smooth compact manifold with a smooth regular circle action and F is the submanifold of fixed points in X then

$$HP_*(X;\mathbb{Q}) \cong HP_*(F;\mathbb{Q})$$

In [BRS] the authors define a manifold-with-coefficients. Given a group presentation, a manifold with coefficients from that group is a manifold with a codimension 1 singular set. Each component of the manifold away from the singular set is labelled by a generator of the group and each component of the singular set is labelled by a relation. The leaves of the non-singular set meeting a given singular point are labelled and oriented so that the relation at the singular point can be read off the leaves.

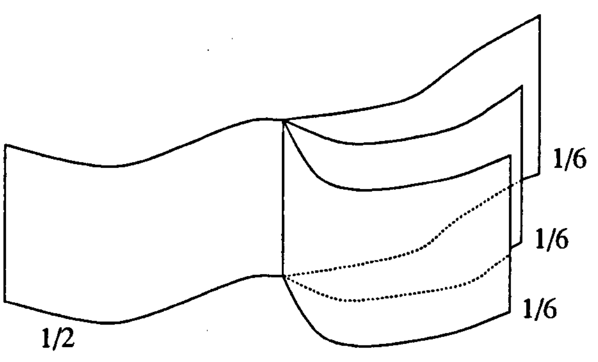

Figure 5.5.1 The singular set in a $\mathbb{Q}$-manifold.

We can now define diffeomorphisms of $\mathbb{Q}$-manifolds, $\mathbb{Q}$-manifolds with boundary and **bordism with coefficients**, $\Omega_n(X;\mathbb{Q})$, for any space X. In fact the singular sets in a $\mathbb{Q}$-manifold can all be resolved

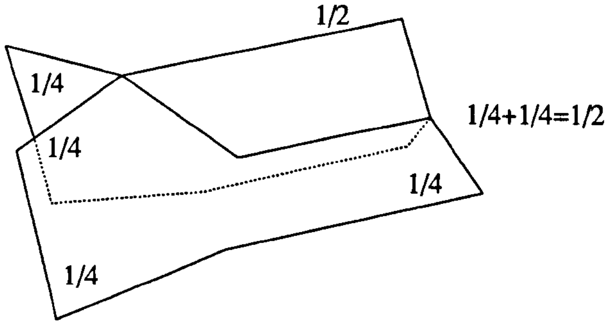

Figure 5.5.2 Resolving singularities in a $\mathbb{Q}$-manifold.

and we deduce that

$$\Omega_n(X;\mathbb{Q}) \cong \Omega_n(X) \otimes \mathbb{Q}$$

Next, define a $\mathbb{Q}$-manifold with a circle actions (actions have the singular set invariant) and check that if M is a $\mathbb{Q}$-manifold whose boundary has a circle action then BM is a $\mathbb{Q}$-manifold. Now we can use **cyclic bordism with coefficients.** Essentially all we need to do is replace the notion of 'manifold' by the notion of 'manifold with coefficients'. The results on cyclic bordism carry through to results with coefficients. The shift map

$$\Omega C_{n+2}(X,\mathbb{Q}) \longrightarrow \Omega C_n(X,\mathbb{Q})$$

gives a definition of **periodic bordism with coefficients** $\Omega P_*(X;\mathbb{Q})$ as the inverse limit.

Using results about regular actions of Lie groups [B] and facts about oriented bordism from [CW], we can prove the following theorem on periodic bordism and fixed points.

Theorem If X is a smooth compact manifold with a smooth regular circle action and F is the submanifold of fixed points in X then

$$\Omega P_*(X;\mathbb{Q}) \cong \Omega P_*(F;\mathbb{Q})$$

This completes the work on cyclic bordism.

Chapter 6. Racks, definitions and examples

In this chapter we begin by introducing racks with some examples, some algebra and rack tables. In the second section, the connection with framed oriented links is described, when we define the rack of a link. This construction gives a perfect invariant of non-split (irreducible) framed links, which we could use if we knew how to determine the isomorphism type of a rack from its presentation. We can, however, weaken the invariant to give invariants which are easier to use. The Alexander invariant is a good example of a classical invariant derived from the rack of a knot, and this is investigated in section three. Finally, in section four, we define the classifying space of a rack, which is a cubical space similar to the simplicial classifying space of a category, or a group, as defined by Segal [S1]. The main reference for this work is [FR]. See also [HR], [DJ], and for a general review of knot theory see [DR]

6.1 Definitions and examples.

Definitions [FR]

A rack is a set equipped with a binary operation, written exponentially,

$$R \times R \longrightarrow R; (a,b) \mapsto a^b$$

satisfying two axioms;

R1 for each b in R the map $\theta_b : R \longrightarrow R; a \mapsto a^b$ is a bijection

and R2 $(a^b)^{(c^b)} = (a^c)^b$ for all $a,\ b,\ c \in R$

Notation: The inverse map of θ_b is written

$$\theta_b^{-1}(a) = a^{\bar{b}}$$

Substituting $d = a^b$ into the rack identity gives the second form of the rack identity;

$$d^{(c^b)} = ((d^{\bar{b}})^c)^b$$

Writing operators as b^{-1} for $\bar{b}$ and b^{+1} for b, this last rack identity allows us to write every element of the rack (non-uniquely) as

$$a^{b_1^{\epsilon_1} \dots b_r^{\epsilon_r}}$$

where ϵ_i are ± 1 and $a,\ b_i$ are rack elements. The omitted brackets here would be

$$(..((a^{b_1^{\epsilon_1}})^{b_2^{\epsilon_2}})..)^{b_r^{\epsilon_r}}$$

Each rack has two groups associated to it; the associated group and the operator group. The **associated group** of R, called $Asgp(R)$, is generated by the rack elements with relations $d \sim b^{-1}cb$ whenever $d = c^b$ in the rack. The **operator group** $Opgp(R)$ is a quotient of the associated group, with relations defined by $a \sim b$ whenever a and b are equivalent as operators; $c^a = c^b$ for all c in the rack. A **quandle** is a rack with $a^a = a$ for all elements a.

Examples of racks

Permutation racks. If ρ is a permutation of the symbols $\{1, 2.., n\}$ then define a rack structure on this set by

$$i^j = \rho(i)$$

When ρ is the identity permutation this gives **the trivial rack** T_n, and when ρ is an n-cycle then we get **the cyclic rack** with n elements C_n. The operator group of a permutation rack is the trivial group, and the associated group is free abelian on the orbits of the permutation. We can see this by putting $i = j$ into $i^j = j^{-1}ij = \rho(i)$. This identifies elements of an orbit, and then $i^j = j^{-1}ij = \rho(i)$ becomes $[j]^{-1}[i][j] = [i]$ showing commutativity of the orbits.

Conjugation racks. If G is a group, define $a^b = b^{-1}ab$. The resulting rack is the conjugation rack of G, written G_{conj} or $conj(G)$. If G is abelian then G_{conj} is a trivial rack. There is an adjunction giving a one-to-one correspondence between the group homomorphisms from the associated group of R to G and rack homomorphisms from R to the conjugation rack of G.

Core racks. If G is a group, define $a^b = ba^{-1}b$.

Coset racks. Given a group G and subgroups $H_1, H_2, ..,$ elements $g_1, g_2, ..$ such that for all i, j, there exists a normal subgroup of G; N_{ij}; with

$$[H_j, g_j] \subset N_{ij} \subset H_i$$

then the coset rack $[G, H_1, H_2, .., g_1, g_2, ..]$ has elements xH_i for $x \in G$ subject to

$$(w_i H_i)^{(v_j H_j)} = v_j g_j \bar{v}_j w H_i$$

Coset racks are studied extensively in [HR], generalising the following result from [DJ].

Lemma An arbitrary quandle can be represented as a rack $[G, H_1, H_2, .., g_1, g_2, ..]$ for some subgroups H_i and elements g_i belonging to the centralizer of H_i.

If S is an abelian group, with an isomorphism $\mu: S \longrightarrow S$ and a homomorphism $\lambda: S \longrightarrow S$ with $\mu\lambda = \lambda\mu$ and $\lambda(\mu + \lambda - 1) = 0$ then $a^b = \mu a + \lambda b$ gives a rack structure on S.

The Alexander rack. Let $S = \mathbb{Z}[t, t^{-1}]$, μ multiplication by t, λ multiplication by $(1 - t)$.

A finite Alexander quotient. Let $S = \mathbb{Z}_n$, μ multiplication by a, λ multiplication by $(1 - a)$ where a is coprime to n.

The dihedral rack. Let $S = \mathbb{Z}_n$, where n is odd, μ multiplication by 2, λ multiplication by -1. This is a subrack of the conjugation rack of the dihedral group D_{2n} and it is an example of a finite Alexander quotient.

The reflection rack. Let S be $\mathbb{R}^n$ and $\mu(x) = 2x, \lambda(x) = -x$.

The sphere rack. Take x and y in S^{n-1}. Consider the line through the origin and y in $\mathbb{R}^n$ and reflect the point x in that line. The resulting point on the sphere in x^y. Alternatively, we can describe x^y as the point on the geodesic through x and y which is the same distance away from y as x, but in the opposite direction.

The projective rack is obtained by identifying antipodal points on the sphere rack.

For finite racks we can draw a rack table, for example

	a	b
a	a	a
b	b	b

Figure 6.1.1 The rack table of C_2.

This is the rack $conj\mathbb{Z}_2$. The group is abelian, so $x^y = x$ for all x, y. Alternatively, it may be viewed as the trivial rack on two elements, the cyclic rack on two elements or the zero-dimensional sphere rack.

In a dihedral group, D_{2i}, say, with elements $\{1, a, b, ab, .., b^{i-1}, ab^{i-1}\}$ subject to relations $a^2 = b^i = 1$ and $aba = b^{-1}$, we have conjugations of the form

$$(b^i)^{(b^j)} = b^i$$

$$(b^i)^{(ab^j)} = b^{-i}$$

$$(ab^i)^{(b^j)} = ab^{i+2j}$$

$$(ab^i)^{(ab^j)} = ab^{2j-i}$$

so the rack table of $conj D_6$ looks like

	1	b	b^2	a	ab	ab^2
1	1	1	1	1	1	1
b	b	b	b	b^2	b^2	b^2
b^2	b^2	b^2	b^2	b	b	b
a	a	ab^2	ab	a	ab^2	ab
ab	ab	a	ab^2	ab^2	ab	a
ab^2	ab^2	ab	a	ab	a	ab^2

Figure 6.1.2 The rack table of $conj D_6$.

The dihedral rack would have only three elements, and its rack table is the bottom right-hand quarter of this one.

Tables of permutation racks look like this:

	a	b	c	d	e	f	g
a	b	b	b	b	b	b	b
b	g	g	g	g	g	g	g
c	f	f	f	f	f	f	f
d	d	d	d	d	d	d	d
e	e	e	e	e	e	e	e
f	c	c	c	c	c	c	c
g	a	a	a	a	a	a	a

Figure 6.1.3 The table of a permutation rack.

A **rack homomorphism** $\theta: R \longrightarrow S$ has $\theta(a^b) = \theta(a)^{\theta(b)}$. An equivalence relation on rack R with the property that

$$a^b \sim c^d \text{ whenever } a \sim c \text{ and } b \sim d$$

is called a **congruence** and we can construct the **quotient rack**. Elements of the quotient rack are equivalence classes, with the binary operation defined by $[a]^{[b]} = [a^b]$. The **free rack** on n symbols $\{a_1,..,a_n\}$ is the set of a_i^v where v lies in the free group on $\{a_1,..,a_n\}$ and the rack identity has $(a^v)^{(b^w)} = a^{vw^{-1}bw}$. The rack is written $FR < a_1,..,a_n >$. A **rack presentation** has generators and relations: build up the free rack on the generators and find the smallest equivalence relation satisfying the relations and the above property. The quotient rack gives the rack of the presentation. Rack presentations are discussed in detail in [FR].

The **free product** of two racks has a presentation with generating set equal to the disjoint union of the racks and relations corresponding to equations $a^b = c$ in either of the two racks. This gives the categorical sum. Another product; the **cartesian product**; has elements from the cartesian product of the sets with rack structure $(a,p)^{(b,q)} = (a^b, p^q)$. This is the categorical product.

6.2 Racks from links.

In [FR], the authors give a definition of the (fundamental) rack of an arbitrary tranversely oriented framed codimension 2 link. Here we will concentrate on codimension 2 links in S^3, where orientation of S^3 and orientation of a link give a transverse orientation (an orientation on the disc bundle). Equivalence of framed links is under maps which preserve the transverse orientation and framing. If L is a framed oriented link, we can think of the framing characterised by a ribbon with one side equal to L, and we can define the rack of the link as follows. Draw a framed diagram of the link and label the arcs of the diagram with symbols $a_1, a_2, .., a_n$. These will generate the rack of the link, and the relations come from the crossings as follows

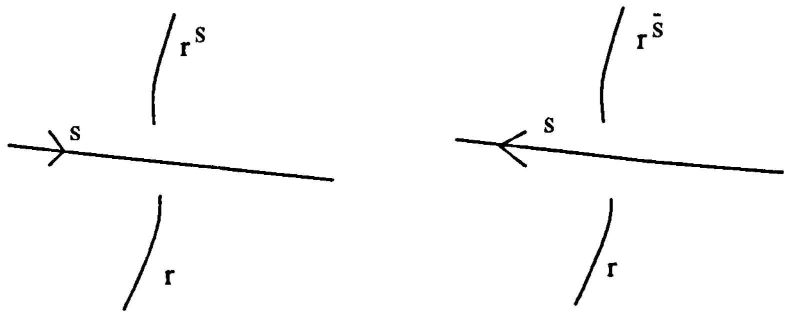

Figure 6.2.1 The relators of the rack of a link.

Note that the orientation of the underpass is irrelevant when writing down these relations. The rack of the trivially framed unknot is the trivial rack with one element. If the framing is non-trivial, we have a diagram

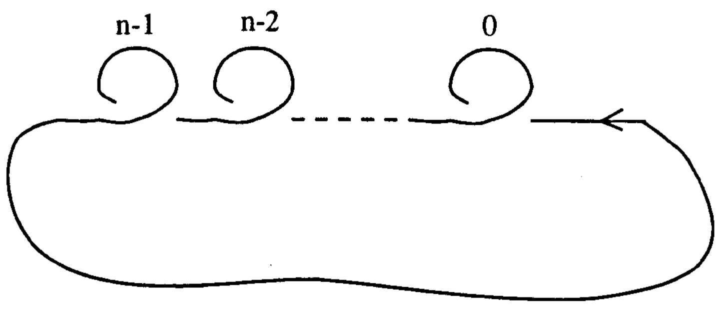

Figure 6.2.2 The rack of a twisted unknot.

giving relations $0^1 = 1, 1^2 = 2, .., (n-1)^0 = 0$. The rack of this link is the cyclic rack on n elements because

$$i^j = i^{((j-1)^j)} = i^{\bar{j}(j-1)j}$$

so

$$i = i^{\bar{j}(j-1)}, \quad i^{\overline{(j-1)}} = i^{\bar{j}}$$

$$i^{(j-1)} = i^j, \quad i^j = i^k$$

for all i, j and k.

The rack of a disjoint union of links (the sum of the links) is the free product of the racks of the links (the 'sum' of the racks).

The rack of a framed oriented, non-split link classifies the link up to equivalence of pairs. This is proved in [FRS]. We can see that the rack is invariant under regular isotopy Reidemeister moves by considering how the presentation changes.

If two diagrams differ by Reidemeister move two then two extra generators are introduced with relations rendering them redundant.

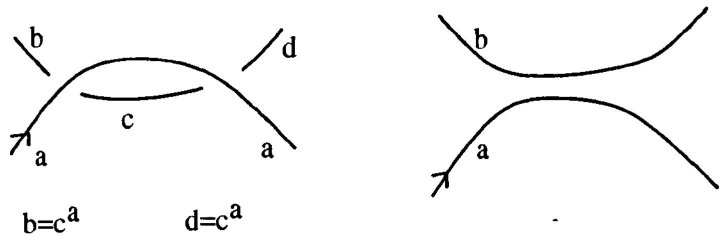

Figure 6.2.3 Reidemeister move two.

If they differ by Reidemeister move three then the rack identity is exactly what is required to make the rack presentations equivalent.

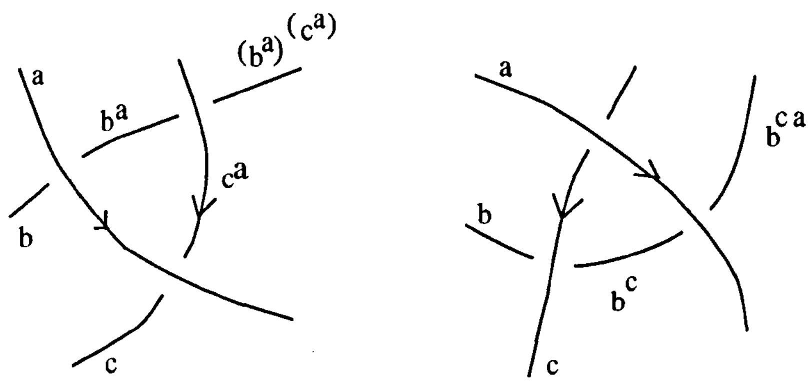

Figure 6.2.4 Reidemeister move three.

The rack of a link is an invariant of the link, but it is hard to look at two rack presentations and decide whether the racks are isomorphic. We can make this invariant easier to use by weakening it. Here are some invariants arising from the rack of a link in a natural way.

The total-writhe. A framed oriented link diagram has the total writhe of each component equal to a multiple of n if and only if there exists a rack homomorphism from the rack of the link to the cyclic rack of order n.

Colouring. A link is three-colourable if and only if there is a homomorphism from the rack of the link to the three-element dihedral rack.

6.3 The Alexander module. [BJS]

During the following construction of the Alexander invariant, the link in question is a knot. The Alexander invariant of a knot is derived from the infinite cyclic cover of the knot exterior. First, construct a cellular decomposition of the knot exterior; the three-sphere with an open neighbourhood of the knot removed. Take a knot K in S^3 and project it to a knot diagram in S^2 as a subset of S^3. Choose an 'outside' and an 'inside' of S^2 in S^3. The words 'up' and 'top' will refer to the outside component of the complement. We can reconstruct K (up to isotopy) in S^3 by pushing the strands up or down as appropriate near crossings in S^2.

The knot exterior has a cell decomposition consisting of

two	3-balls,	
three	2-cubes	at each crossing (one over the overpass, one between the strands and one under the underpass),
one	2-cube	for each region of S^2 less a neighbourhood of the diagram,
two	2-cubes	along each arc between crossings,
eight	1-cells	for each crossing (across each of the strands near the crossing),
two	1-cells	between each crossing along the sides of the arc
and four	vertices	at each crossing

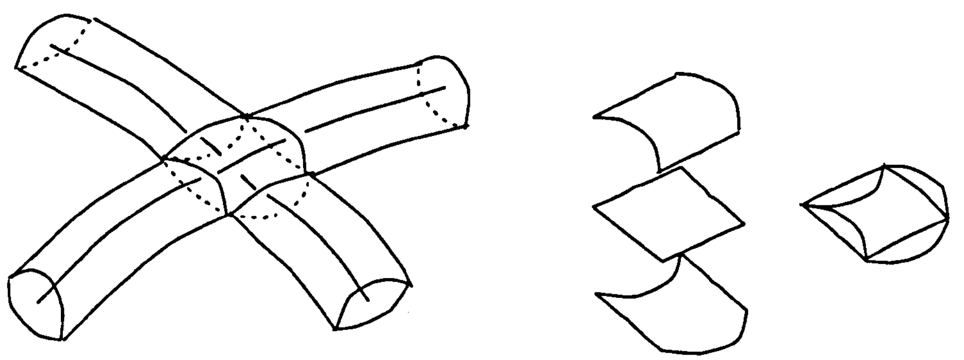

A crossing in the link diagram

four vertices,
three 2-cubes and eight 1-cells
for each crossing

Figure 6.3.1 A cellular decomposition of a knot exterior.

Within homotopy-equivalence we can contract one of the 3-balls (the top one) to a basepoint. The space that remains has cell decomposition

one	3-ball,	
two	2-cubes	at each crossing (one between the strands and one under the underpass),
one	2-cube	along each arc between crossings,
four	1-cells	for each crossing (bounding the underpass 2-cube)
and one	vertex,	the basepoint

Now collapse the 2-cube along the arcs between crossings to a 1-cube below the arc. The space now has

one	3-ball,	
two	2-cubes	at each crossing (one between the strands and one under the underpass),
four	1-cells	for each crossing with pairs from adjacent crossings identified this amounts to one per arc of the diagram less crossings.
and one	vertex,	the basepoint

The first homotopy group of this space is generated by loops down from the basepoint passing under each arc of the knot diagram. Finally, collapse the middle 2-cell in each crossing to a one-cube looping under the overpass. This collapse identifies the fundamental group generators passing under the overpass on each side of a crossing. This leaves

one	3-ball,	
one	2-cube	at each crossing (the one under the underpass),
one	1-cell	for each arc of the diagram including crossings.
and one	vertex,	the basepoint

The fundamental group of this space is generated by the 1-cells (in correspondence with the arcs of the knot diagram). Near each 2-cell there are three generating loops, one under the overpass, called a, say, and one under the underpass on each side of the crossing, called b and b^a. Each 2-cell gives a relation of the form $ab^a a^{-1} b^{-1}$. So $b^a = a^{-1}ba$ in the fundamental group.

We now construct the infinite cyclic cover of this space. We shall use t as a generator of the infinite cyclic group, and there is a vertex for each t^i. There are 1-cells $t^i a$ from t^{i+1} to t^i, and 2-cells with boundary reading $ta, b^a, a^{-1}, (tb)^{-1}$. The homology of this space is the homology of the sequence

$$0 \longrightarrow \mathbb{Z}[t,t^{-1}] \longrightarrow \mathbb{Z}[t,t^{-1}]^{(crossings)} \longrightarrow \mathbb{Z}[t,t^{-1}]^{(arcs)} \longrightarrow \mathbb{Z}[t,t^{-1}] \longrightarrow 0$$

We are interested in the first homology group of this space. The image of the boundary map from 2-chains to 1-chains is generated by expressions of the form

$$tb + a - b^a - ta$$

The boundary map sends a 1-cell $t^i a$ to $t^{i+1} - t^i$. As a $\mathbb{Z}[t,t^{-1}]$-module, the kernel is generated by the differences $a - w, b - w, \ldots.$ for some 1-cell (some arc of the diagram) w.

Consider the matrix representation of the boundary map on 2-cells. It has n columns (one for each 2-cell) and n rows (one for each 1-cell). With respect to bases of the individual cells, the columns of the matrix are all zeros except for -1, t and $1-t$. Change the basis of the image space to $a-w, b-w, \ldots.$ where w is the last in our old basis. The matrix will change to one with only $n-1$ rows, we have added all the rows except the last to the last row and then missed out the last row.

The 3-balls in the covering space have boundary which must map to zero under the next boundary map. We can choose a 3-ball whose image has a single occurrence of some 2-cell in its boundary. The boundary of the 3-ball gives a dependence in the relations, and allows us to forget one of the columns of the matrix.

The matrix has now been reduced to an $n-1$ by $n-1$ matrix, and the Alexander invariant is the cokernel of the matrix.

Any $\mathbb{Z}[t,t^{-1}]$-module becomes a rack under $a^b = ta + (1-t)b$. Call racks from such constructions $\mathbb{Z}[t,t^{-1}]$-racks. There are natural definitions of $\mathbb{Z}[t,t^{-1}]$-subracks, $\mathbb{Z}[t,t^{-1}]$-rack homomorphisms and so on.

The universal property of the Alexander module

The Alexander module of a knot K is a universal $\mathbb{Z}[t,t^{-1}]$-rack under the property that there exists a rack homomorphism from the rack of the knot to the Alexander module.

This means that there is a rack homomorphism from $R(K)$ to the Alexander module, and if M is another $\mathbb{Z}[t,t^{-1}]$-rack with a homomorphism from $R(K)$ to M then the map factors uniquely through the Alexander module.

Proof Label the arcs of a knot diagram $x_1,..,x_n$ (for the purposes of generating the rack of the link) and label them in the same order $a_1,..,a_{n-1}$ omitting the last (to generate the Alexander module).

We need to produce a map from $R(L)$ to the Alexander module which is a rack homomorphism. This map is defined on the generators, sending x_i to a_i for i less than n and x_n to 0.

Also, if we are given a $\mathbb{Z}[t,t^{-1}]$-rack M and homomorphism $\phi\colon R(L) \longrightarrow M$, we need a unique rack homomorphism from the Alexander module to M. The completing map is defined by $a_i \mapsto \phi(x_i)$. This is necessary and sufficient for commutativity of the following diagram

$$\begin{array}{ccc} & & Alex(L) \\ & \nearrow & \downarrow \\ R(L) & \longrightarrow & M \end{array}$$

Figure 6.3.2 The universal property of the Alexander rack.

□

6.4 The Classifying space of a rack.

Cubical sets, classifying spaces and species (or trunks) are introduced and discussed in [FRS]. The **classifying space** of a rack is defined using a cubical complex, the n-cubes correspond to n-tuples in the product $X \times ... \times X$. There is a single 0-cube, the basepoint, and the cubes are glued by the boundary maps

$$\partial_i^0(x_1,..,x_i,..,x_n) = (x_1,..,\hat{x}_i,..,x_n)$$
$$\partial_i^1(x_1,..,x_i,..,x_n) = ({x_1}^{x_i},..,{x_{i-1}}^{x_i},x_{i+1},..,x_n)$$

The classifying space, $\mathbb{B}R$, is the realisation, without degeneracies, of this cubical set. Usually, there is no topology specified on R, and we assume the discrete topology. If R has a topology, then the above construction gives a cubical space, and the classifying space is the realisation, without degeneracies of that cubical space. The classifying space of a rack is also referred to as **the rack space.** When the rack came from a link, all the familiar topological invariants of this space are invariants of the link.

There is an analogy between categories and **trunks.** A category is a set of objects with edges (morphisms) between them and specified triples of edges (commuting triangles). The classifying space of a category is a simplicial set whose n-simplices are generated by n-tuples of edges whose 2-faces are all specified (commuting) triangles. In the cubical case, we define a trunk, having objects and edges between them with specified oriented squares of edges (these specified squares are four-tuples of edges). The edges do not have a composition map, so these preferred squares are *not* commuting diagrams of edges. The classifying space of a trunk is a cubical realisation, where all the 2-faces of each n-cube are one of the specified squares. The trunk of a rack has one object (the basepoint), edges in one-to-one correspondence with the rack elements and preferred squares are in one-to-one correspondence with pairs of racks elements (r, s), the four-tuple is (r, s, r^s, s).

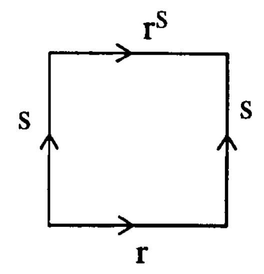

Figure 6.4.1 A preferred square.

It is easy to see that isomorphic racks have homeomorphic classifying spaces.

Chapter 7. The second homotopy group of a rack space

In this chapter we discuss two methods of calculating the second homotopy group of the classifying space of a rack. Racks give link invariants, so homotopy groups of classifying spaces of racks do as well. The first method of calculation is algebraic, and depends upon a cellular construction of the universal cover of a cubical space. This method is used explicitly to find the second homotopy group of the cyclic rack of order 2. The algebra is unwieldy by hand, but there may be scope for writing a computer program to deal with larger racks. The second method of calculation (geometric) uses transversality of homotopy representatives; we can ensure that preimages of certain points in the classifying space form link diagrams in the sphere, and manipulation of such link diagrams in bordism gives homotopy of the 2-spheres ([FRS]). This method is applied to find the second homotopy group of the trivial rack, all the cyclic racks, and all the permutation racks. This geometric approach is much easier to use, but it would be hard to program a computer to apply such a method.

The fundamental group of $\mathbb{B}R$ is calculated, as for any CW-complex with a single vertex, using the 1-cells as generators and the 2-cells to provide relations.

$$\pi_1(\mathbb{B}R) \; = \; < r \in R \mid sr^s s^{-1} r^{-1} > \; = \; < r \in R \mid r^s = s^{-1} r s > \; = Asgp(R)$$

In particular, $\pi_1(\mathbb{B}R(L))$ is the fundamental group of the link. Other examples:

$$\pi_1(\mathbb{B}T_n) \cong \mathbb{Z}^n$$

$$\pi_1(\mathbb{B}C_n) \cong \mathbb{Z}$$

7.1 Algebraic calculation of the second homotopy group.

If X is a cell complex with a single 0-cell then

$$\pi_2(X) \cong \pi_2(X^{(3)}) \cong \pi_2(\widetilde{X^{(3)}}) \cong H_2(\widetilde{X^{(3)}})$$

where $X^{(3)}$ is the 3-skeleton of X and the tilde indicates universal cover.

The universal cover of a cubical complex

Let X be a connected cubical complex with a single vertex, the basepoint, and let ${\delta_i}^\epsilon$ be the inclusion of the (i,ϵ) face of a cube. An attaching map of a k-cube, f_j^k, composes with the boundary inclusion to give ${f_j}^k {\delta_i}^\epsilon$ as a $k-1$-face of the k-cube.

For each ${\delta_i}^\epsilon$, choose a path in the i-skeleton of I^k from the basepoint of I^k to the basepoint of the face ${\delta_i}^\epsilon(I^{k-1})$. This path ${\sigma_i}^{\epsilon k}$ is unique up to homotopy in the cube I^k, and we can compose with the attaching map to give

$${f_j}^k {\sigma_i}^{\epsilon k} = \phi_{ji}^{\epsilon k}$$

a loop in X.

Define $\tilde{X}$ as a cubical complex with the set of k-cubes indexed by $\pi_1(X) \times \{k \text{ cubes of } X\}$ The attaching map of a k-cell in $\tilde{X}$ is defined on each face; the face $([\xi], {e_j}^k){\delta_i}^\epsilon$ is identified with the $k-1$-cube $([\xi][{f_j}^k {\sigma_i}^{\epsilon k}], {\delta_i}^\epsilon {e_j}^k)$.

Lemma This cubical complex is well-defined.

We need to check the attachment of double-boundaries, for example if $i > j$ then the maps $\delta_j{}^{\epsilon_j}\delta_i{}^{\epsilon_i}$ and $\delta_i{}^{\epsilon_i}\delta_{j-1}{}^{\epsilon_j}$ on I^{k-2} are equal. (for $k \geq 2$). The faces

$$([\xi], e^k)\delta_j{}^{\epsilon_j}\delta_i{}^{\epsilon_i} \text{ and } ([\xi], e^k)\delta_i{}^{\epsilon_i}\delta_{j-1}{}^{\epsilon_j}$$

are identified with the $k-2$-cells

$$([\xi][\phi_j^{\epsilon_j k}][\phi_i^{\epsilon_i(k-1)}], e^k\delta_j^{\epsilon_j}\delta_i^{\epsilon_i}) \text{ and } ([\xi][\phi_i^{\epsilon_i k}][\phi_{(j-1)}^{\epsilon_j(k-1)}], e^k\delta_i^{\epsilon_i}\delta_{(j-1)}^{\epsilon_j})$$

It remains to check that

$$[\phi_j^{\epsilon_j k}][\phi_i^{\epsilon_i(k-1)}] = [\phi_i^{\epsilon_i k}][\phi_{(j-1)}^{\epsilon_j(k-1)}]$$

that is, two paths from the origin of the k-cube to the origin of a certain $k-2$-face are homotopic in X. This is true because a k-cube is simply-connected. □

Theorem The cubical space $\tilde{X}$ is the universal cover of X.

Proof First show that the projection map $([\rho], x) \mapsto x$ is a covering map and then show that the space $\tilde{X}$ is connected and simply connected.

Above $x \in X$ there is a copy of $\pi_1(X)$; $([\rho_1], x), ([\rho_2], x), .., ([\rho_n], x), \ldots$ Each cell in X attaching to $x \in X$; $x \in e_j^k\delta_i^\epsilon$ has copies in $\tilde{X}$ $([\rho_1], e_j^k), ([\rho_2], e_j^k), .., ([\rho_n], e_j^k), \ldots$ The cell $([\rho_i], e_j^k)$ attaches to $([\rho_j], x)$ if and only if

$$([\rho_j], x) \in ([\rho_i], e_j^k)\delta_i^\epsilon = ([\rho_i][\phi_i^{\epsilon k}], e_j^k\delta_i^\epsilon)$$

if and only if

$$[\rho_j] = [\rho_i][\phi_i^{\epsilon k}]$$

The neighbourhood of a point in X consists of points in the interior of a cell (if x is in the interior of a cell) and points near the boundaries of cells which attach at x. In $\tilde{X}$ we have the same interior points in the copy of the cube, and a unique copy of each attached cell attaching in the same way. Thus sufficiently small neighbourhoods lift to disjoint copies of the base neighbourhood, and we have an even covering.

This covering property allows us to lift paths from X to $\tilde{X}$. Given two points $([\rho_1], x_1)$ and $([\rho_2], x_2)$ in the cover, find a path between x_1 and x_2 in X, α, and lift it to a path in $\tilde{X}$ starting at $([\rho_1], x_1)$. If the endpoint of this path is $([\sigma], x_2)$ then lift the path $\alpha\sigma^{-1}\rho_2$ from $([\rho_1], x_1)$. This gives a path in the cover from $([\rho_1], x_1)$ to $([\rho_2], x_2)$. So $\tilde{X}$ is path-connected.

To see that $\tilde{X}$ is simply-connected. take a loop in the covering space. Homotope it to a word in the edges of $\tilde{X}$. An edge in the lift is $([\rho], e_j)$ from $([\rho], *)$ to $([\rho][e_j], *)$. A path of edges in the cover from the basepoint is a sequence in which adjacent edges are related by one of the following four moves

$$.., ([\rho], e), ([\rho][e], f), ..$$

$$.., ([\rho], e), ([\rho][e][f]^{-1}, f)^{-1}, ..$$

$$.., ([\rho], e)^{-1}, ([\rho], f), ..$$

$$..,([\rho],e)^{-1},([\rho][f]^{-1},f)^{-1},..$$

These four are described in the following single expression

$$..,([\rho],e_1)^{\epsilon_1},([\rho][e_1]^{\frac{1+\epsilon_1}{2}}[e_2]^{\frac{-1+\epsilon_2}{2}},e_2)^{\epsilon_2},..$$

A path in the cover is determined by the sequence of pairs e_i,ϵ_i. Such a path is a loop in the cover if and only if the path $e_1^{\epsilon_1}e_2^{\epsilon_2}..e_n^{\epsilon_n}$ is null-homotopic in X. Null-homotopic word-paths in X can be reduced to the null-word under moves of inserting or deleting boundaries of 2-cubes and inserting or deleting cancelling pairs $e^{\epsilon},e^{-\epsilon}$. If these moves lift to alter the path in the cover appropriately, we'll reduce the loop in the covering space to the null-loop.

Insert the boundary of the 2-cell e^2 in X. We want to lift the loop

$$(e^2\delta_0^0)(e^2\delta_1^1)(e^2\delta_0^1)^{-1}(e^2\delta_1^0)^{-1}$$

into the path $..,([\rho],e_j)^{\epsilon_j},([\rho][e_j]^{\frac{1+\epsilon_j}{2}}[e_{j+1}]^{\frac{-1+\epsilon_{j+1}}{2}},e_{j+1})^{\epsilon_{j+1}},..$ giving

$$..,([\rho],e_j)^{\epsilon_j},([\rho][e_j]^{\frac{1+\epsilon_j}{2}},e^2\delta_0^0),([\rho][e_j]^{\frac{1+\epsilon_j}{2}}[e^2\delta_0^0],e^2\delta_1^1),$$
$$([\rho][e_j]^{\frac{1+\epsilon_j}{2}}[e^2\delta_0^0][e^2\delta_1^1][e^2\delta_0^1]^{-1},e^2\delta_0^1)^{-1},$$
$$([\rho][e_j]^{\frac{1+\epsilon_j}{2}}[e^2\delta_0^0][e^2\delta_1^1][e^2\delta_0^1]^{-1}[e^2\delta_1^0]^{-1},e^2\delta_1^0)^{-1},$$
$$([\rho][e_j]^{\frac{1+\epsilon_j}{2}}[e^2\delta_0^0][e^2\delta_1^1][e^2\delta_0^1]^{-1}[e^2\delta_1^0]^{-1}[e_{j+1}]^{\frac{-1+\epsilon_{j+1}}{2}},e_{j+1})^{\epsilon_{j+1}},..$$

The last edge in this word is equal to $([\rho][e_j]^{\frac{1+\epsilon_j}{2}}[e_{j+1}]^{\frac{-1+\epsilon_{j+1}}{2}},e_{j+1})^{\epsilon_{j+1}}$ by homotopy through e^2 in X. The new four edges in the sequence of edges in $\tilde{X}$ form the boundary of the lift $([\rho][e_j]^{\frac{1+\epsilon_j}{2}},e^2)$ in the cover, so the homotopy type of the loop in $\tilde{X}$ is unchanged.

A cancelling pair $e^{\epsilon},e^{-\epsilon}$ in $e_j^{\epsilon_j},e_{j+1}^{\epsilon_{j+1}}$ lifts to

$$...([\rho],e_j)^{\epsilon_j},([\rho][e_j]^{\frac{1+\epsilon_j}{2}}[e]^{\frac{-1+\epsilon}{2}},e)^{\epsilon},([\rho][e_j]^{\frac{1+\epsilon_j}{2}}[e]^{\epsilon}[e]^{\frac{-1-\epsilon}{2}},e)^{-\epsilon},$$
$$([\rho],[e_j]^{\frac{1+\epsilon_j}{2}}[e]^{\epsilon}[e]^{-\epsilon}[e_{j+1}]^{\frac{-1+\epsilon_{j+1}}{2}},e_{j+1})^{\epsilon_{j+1}}$$

The last of these is equal to $([\rho][e_j]^{\frac{1+\epsilon_j}{2}}[e_{j+1}]^{\frac{-1+\epsilon_{j+1}}{2}},e_{j+1})^{\epsilon_{j+1}}$. The two new edges are equal and opposite, cancelling in $\tilde{X}$. The sequence of moves reducing the edge-word to the null-word in X also reduces the loop in the covering space to a homotopic null-word. All loops are contractible in $\tilde{X}$ □

The j-dimensional chain groups for cellular homology of $\tilde{X}$ are given by $\mathbb{Z}\pi_1(X)\otimes C(j)$ where $C(j)$ is the cellular chain group for X. We need to calculate the homology of

$$\mathbb{Z}\pi_1(X)\otimes C(3)\longrightarrow\mathbb{Z}\pi_1(X)\otimes C(2)\longrightarrow\mathbb{Z}\pi_1(X)\otimes C(1)$$

The boundary maps are extended from their action on the cells; the image of $([\rho],e^j)$ is

$$\sum_{1\le i\le j,\ \epsilon\in\{0,1\}}(-1)^i(-1)^{\epsilon}([\rho],e^j)\delta_i^{\epsilon}$$

An example: $\pi_2(\mathbb{B}C_2)$ Let X be $\mathbb{B}C_2$. Here is the rack table for C_2

	a	b
a	b	b
b	a	a

The one-cells in the classifying space are labelled a and b. The two-cells give homotopy relators $aab^{-1}a^{-1}$, $abb^{-1}b^{-1}$, $baa^{-1}a^{-1}$ and $bba^{-1}b^{-1}$ from the cells $e(a,a)$, $e(a,b)$, $e(b,a)$, $e(b,b)$ respectively. This leaves

$$\pi_1(\mathbb{B}C_2) \cong \mathbb{Z}$$

with generator either a or b.

The set of j-cells in the universal cover is $\pi_1(X) \times \{j\text{-cells of } X\} \cong \mathbb{Z} \times (C_2)^j$ We can write 1-cells in the covering space $\tilde{X}$ in the form $e(n,a)$, $e(n,b)$, the 2-cells as $e(n,a,a)$, $e(n,a,b)$, $e(n,b,a)$ and $e(n,b,b)$ and so on. To calculate the boundaries of these cells, we change the element of the fundamental group (n) according to a path from the origin of the cube to the origin of the face under consideration.

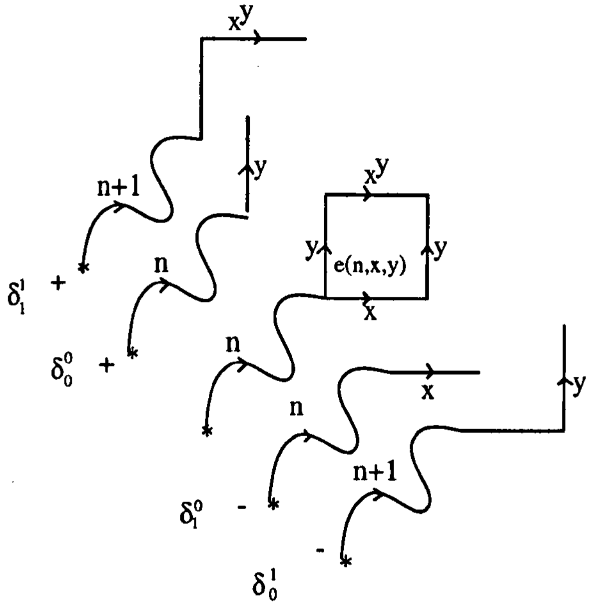

Figure 7.1.1 A boundary in the universal cover.

As a result we get

$$\begin{array}{rl} \text{boundary : 2-cells} & \longrightarrow \text{1-cells} \\ e(n,a,a) \mapsto & -e(n,a) + e(n,a) + e(n+1,b) - e(n+1,a) \\ e(n,a,b) \mapsto & -e(n,a) + e(n,b) + e(n+1,b) - e(n+1,b) \\ e(n,b,a) \mapsto & -e(n,b) + e(n,a) + e(n+1,a) - e(n+1,a) \\ e(n,b,b) \mapsto & -e(n,b) + e(n,b) + e(n+1,a) - e(n+1,b) \end{array}$$

ie.

$$
\begin{array}{llllll}
\text{boundary: 2-cells} & \longrightarrow & \text{1-cells} \\
e(n,a,a) & \mapsto & e(n+1,b) - e(n+1,a) \\
e(n,a,b) & \mapsto & -e(n,a) + e(n,b) \\
e(n,b,a) & \mapsto & -e(n,b) + e(n,a) \\
e(n,b,b) & \mapsto & e(n+1,a) - e(n+1,b)
\end{array}
$$

The kernel of this map is generated by chains

$$e(n,a,a) + e(n+1,b,a)$$

$$e(n,a,a) + e(n,b,b)$$

$$e(n,a,b) + e(n,b,a)$$

Call these generators X_n, Y_n, Z_n respectively.

$$
\begin{array}{llllll}
\text{boundary : 3-cells} & \longrightarrow & \text{2-cells} \\
e(n,a,a,a) & \mapsto & +e(n,a,a) & -e(n,a,a) & +e(n,a,a) \\
 & & -e(n+1,b,b) & +e(n+1,b,a) & -e(n+1,a,a) \\
e(n,a,a,b) & \mapsto & +e(n,a,a) & -e(n,a,b) & +e(n,a,b) \\
 & & -e(n+1,b,b) & +e(n+1,b,b) & -e(n+1,a,b) \\
e(n,a,b,a) & \mapsto & +e(n,a,b) & -e(n,a,a) & +e(n,b,a) \\
 & & -e(n+1,b,a) & +e(n+1,b,a) & -e(n+1,b,a) \\
e(n,a,b,b) & \mapsto & +e(n,a,b) & -e(n,a,b) & +e(n,b,b) \\
 & & -e(n+1,b,a) & +e(n+1,b,b) & -e(n+1,b,b) \\
e(n,b,a,a) & \mapsto & +e(n,b,a) & -e(n,b,a) & +e(n,a,a) \\
 & & -e(n+1,a,b) & +e(n+1,a,a) & -e(n+1,a,a) \\
e(n,b,a,b) & \mapsto & +e(n,b,a) & -e(n,b,b) & +e(n,a,b) \\
 & & -e(n+1,a,b) & +e(n+1,a,b) & -e(n+1,a,b) \\
e(n,b,b,a) & \mapsto & +e(n,b,b) & -e(n,b,a) & +e(n,b,a) \\
 & & -e(n+1,a,a) & +e(n+1,a,a) & -e(n+1,b,a) \\
e(n,b,b,b) & \mapsto & +e(n,b,b) & -e(n,b,b) & +e(n,b,b) \\
 & & -e(n+1,a,a) & +e(n+1,a,b) & -e(n+1,b,b)
\end{array}
$$

This simplifies to

$$
\begin{array}{llllll}
\text{boundary : 3-cells} & \longrightarrow & \text{2-cells} \\
e(n,a,a,a) & \mapsto & X_n - Y_{n+1} \\
e(n,a,a,b) & \mapsto & X_n - Z_{n+1} \\
e(n,a,b,a) & \mapsto & Z_n - X_n \\
e(n,a,b,b) & \mapsto & Y_n - X_n \\
e(n,b,a,a) & \mapsto & X_n - Z_{n+1} \\
e(n,b,a,b) & \mapsto & X_n - Y_n & +Z_n - Z_{n+1} \\
e(n,b,b,a) & \mapsto & Y_n - X_n \\
e(n,b,b,b) & \mapsto & Y_n - X_n & +Z_{n+1} - Y_{n+1}
\end{array}
$$

We have $X_n = Y_n = Z_n = Y_{n+1}$ for all n and the second homology of the covering space has a single generator,

$$\pi_2(\mathbb{B}C_2) \cong \mathbb{Z}$$

7.2 A geometric approach to π_2 of a classifying space, [FRS].

Given a map f mapping S^2 to $\mathbb{B}R$, we can use homotopy until it falls into the 2-skeleton. Then make it transverse to the centres of 2-cells. The preimages of these points have a neighbourhood mapping homeomorphically onto a neighbourhood of the centre of the appropriate 2-cell of $\mathbb{B}R$. Push points mapping outside this neighbourhood to the boundary of the 2-cell. Then all points mapping to 2-cells belong to a homeomorphic preimage. Now do the same for the centres of the 1-cells, giving 1-manifolds in S^2 with a neighbourhood of preimages. Locally the preimage neighbourhood maps to $\mathbb{B}R$ simply by projection onto a normal fibre identified with the 1-cell. The rest of the sphere maps to the basepoint of $\mathbb{B}R$. After such homotopy, the map can be encoded by a framed link diagram whose arcs (the preimage of 1-cell centres) are labelled by rack elements and the crossings (preimages of 2-cell centres) have labels changing according to the following rule

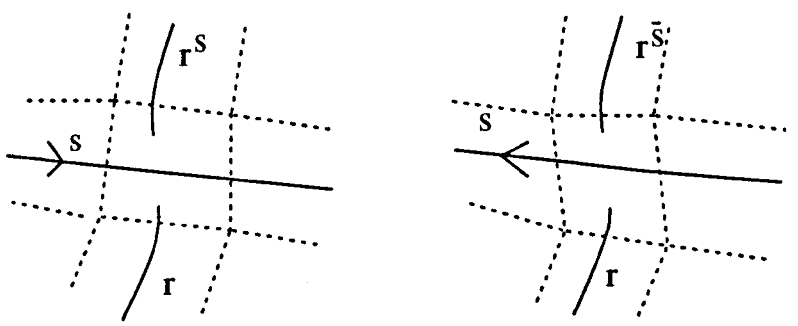

Figure 7.2.1 Crossings in transverse preimage diagrams.

Here framing and orientation of diagrams are identified by the following rule

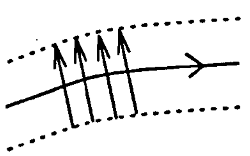

Figure 7.2.2 The orientation convention.

Homotopy between representatives is cobordism of such link diagrams with added rules for passing through the 3-cells.

Theorem There is a one-to-one correspondence between $\pi_2(\mathbb{B}R)$ and the set of link diagrams which are framed (or oriented, in oriented S^2) and labelled by rack elements, under equivalence of birth, death, bridging between equally labelled arcs and Reidermeister moves 2 and 3.

Proof A cobordism between link diagrams has singular points at maxima and minima of the surface allowing birth and death of unknots,

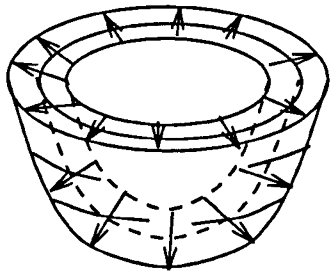

Figure 7.2.3 A minimum in the framed surface.

at saddle points of the surface allowing bridging of arcs

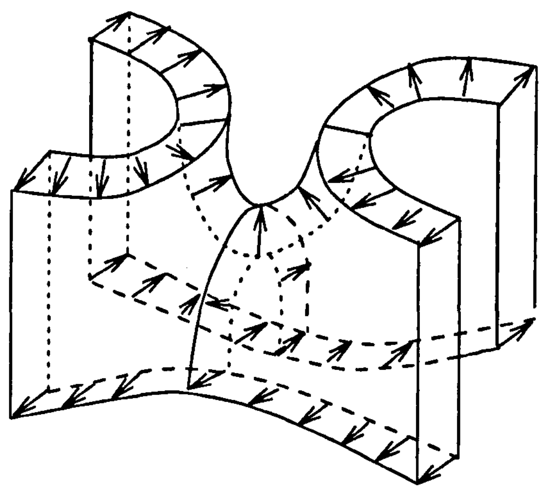

Figure 7.2.4 A saddle point in the framed surface.

at maxima and minima of the lines of crossings giving Reidermeister move 2

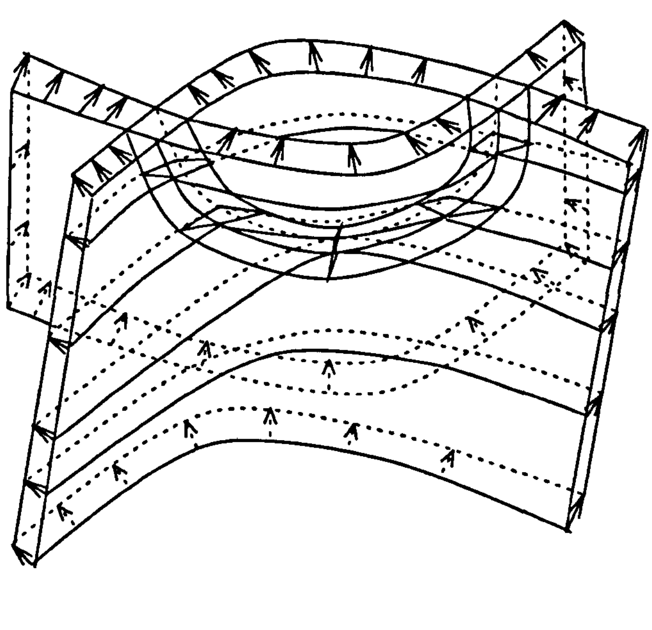

Figure 7.2.5 A minimum in the line of singular points.

Finally, passing the surface through 3-cells gives Reidermeister move 3.

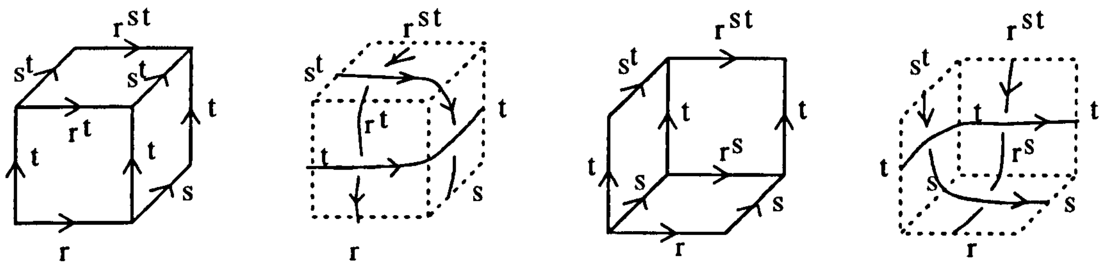

Figure 7.2.6 Boundaries of 3-cubes in the classifying space.

□

7.3 Calculation of $\pi_2(\mathbb{B}R)$ where R is the trivial rack with one element.

Take a framed oriented diagram labelled by the rack. It represents a homotopy class. In this case every arc is labelled by the single rack element, and bridging can be applied between any pair of oppositely oriented arcs. Apply the following move near every crossing on the diagram

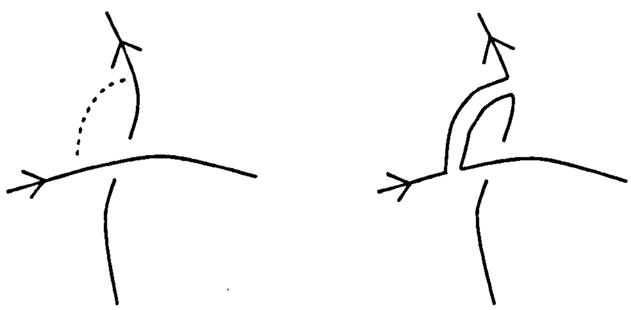

Figure 7.3.1 Bridging near a crossing.

The resulting diagram has the same number of crossings as before, but ignoring the twists, it consists of unlinked unknots. Either an unknot has no twists in it, in which case we can kill it using birth and death, or it has some twists in it. Apply the following move near each twist until the whole diagram is a sum of figures-of-eight.

Figure 7.3.2 Splitting off a crossing.

A figure of eight can be drawn without a orientation

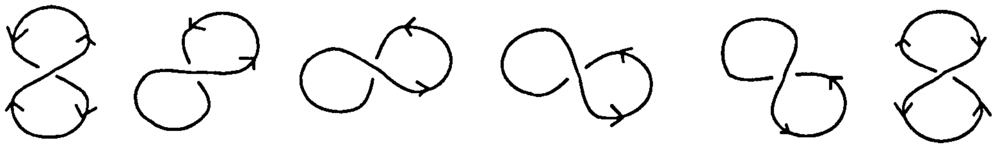

Figure 7.3.3 Orientation of the figure of eight.

and we can talk about right-handed or left-handed figures of eight according to the sign of the crossing. Under the moves above, right-handed and left-handed figures-of-eight cancel out

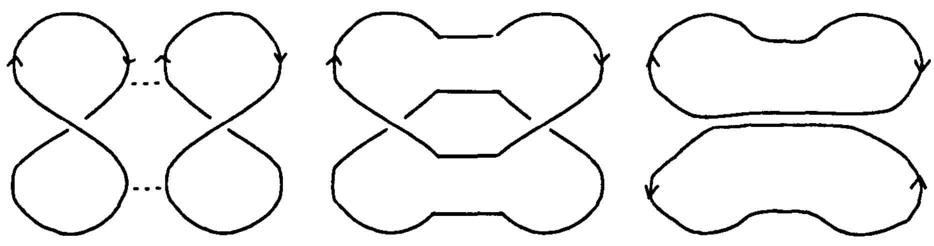

Figure 7.3.4 Inverse figures of eight.

Thus every knot diagram reduces to a sum of figures of eight and the generator is explicit.

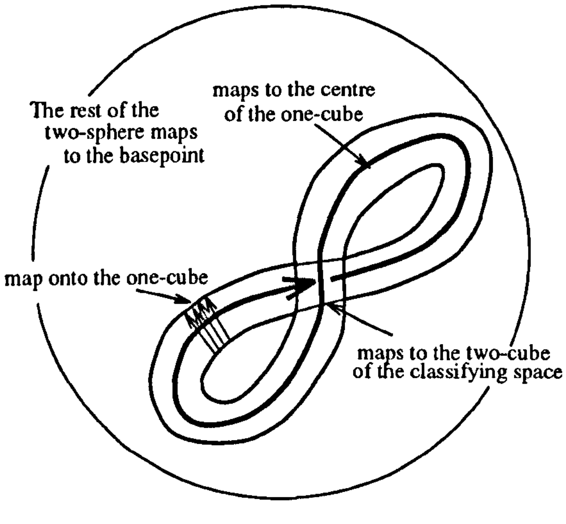

Figure 7.3.5 A generator.

This generator is of infinite order because manipulation of a diagram representing a homotopy class leaves the writhe of the diagram invariant. The writhe of the diagram representative is the number of generators it splits up into.

$$\pi_2(\mathbb{B}(*)) \cong \mathbb{Z}$$

7.4 Calculation of $\pi_2(\mathbb{B}C_n)$, the cyclic rack.

Here the link diagrams representing homotopy classes are labelled by the rack C_n and crossings look like

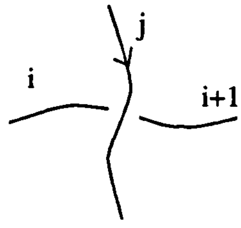

Figure 7.4.1 A crossing.

Adding a twist (only allowed if you also add the opposite twist) changes the labels thus

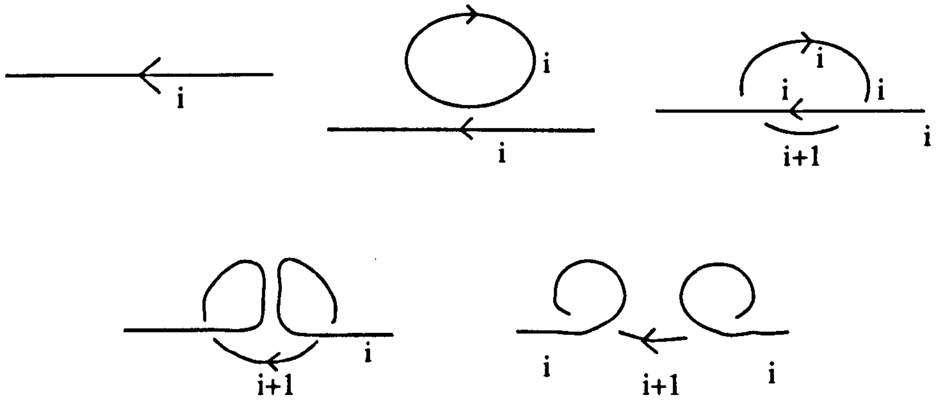

Figure 7.4.2 Introducing opposite twists by bridging.

All the labels are integers mod n so given any pair i, j, we can add enough twists to the i-labelled arc to change the label to a j

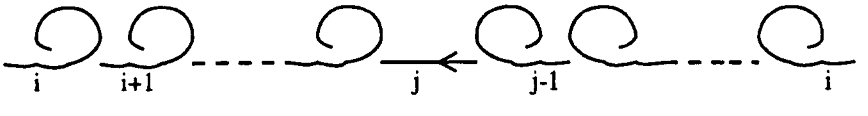

Figure 7.4.3 Changing the label on an arc.

Do this near each crossing on the underpass

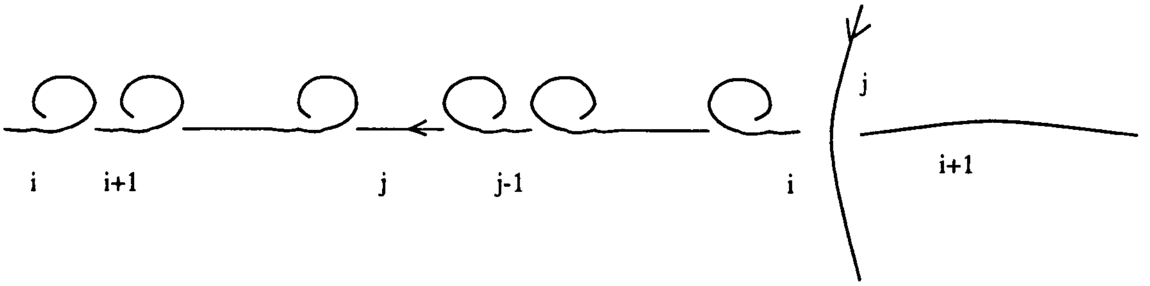

Figure 7.4.4 Changing the label near a crossing.

and using Reidermeister moves 2 and 3 move the twists under the overpass

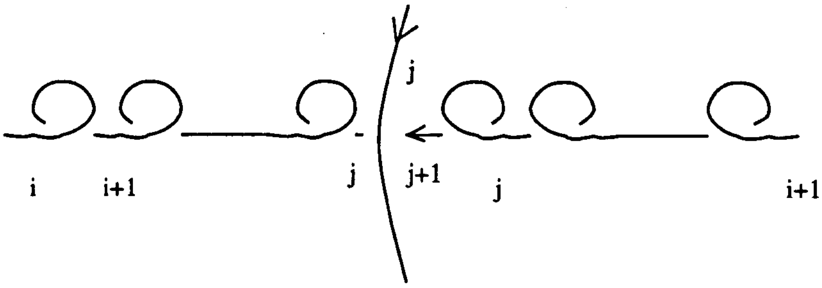

Figure 7.4.5 Changing the label at a crossing.

Now we can undo all crossings by bridging between equally labelled oppositely oriented arcs

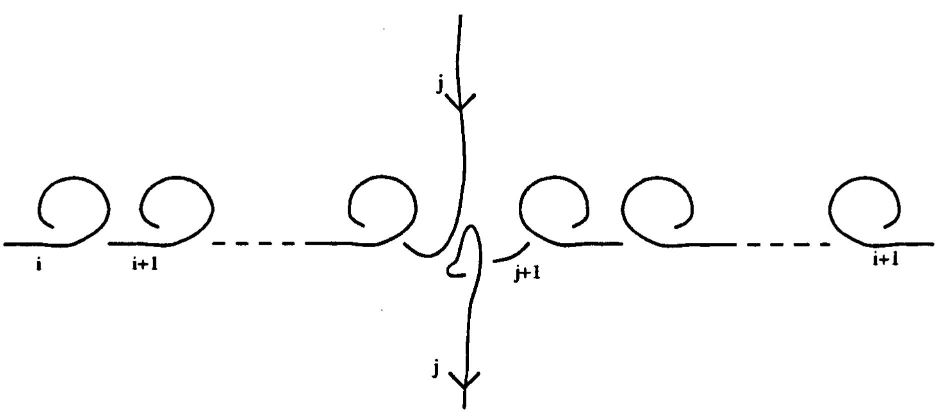

Figure 7.4.6 Bridging near crossings.

This reduces the link diagram to twisted unlinked unknots, as in the previous calculation, and each of these must have a multiple of n twists. Opposite twists cancel out and the unknots split after each n twists into the following.

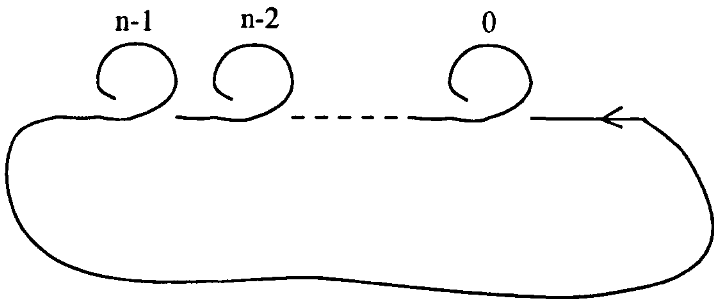

Figure 7.4.7 A generator.

Every C_n-labelled link diagram is bordant to an integer sum of this generator.The generator is seen to be of infinite order using a writhe argument on diagram representatives, as in the trivial rack case. Deduce that

$$\pi_2(\mathbb{B}C_n) \cong \mathbb{Z}$$

Consistent labelling on a diagram representative ensures that the writhe is a multiple of n. The integer corresponding to that element of $\pi_2(\mathbb{B}C_n)$ is the writhe divided by n.

7.5 Calculation of $\pi_2(\mathbb{B}P_\rho)$, any permutation rack.

If a link diagram is labelled by the permutation rack P_ρ then the crossings look like

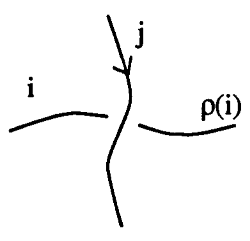

Figure 7.5.1 A crossing.

Either i and j are in the same orbit of ρ or they are not. If they are in the same orbit, we can take the crossing apart leaving twists as in the cyclic rack case. If i and j are in different orbits then we can reverse the crossing as follows

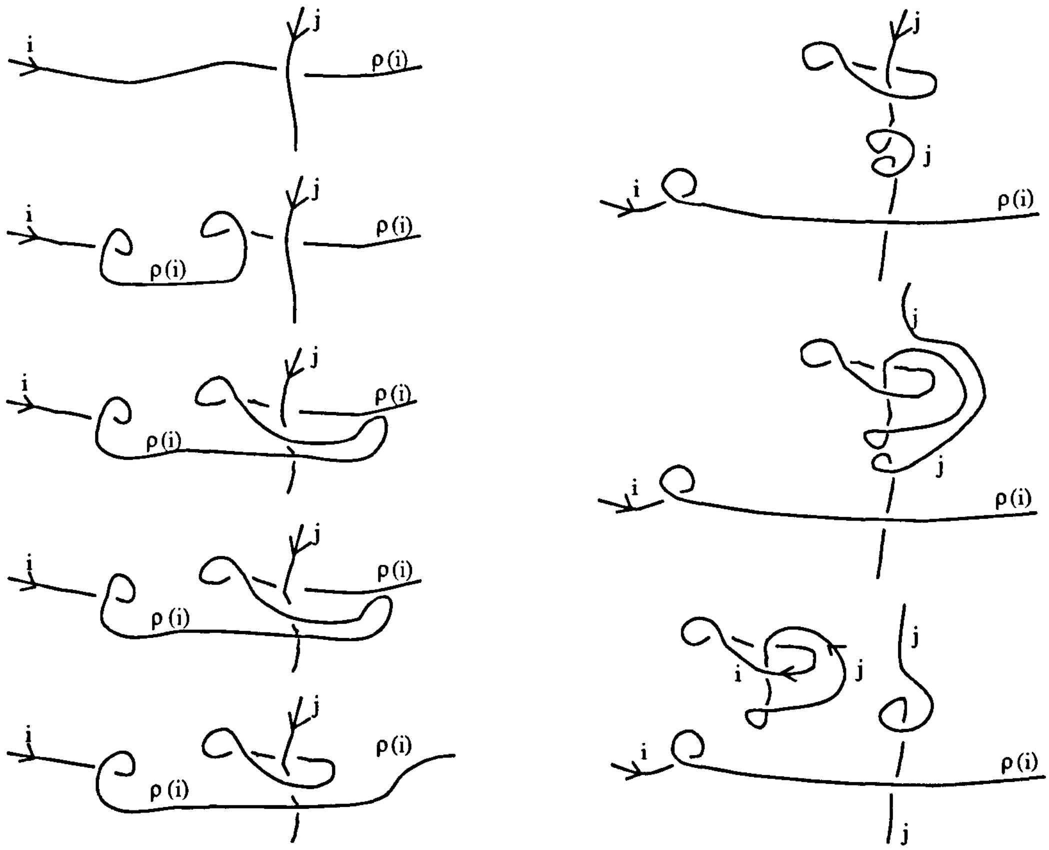

Figure 7.5.2 Reversing crossings.

We are left with a sum of generators, a twisted unknot for each orbit with a minimal positive number of twists (the number of twists required is the length of the orbit), and linked unknots for each pair of orbits.

Figure 7.5.3 A generator.

We can change each label on this orbit by rotating the appropriate unknot, and we only need one generator per pair of orbits. The number of generators required is then $k(k+1)/2$ where k is the number of orbits of the premutation ρ.

Further work on the second homotopy group.

In [FRS], it was proved that if L is a link which has r non-trivial non-split components then the second homotopy group of the classifying space is free abelian on r generators.

In particular, taking L as the disjoint union of two figures of eight, the rack of the link is generated by a and b, say, subject to relations $a^a = a$ and $b^b = b$. Elements of this rack are of the form a^w or b^w with w in the free group generated by a and b. As a result of the theorem, $\pi_2(\mathbb{B}R(L)) \cong \mathbb{Z}^r \cong \mathbb{Z}^2$. Every link diagram labelled with rack elements should be reducible under bridging moves and framed isotopy to a sum of the figures of eight.

An algorithm for reducing any link labelled by the rack $\{a^w, b^w\}$ to figures of eight must include a method of cancelling crossings between arcs labelled a^w and arcs labelled b^w. Such an algorithm is a first step to finding a geometric proof of the theorem, we need to reduce any link diagram labelled by $R(L)$ to a sum of the non-trivial components of L. We must be able to eliminate crossings between arcs labelled by rack elements from different operator group orbits.

Chapter 8. The second homotopy group of Alexander quotients

In this chapter we use the geometric approach to find the second homotopy group of a complex family of racks. In all the previous calculations we have been able to simplify a link diagram homotopy representative by undoing or detaching the crossings. This is because the label on the overpass is unimportant in a permutation rack. Here, some more subtle manoeuvring is required. The chapter finishes with an application, we describe an explicit set of generators for the second homotopy group of the dihedral rack of order 3.

8.1 On Alexander quotients.

Define a family of racks called R_a on the set $\mathbb{Z}_n$ with $i^j = ai + (1-a)j$. To satisfy the rack laws, a must be invertible. For example the dihedral rack has $i^j = 2i - j$. From now on, take n, the order of the rack, to be prime. If $a = 1$ then the rack is trivial, so assume that $a \in \{2, .., n-1\}$.

Lemma $R_a \cong R_b$ if and only if $a = b$.

Proof Take an isomorphism $\rho: R_a \longrightarrow R_b$. It is a rack homomorphism so it satisfies

$$\rho(ai + (1-a)j) = b\rho(i) + (1-b)\rho(j)$$

If ρ is a rack isomorphism then so is $\hat{\rho}$ defined by $\hat{\rho}(t) = \rho(t) + k$ and so is $\tilde{\rho}$ defined by $\tilde{\rho}(t) = \lambda\rho(t)$ (with λ invertible in a prime order rack). Choosing k and λ appropriately, we may assume that $\rho(0) = 0$ and $\rho(1) = 1$. Look again at $\rho(ai + (1-a)j) = b\rho(i) + (1-b)\rho(j)$ and put $i = 0$ and $i = 1$ giving

$$\rho((1-a)j) = (1-b)\rho(j) \quad \rho(a + (1-a)j) = b + (1-b)\rho(j)$$

$$\rho(a + (1-a)j) = b + \rho((1-a)j)$$

Put $j = 0$ and get $\rho(a) = b$. Let us assume a is not 1 (otherwise we have the trivial rack) so we can find j with $(1-a)j = a$ and get $\rho(2a) = 2b$, and so on.

$$\rho(x) = (\frac{b}{a})x$$

But $\rho(1) = 1$ so $\frac{b}{a} = 1$ and $b = a$ as required. □

Take a link diagram representing an element of the second homotopy group of the classifying space of the rack. The rack acts transitively on itself, for any choice of x and y in the rack, there is a z with $x^z = y$ (this is $ax + (1-a)z = y$ and unless the rack is trivial, $(1-a)$ is invertible and z can be found). We can use this transitivity to undo the crossings in the diagram.

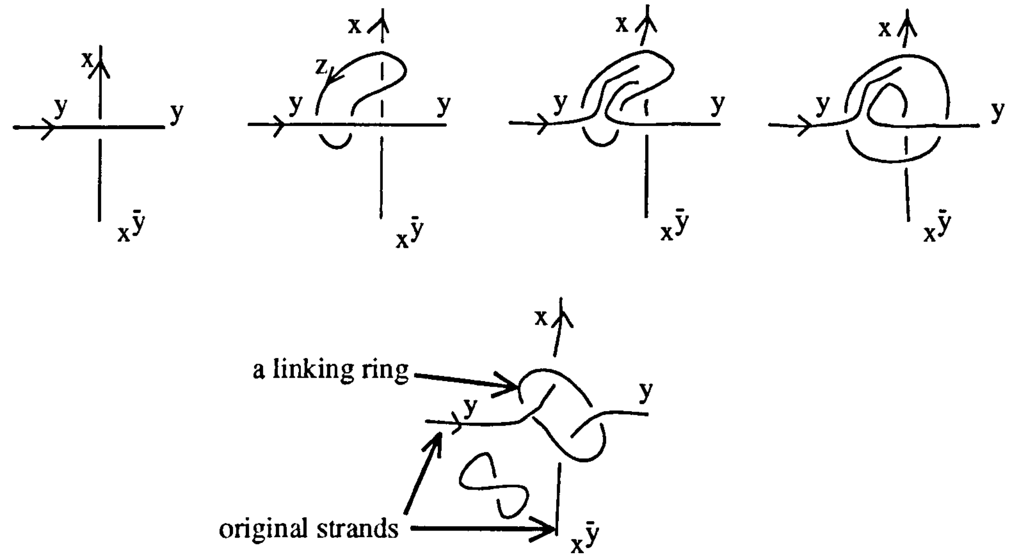

Figure 8.1.1 Undoing crossings.

The figure-of-eight that appears here is a generator of $\pi_2(\mathbb{B}R)$, as usual in a quandle. The labelling on this generator is unimportant; by transitivity of the rack action. We are left with nested unknots of original strands connected by the linking rings which are small. We can connect the unknots that arose from original strands by introducing new linking rings.

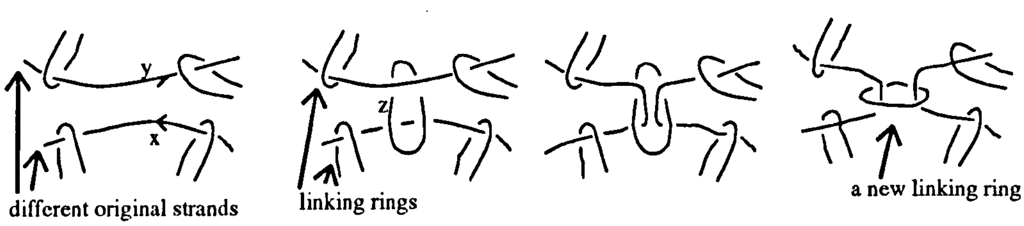

Figure 8.1.2 Bridging between equally oriented original strands.

If the orientations do not match as above then just pass one unknot over the other, and over all its linking rings

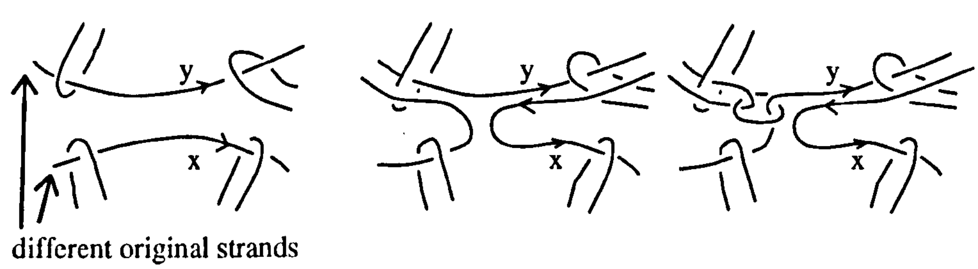

Figure 8.1.3 Bridging between oppositely oriented original strands.

The original strands have joined to form an unknot in the diagram, with small, untwisted linking rings. Apply an isotopy to the diagram until the unknot is a circle and linking rings are stretched but they still bound a tewisted neighbourhood of a path from one point on the unknot to another. The path can be chosen disjoint from other linking rings, but it may pass over or under the unknot. Now comb the linking rings so that they lie inside the unknot except for where the link with the unknot in two places.

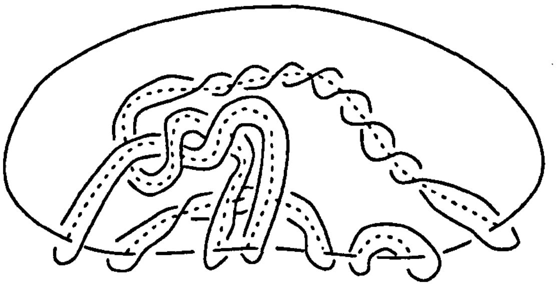

Figure 8.1.4 A first simplification of a homotopy representative.

The paths which the linking rings follow may now have become tangled and the linking rings may twist around those paths. We can reverse crossings in the paths by introducing another generator (we already have the figure-of-eight). The generator is

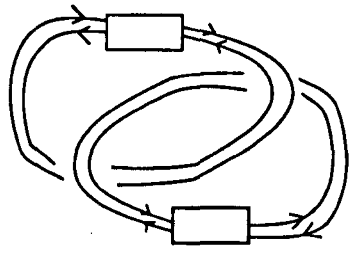

Figure 8.1.5 A generator of type 2.

The boxes in the diagram represent an undetermined number of whole twists, which have the effect of adding a constant to the labels. Labelling on the diagram is consistent, by the following results.

$$i - i^j = (1-a)(i-j)$$

$$i - i^{\bar{j}} = (1-a^{-1})(i-j)$$

$$i - i^{j\bar{k}} = (1-a^{-1})(j-k)$$

$$i - i^{\bar{j}k} = (1-a)(j-k)$$

$$i^k - j^k = a(i-j)$$

$$i^{\bar{k}} - j^{\bar{k}} = a^{-1}(i-j)$$

and here are some link diagram portions.

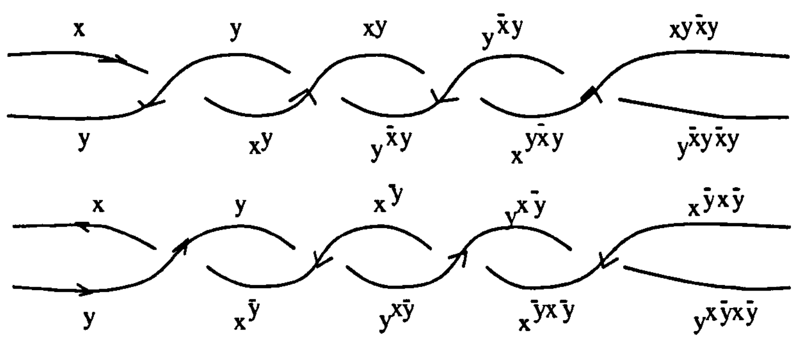

Figure 8.1.6 A whole number of twists labelled by rack elements.

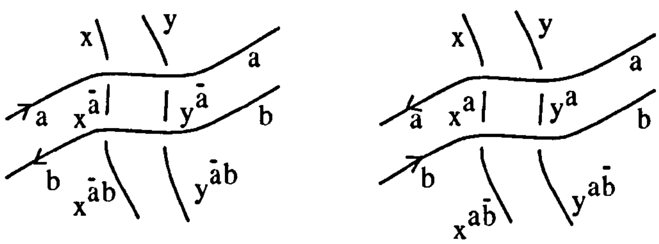

Figure 8.1.7 Passing under a linking ring.

We see that passing under a pair of oppositely oriented strands adds a constant to the labels of the underpasses. We can rectify this by putting in some twists before re-attaching the strands. This generator allows us to reverse the crossings (and introduce twists) by the following bridging moves.

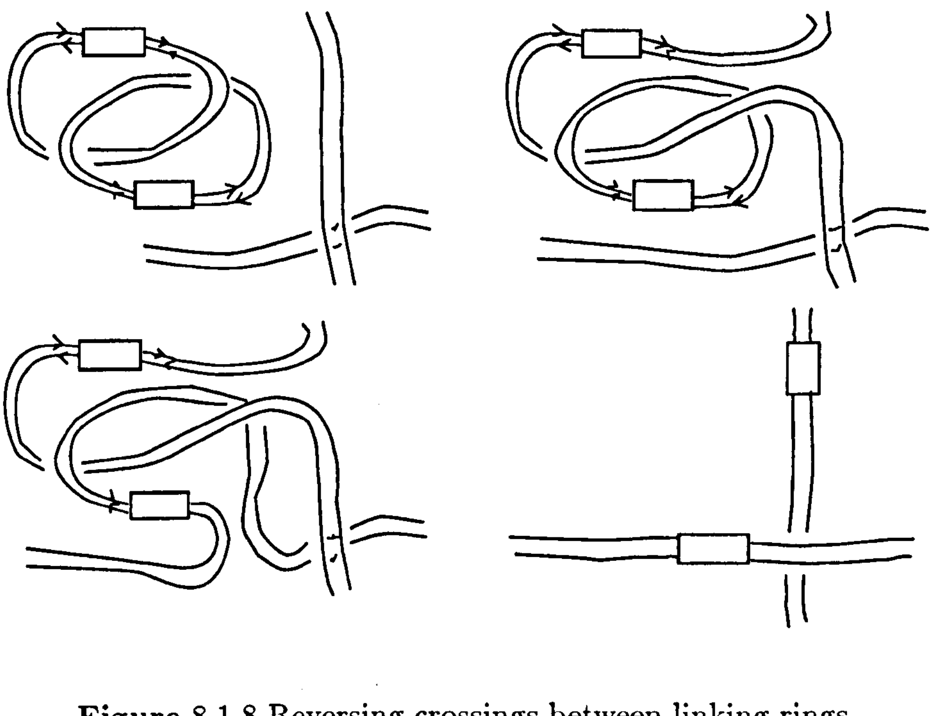

Figure 8.1.8 Reversing crossings between linking rings.

Once we can untangle the paths which the linking rings follow, and use the boxes in pictures to indicate twisting, the knot diagram looks like

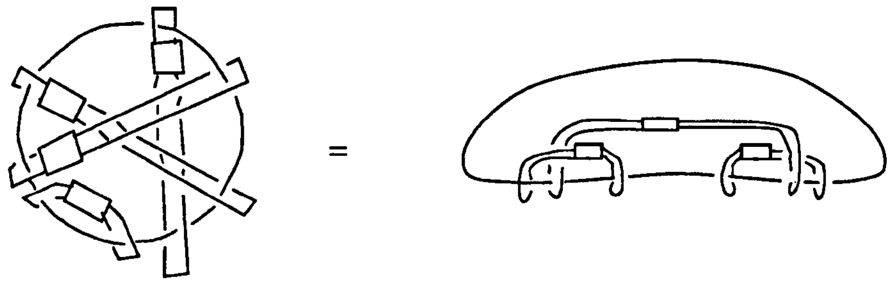

Figure 8.1.9 A second simplification of homotopy representatives.

The next step in reducing the diagram to a sum of generators is to swap the ends of linking rings over, so that the pairs of points where linking rings meet the circle become un-nested. This move requires another generator

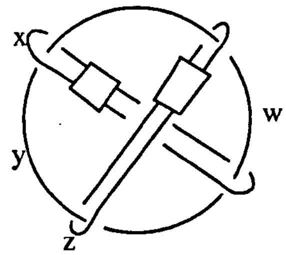

Figure 8.1.10 A generator of type 3.

We can label this diagram; given numbers of twists in the boxes, all labels are determined by x, y and z. But there are two ways to deduce w from these three. The following lemmas check that whatever the orientation of this generator, and however the linking rings link with the circle, the two ways of calculating w give the same result.

Lemma If $x - x^{wx} = q - q^{\bar{p}wpq}$ and $y - y^{\bar{x}wxy} = p - p^{wp}$ (in the diagrams below)

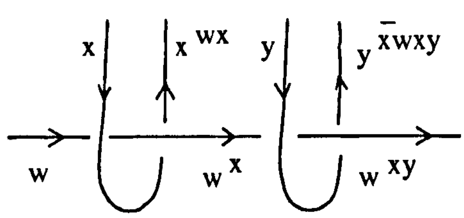

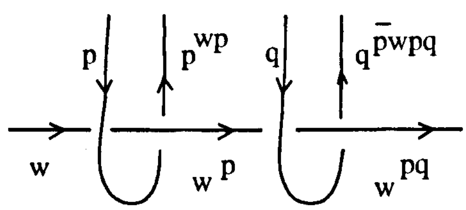

then $w^{xy} = w^{pq}$

Proof

$$\begin{aligned} x - x^{wx} &= x^x - x^{wx} \\ &= a(x - x^w) \end{aligned}$$

$$
\begin{aligned}
& & &= a(1-a)(x-w)\\
&\text{and} & q - q^{\bar{p}wpq} &= q^{q} - q^{\bar{p}wpq}\\
& & &= a(q - q^{\bar{p}wp})\\
& & &= a^2(q^{\bar{p}} - q^{\bar{p}w})\\
& & &= a^2(1-a)(q^{\bar{p}} - w)\\
& & &= a^2(1-a)(a^{-1}q + (1-a^{-1})p - w)\\
&\text{so} & a(1-a)(x-w) &= a^2(1-a)(a^{-1}q + (1-a^{-1})p - w)\\
& & (x-w) &= q + (a-1)p - aw\\
& & x + (1-a)p &= q + (1-a)w\\
&\text{similarly} & p + (1-a)x &= y + (1-a)w
\end{aligned}
$$

$$
\begin{aligned}
&\text{now} & w^{pq} - w^{xy} &= aw^{p} + (1-a)q - aw^{x} - (1-a)y\\
& & &= (a^2w + a(1-a)p + (1-a)q)\\
& & &\quad -(a^2w + a(1-a)x + (1-a)y)\\
& & &= (1-a)(ap + q - ax - y)\\
&\text{and} & ap + q - ax - y &= (x + p - (1-a)w) - (p + x + (1-a)w)\\
& & &= 0
\end{aligned}
$$

as required.

□

Proofs of the following lemmas are similar and will be omitted

Lemma

If $x - x^{wx} = q - q^{pw\bar{p}q}$ and $p - p^{w\bar{p}} = y - y^{\bar{x}wx\bar{y}}$ (in the diagrams below)

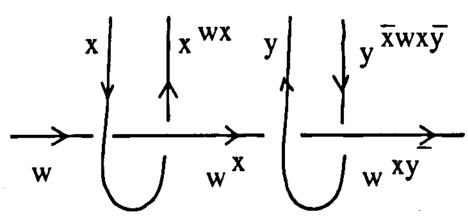

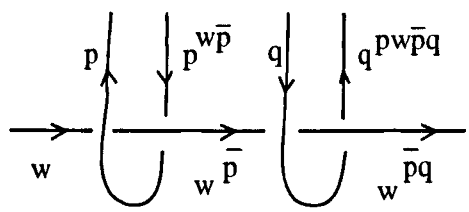

then $w^{x\bar{y}} = w^{\bar{p}q}$ □

Lemma

If $x - x^{w\bar{x}} = q - q^{pw\overline{pq}}$ and $p - p^{w\bar{p}} = y - y^{xw\overline{xy}}$ (in the diagrams below)

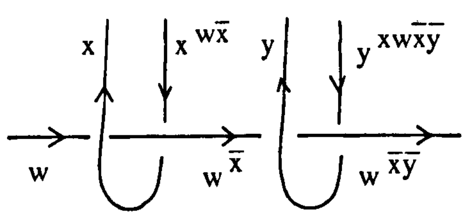

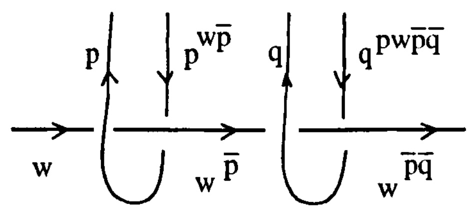

then $w^{\overline{xy}} = w^{\overline{pq}}$ □

The generator allows us to manouevre the diagram as follows

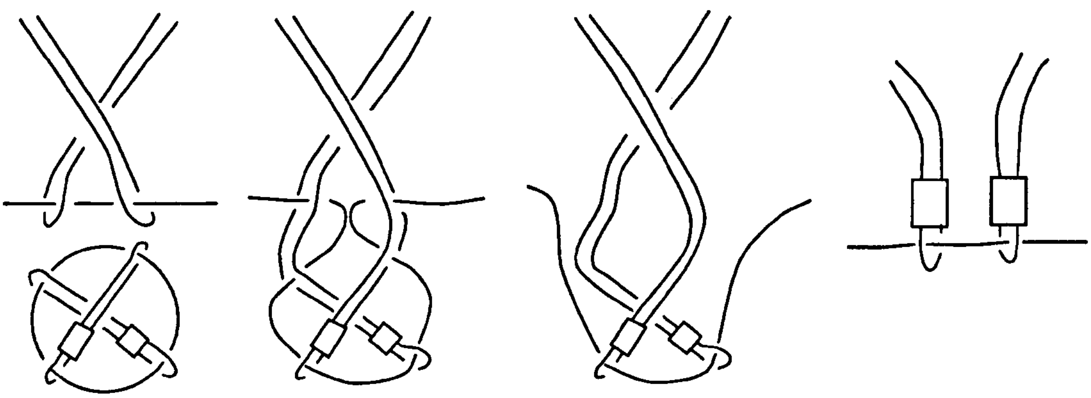

Figure 8.1.11 Exchanging ends of linking rings.

Once the ends of the linking rings are nested around the unknot, we can take a minimal example which looks like

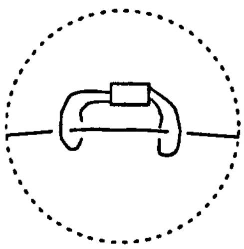

This describes a disc which maps into the classifying space. The boundary of the disc is therefore null-homotopic. The word of the two labels is zero in $\pi_1(\mathbb{B}R_a)$ which is just the associated group of the rack. The labels are equal in the associated group, so they are equal in the operator group (a quotient of the associated group). Invertibility of $(1-a)$ shows that equal operators are equal elements of the rack, so the labels on either end of this link portion are equal. We also could have checked this algebraically. Apply bridging between these equally labelled arcs. The homotopy link diagram has been reduced to a sum of the following types of generator.

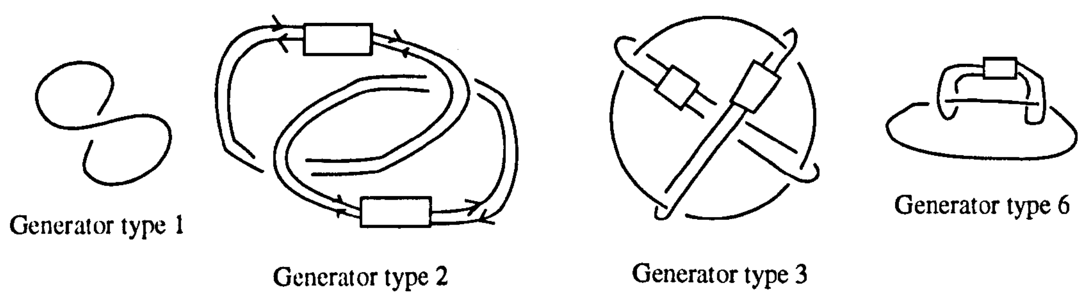

Figure 8.1.12 Generators of types 1,2,3 and 4.

The number of twists in the boxes in these diagrams is determined by the required change in label, up to mod n. n whole twists leaves the labels invariant. We can use a generator of type 5 to eliminate ambiguity over how many twists are in each diagram. This generator has a full complement of positive twists.

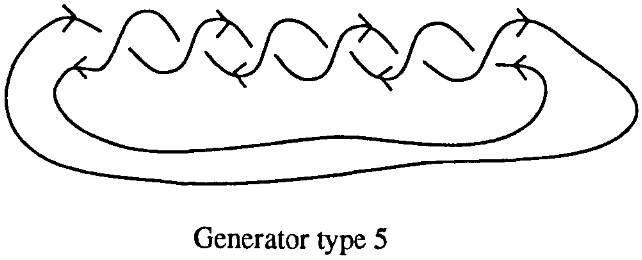

Figure 8.1.13 Generators of type 5.

We can simplify the second and third generator further. In the twists of a generator of type 4 there will be an arc of equal label and opposite orientation to the arc of the original strand below the twists. (If there is not such an arc in the twists, add or subtract generator 5 until there is such an arc). Split up the twists there, and apply the following bridging moves.

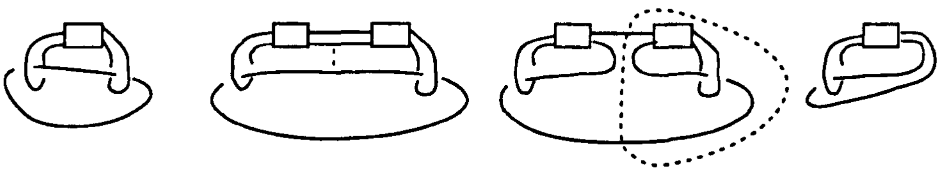

Figure 8.1.14 Reducing generator type 4.

leaving us with a new generator set

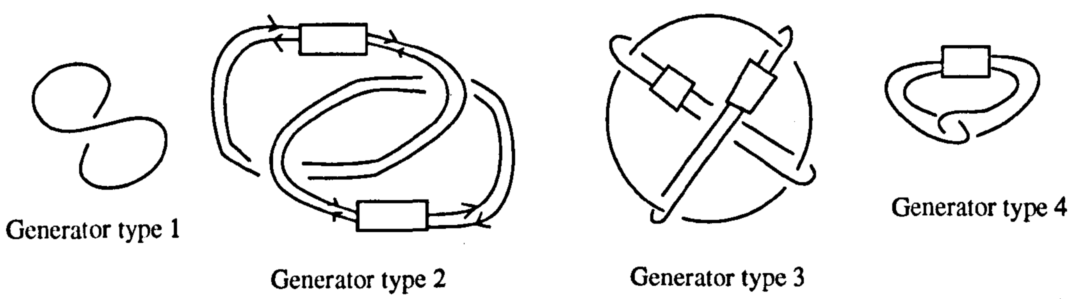

Figure 8.1.15 Generators of type 1,2,3 and 6.

8.2 Reducing the generator set.

To simplify further, I shall make another assumption about the rack. From now on, assume that $a \in \mathbb{Z}_n$ multiplicatively generates $\{1, 2, .., n-1\}$ so any non-zero element of R can be written as a product of a's. We are still assuming that the order n is prime.

Lemma Under the above conditions, the operator group of the rack acts doubly transitively on the rack.

Proof Take distinct elements x and y. 1 does not generate $\mathbb{Z}_n$, so $a \neq 1$ and $a - 1$ is invertible. If x is non-zero, let $w = -(ax)^{-1}(1-a)$ then $x^w = 0$. Then y^w is non-zero (because x and y were distinct). If x was zero, let w be the empty word. Now take integer j such that a^j is the multiplicative inverse of y^w. Let v be the word of j zeros. Then $x^{wv} = 0^v = 0$ and $y^{wv} = 1$. To find and operator which sends x to s and y to t, (x, y and s, t distinct) find operators w and v with $x^w = s^v = 0$ and $y^w = t^v = 1$ then $x^{w\overline{v}} = s$ and $y^{w\overline{v}} = t$. □

Now we can count the generators in more detail. The type of a generator indicates the shape of the link diagram representing the homotopy class. There can be many link diagrams, with varying labelling and varying orientation fitting the same type. The next two lemmas show that these alternative generators of a given type can be equivalent under homotopy of maps to the classifying space, bordism of the labelled link diagrams.

Lemma It is sufficient to include only one generator of type 6 in a generating set.

Proof Here are labelled diagrams of all possibilities

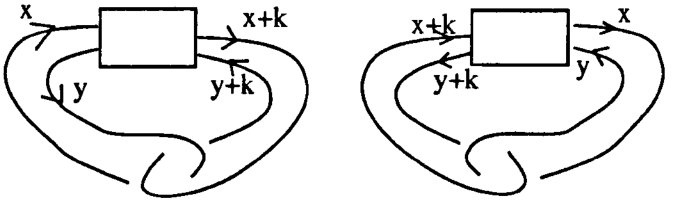

Figure 8.2.1 Labelled generators of type 6.

In the first case we have $y + k = (x + k)^y$ and $x = y^{(x+k)}$ which both give $k = (1-a)^{-1}a(x-y)$. In the second case we have $y = x^{(y+k)}$ and $x + k = (y+k)^x$ which both give $k = (1-a)^{-1}a(x-y)$. This determines the number of twists in the box in terms of labels x and y. We can pass an unknot over the whole diagram and back underneath, to change the label x into 0, say. Then $0^0 = 0$ so provided x and y were different (if they were the same the diagram collapses to the empty diagram) we can repeatedly pass a 0-labelled unknot over the diagram. a generates the rack, and $r^0 = ar$ so eventually the other label, which started as y will become 1.

Without loss of generality, $x = 0$ and $y = 1$ thus the number of whole twists is 1 or -1, and these are inverse. □

Lemma It is sufficient to include only one generator of type 5 in a generating set.

Proof The only decision to be made about a generator of type 5 is the labelling. Double transitivity of the action of the operator group means we may assume two given labels are 0 and 1. This fixes all other labels. □

Finally we can use one more generator

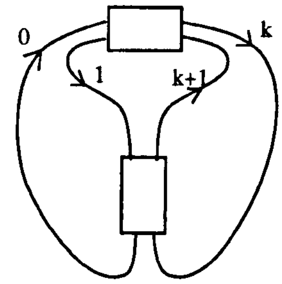

Generator type 7

Figure 8.2.2 Generators type 7.

The crossings in this diagram are all positive. The diagram is an alternating knot diagram.

Lemma It is sufficient to include $\frac{n-1}{2}$ generators of type 7 in a generating set.

Proof Given the labels 0 and 1, the numbers of twists mod n determine and are determined by the label k. If k is zero then the diagram can be reduced to the empty diagram by bridging moves. k can be chosen from 1, 2, ..,$n-1$. But the inverse of the k^{th} generator is the $n-k^{th}$ generator.

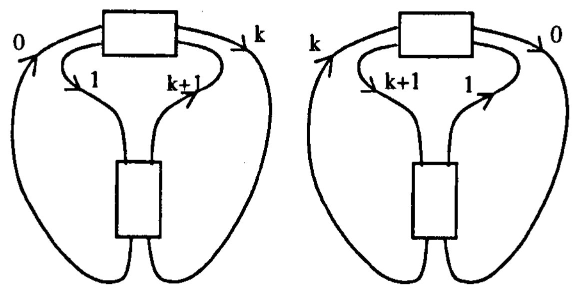

Generator type 7 The inverse.

Figure 8.2.3 The inverse of a generator of type 7.

Now use double transitivity to change the inverse of the k^{th} generator into a known generator. First take r with $k^r = 0$ so $ak + (1-a)r = 0$. This equation defines r mod n.

Next apply $-^0$ enough times to $(k+1)^r$ to change it to 1.

$$(k+1)^r = a(k+1) + (1-a)r = a(k+1) - ak = a$$

Recall that $x^0 = ax$ so we find an integer s with $a^{(s+1)} = 1$. In this last equation, the exponent is a power, meaning a multiplied $s+1$ times, and is not the rack exponent. Finally, apply these rack operators (r then 0 s times) to the label 0. It becomes $-ak.a^s = -k = n-k$.

So the $n-1$ generators pair off as inverses leaving us with $\frac{n-1}{2}$. □

We can now eliminate generators of types 2 and 3 using the type 7.

Lemma Any generator of type 2 is a sum of generators of types 1, 5 and 7.

Proof Use double transitivity of the rack action (as in the previous lemma) and we can assume that two independent strands are labelled 0 and 1. Then rotate the lower circle (and possibly replace m twists by $n-m$ reversed twists) until the neighbouring strand is also labelled 0. We can then bridge as shown.

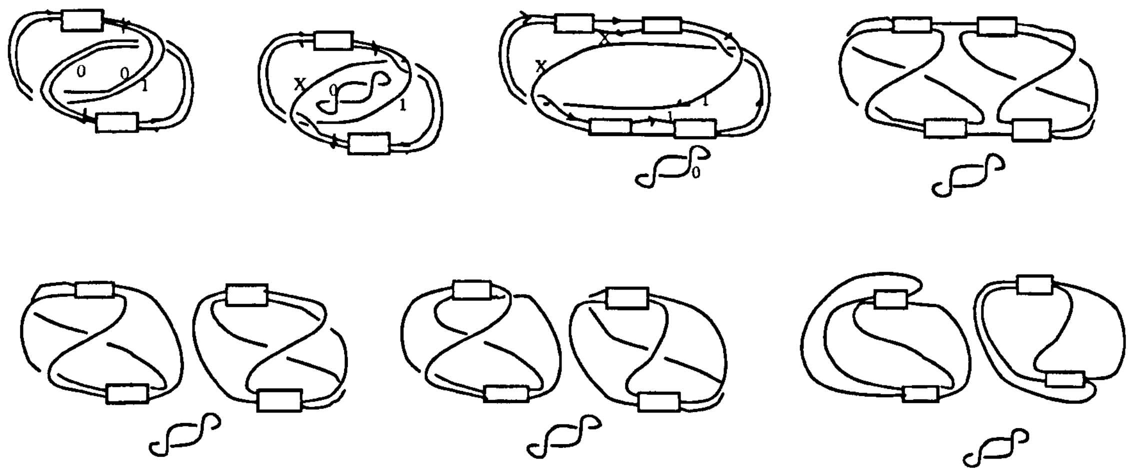

Figure 8.2.4 Reducing generators of type 2.

□

Lemma Any generator of type 3 is a sum of generators of types 1, 5 and 7.

Proof

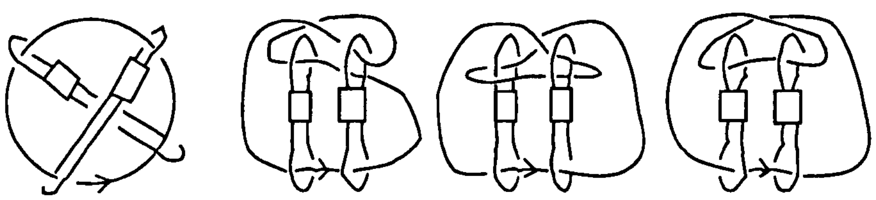

There are four possible combinations of orientations on the twisted linking rings but the the proofs are all similar;

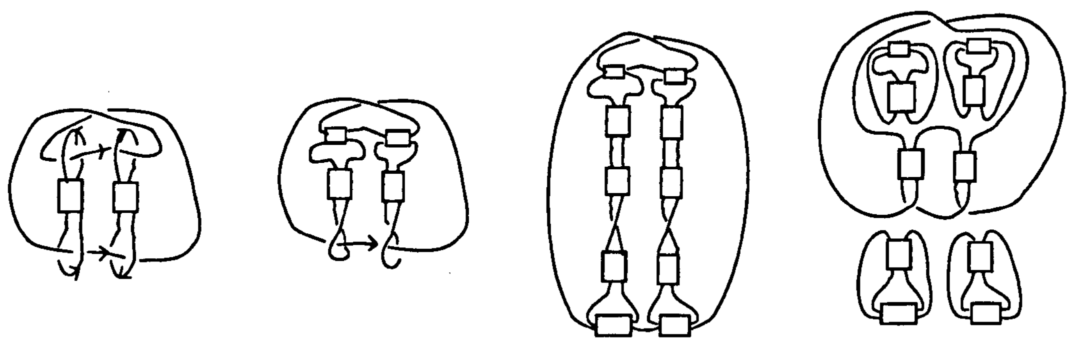

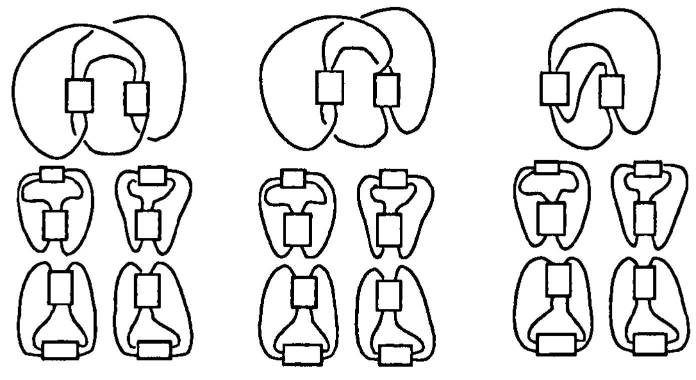

Figure 8.2.5 Reducing a generator of type 3.

□

Now note that generator type 6 is a specific instance of a generator type 7, with the number of whole twists at the bottom fixed at 1. Thus every link diagram representative has been reduced to a sum of $\frac{n+3}{2}$ generators; a positive figure-of-eight labelled 0, a pair of strands labelled 0 and 1 twisted positively n times and reattached, and $\frac{n-1}{2}$ generators of type 7 (with $k = 1, 2, .., \frac{n-1}{2}$).

Conjecture If R_a is an Alexander quotient on an odd prime order group $\mathbb{Z}_n$, where $a \in \{2, 3, .., n-1\}$ generates the group by multiplication, then $\pi_2(\mathbb{B}R_a) \cong \mathbb{Z}^{(\frac{n+3}{2})}$

8.3 Example $\pi_2(\mathbb{B}D_3)$.

The dihedral rack of order three has table

	a	b	c
a	a	c	b
b	c	b	a
c	b	a	c

The above procedure reduces every labelled diagram to a sum of the twisted generator, the figure-of-eight and the k-th generator where $k = 1$ (this is just a trefoil).

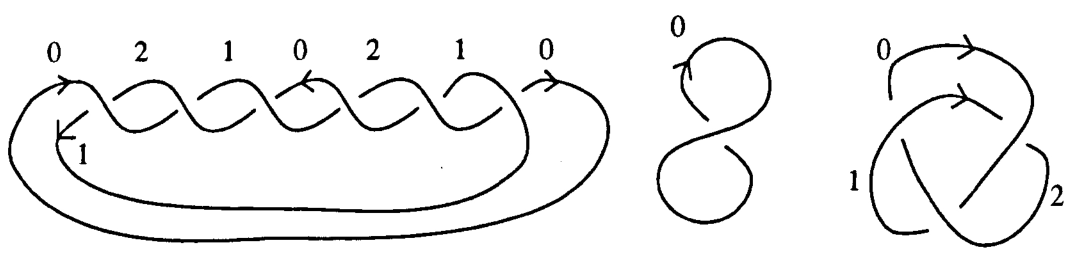

Figure 8.3.1 A generating set for $\pi_2(\mathbb{B}D_3)$.

Chapter 9. Topological racks

We have discussed the classifying space of rack, and the first and second homotopy groups of that space. The classifying space was the realisation of a cubical set. If the rack itself has a topology, with the rack operations all continuous, then instead of a cubical set, we get a cubical space, whose realisation inherits a topology from the rack itself. In this chapter we introduce this topic, starting with the cell structure of the classifying space, then describing a method of calculation of the second homotopy groups by diagram manipulation. The second homotopy group of the plane racks and the sphere racks are calculated explicitly

9.1 A non-CW structure on the classifying space.

Given a topological rack R with a CW structure, the classifying space $\mathbb{B}R$ inherits a cellular structure. Cells of $\mathbb{B}R$ are

$$e(e_1,..,e_r) = \{(t_1,..,t_r,x_1,..,x_r) \ : \ x_i \in e_i\}$$

where the e_i are cells of R. I will abbreviate $e(e_{i_1},..,e_{i_r})$ to $e(i_1,..,i_r)$. The dimension of the cell $e(i_1,..,i_r)$ is $r + \dim e_{i_1} + .. + \dim e_{i_r}$

This cellular structure on $\mathbb{B}R$ in general will fail to be a CW complex. For example, if v, w are vertices of R then the cell $e(v,w)$ has boundary points in the interiors of $e(v)$ and $e(w)$, and there are boundary points (t, v^w). v^w is a point in the rack which will fall into the interior of a cell e^j for some j. Then the boundary of the 2-dimensional cell $e(v,w)$ will meet the interior of the $j+1$-dimensional cell $e(e^j)$.

We can, however, place constraints on R to ensure that that the cellular structure of $\mathbb{B}R$ is a CW-structure, or that it is well-behaved enough to simplify representatives of homotopy elements.

Given a map $X \longrightarrow \mathbb{B}R$, X a compact n-dimensional manifold, take a cell of $\mathbb{B}R$ of dimension greater than n, e. If the image of X only meets cells which meet the boundary of e then the image of X can be pushed out of the interior of e. We will place a partial order on the cells of the classifying space to ensure that such moves are possible and do not push the image of X into less desirable cells.

Say that $e(i_1,..,i_r)$ is less than $e(j_1,..,j_s)$ if and only if either $r < s$ or, if $r = s$ then the dimension of $e(i_1,..,i_r)$ is less than that of $e(j_1,..,j_s)$

Lemma If a point in the boundary of $e(j_1,..,j_s)$ meets the interior of $e(i_1,..,i_r)$ then $e(i_1,..,i_r) < e(j_1,..,j_s)$.

Proof Points in the boundary of $e(j_1,..,j_s)$ are either obtained by taking a boundary point of the s-cube

$$(t_1,..,t_{k-1},0,t_{k+1},..,t_s,x_1,..,x_s) \sim (t_1,..,t_{k-1},t_{k+1},..,t_s,x_1,..,x_{k-1},x_{k+1},..,x_s)$$

and

$$(t_1,..,t_{k-1},1,t_{k+1},..,t_s,x_1,..,x_s) \sim (t_1,..,t_{k-1},t_{k+1},..,t_s,x_1^{x_k},..,x_{k-1}^{x_k},x_{k+1},..,x_s)$$

in which case the index r of $e(i_1,..,i_r)$ is $s-1$ and $e(i_1,..,i_r) < e(j_1,..,j_s)$

or the points on the boundary are obtained by taking a point x_k in the boundary of one of the cells e_{j_k}. R has a CW-structure. This ensures that the point x_k belongs to the interior of a cell of lower dimension, and $e(i_1,..,i_r) < e(j_1,..,j_s)$ again, as required. □

If I push the image of X out of the highest (in this partial order) cell which it meets, then we have reduced this maximum-order cell. We have the following result

Theorem If R is a rack with a CW structure and $f: X \longrightarrow \mathbb{B}R$ where X is a compact n-dimensional manifold then there exists $g: X \longrightarrow \mathbb{B}R$, homotopic to f, such that a cell $e(i_1,..,i_r)$ whose interior meets $g(X)$ has $r < n$ or $r = n$ and all the cells e_{i_k} being vertices of R.

Proof X is compact, so meets the interior of finitely many cells of $\mathbb{B}R$. The boundary of any cell of $\mathbb{B}R$ is itself compact, and meets the interiors of only finitely many other cells. Moreover, these other cells are smaller in the partial order, either with the index r reduced, or the dimension reduced. We can push X out of finitely many cells until the highest-order cell whose interior meets the image of X is of dimension n or less.

A cell $e(i_1,..,i_r)$ with $r > n$ has dimension greater than n. So the highest order cell meeting the image must be $e(i_1,..,i_r)$ with $r \leq n$. If a cell $e(i_1,..,i_n)$ has dimension less than or equal to n, it must be equal to n and all the cells e_{i_k} must be vertices of R. □

We can strengthen this result by imposing further conditions on the CW-structure of R. In practice we can see that these are not restrictive.

Theorem If R is a CW-rack in which the 0-skeleton, 1-skeleton,..,n-skeleton are all subracks, and $f: X \longrightarrow \mathbb{B}R$ where X is a compact n-dimensional manifold then there exists a homotopic map g such that $g(X)$ only meets cells of the form $e(i_1,..,i_r)$ where the dimension of this cell is less than or equal to n and each cell e_{i_k} lies in the n-skeleton of R.

Proof Place a partial order on the cells of $\mathbb{B}R$ as follows: describe a cell $e(i_1,..,i_r)$ as *good* if all the cells e_{i_k} lie in the n-skeleton of R, and *bad* otherwise. Then, on the set of good cells, and on the set of bad cells, define $e(i_1,..,i_r) < e(j_1,..,j_s)$ if and only if $r < s$ or $r = s$ and the dimensions have $dim[e(i_1,..,i_r)] < dim[e(j_1,..,j_s)]$. Further, define that all good cells are less than all bad cells.

Take a cell in the classifying space, $e(j_1,..,j_s)$ whose boundary meets the interior of $e(i_1,..,i_r)$.

Either this boundary point was obtained by taking the boundary of the s-cube, in which case we have $r < s$ and if $e(j_1,..,j_s)$ was good then so is $e(i_1,..,i_r)$ by the skeletal condition on R, giving $e(i_1,..,i_r) < e(j_1,..,j_s)$

or the point $(t_1,..,t_s,x_1,..,x_s)$ has some x_k in the boundary of e_{i_k}. The rack is a CW-complex, and goodness is preserved under taking cell boundaries, so we have again $e(i_1,..,i_r) < e(j_1,..,j_s)$.

The finiteness argument from the previous proof holds here and pushing the image of X out of finitely many cells in $\mathbb{B}R$, we have the maximal cell whose interior meets the image of X is at most n dimensional. A bad cell has dimension at least $n+1$, so the new image of X only meets the interior of good cells. The dimension of $e(i_1,..,i_r)$ is at least r, so the image of X meets good cells $e(i_1,..,i_r)$ with r less than or equal to n. If $r=n$ then all the e_{i_k} are vertices of R. □

Corollary If R is a CW-rack in which the 0-, 1-, and 2-skeleta are subracks then we may assume that any homotopy representative $f: S^2 \longrightarrow \mathbb{B}R$ meets only cells $e(i_1,..,i_r)$ with $r \leq 2$ and e_{i_k} in the 1-skeleton or R.

Moreover, any homotopy between such representatives can be made to meet only cells $e(i_1,..,i_r)$ with $r \leq 3$ and e_{i_k} in the 2-skeleton of R □

Maps $f: S^2 \longrightarrow \mathbb{B}R$ meeting only the basepoint, $e(v_i)$, $e(e_i)$, and $e(v_i, v_j)$ (where the v_i are vertices of R and the e_i are 1-cells of R) can be made transverse to the centres of these cells, and the preimages form a link diagram in the two-sphere, with specialised points on the arcs.

The neighbourhoods of these points map to a cell $e(e_i)$ in $\mathbb{B}R$. The labels on each side of the specialised points are the vertices at each end of the edge e in R. They're marked on diagrams as follows

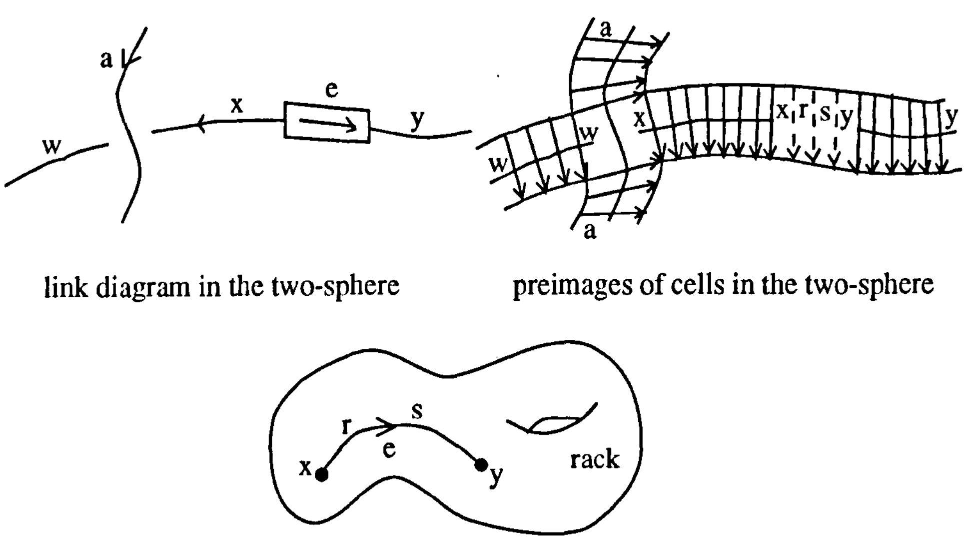

Figure 9.1.1 The origin of specialised points.

9.2 Allowed moves on representative diagrams.

Homotopy between such representatives is confined to cells of the form $e(v_i, v_j, v_k)$ (giving Reidemeister move 3) $e(e_i, v_j)$ and $e(v_i, e_j)$. These last two boundaries give us allowed moves on diagrams about how to pass specialised points over and under crossings.

Passing the 2-sphere through a cell $e(e, v)$ (now e is an edge of R and v is a vertex) corresponds to a diagram relator as shown below

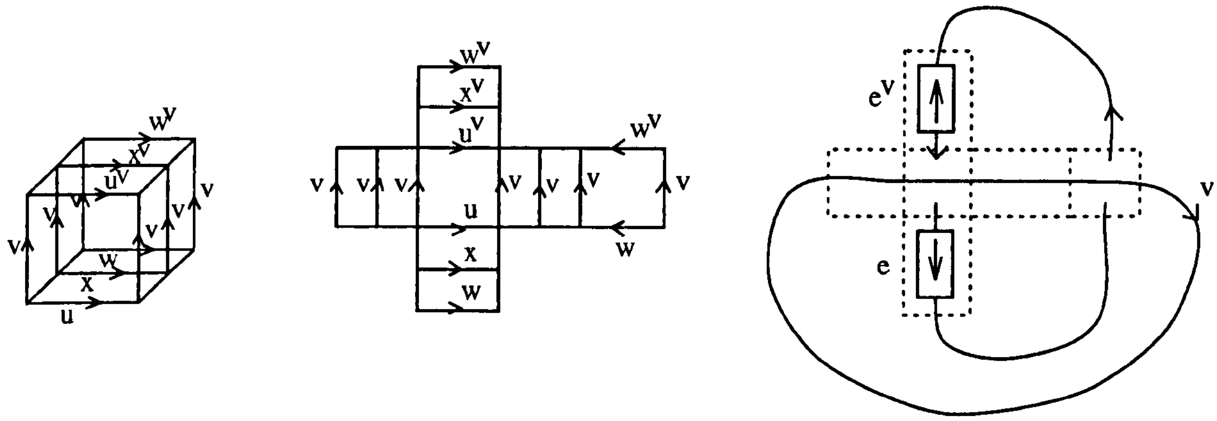

Figure 9.2.1 Relator from the 3-cell $e(e, v)$.

Theorem The following moves are allowed on diagram representatives of π_2 elements

Figure 9.2.2 Rules from the 3-cell $e(e, v)$.

Proof

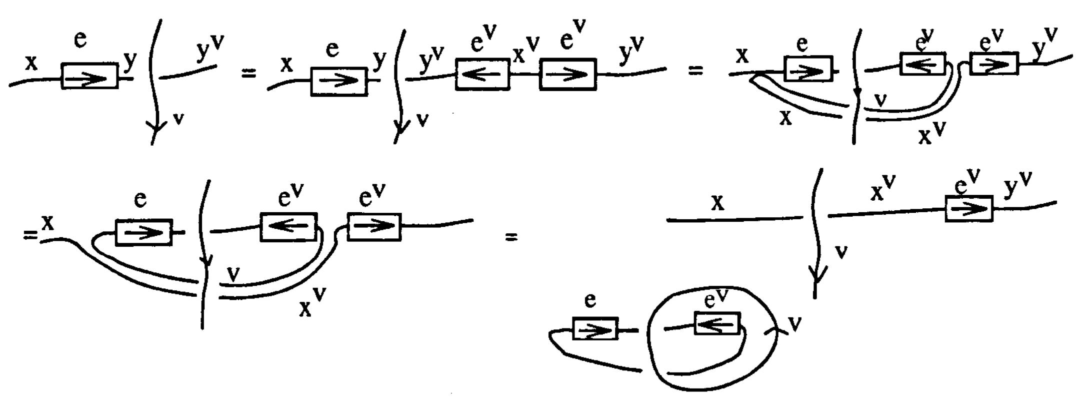

□

Passing the 2-sphere through a cell $e(v, e)$ gives a diagram relator

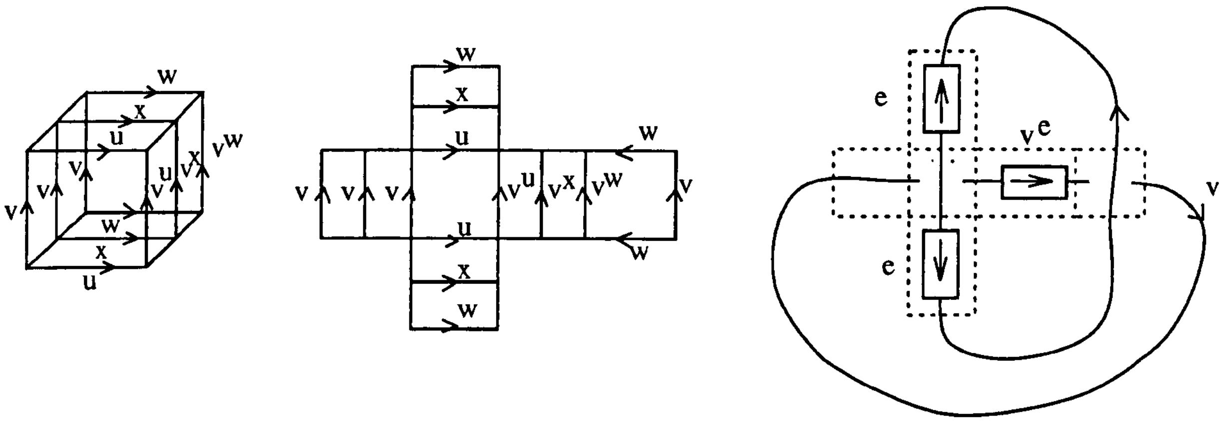

Figure 9.2.3 Relator from the 3-cell $e(v, e)$.

Theorem The following moves are allowed on diagram representatives of π_2 elements

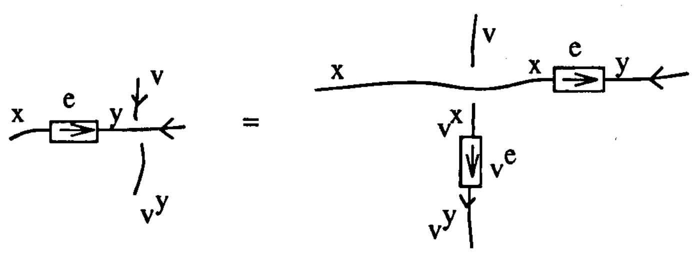

Figure 9.2.4 Rules from the 3-cell $e(v, e)$.

Proof

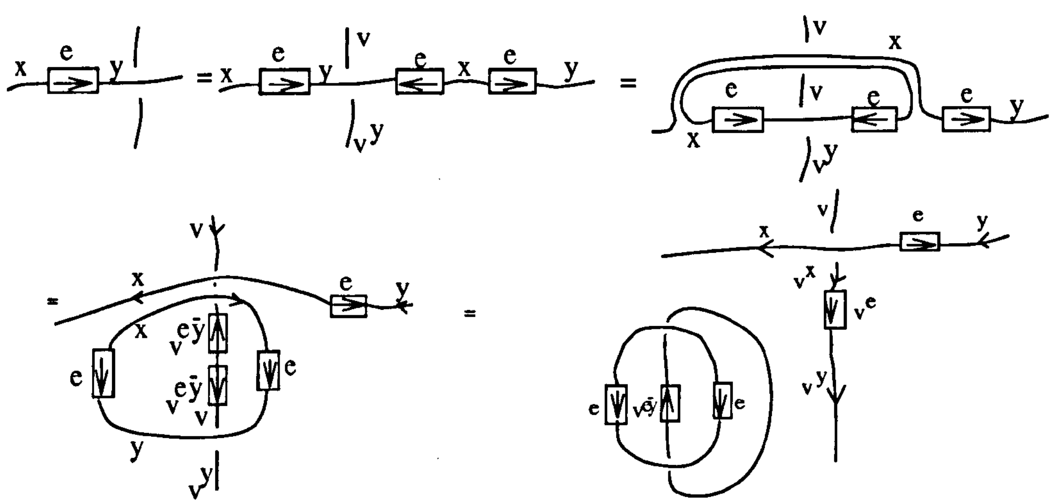

□

The 2-sphere also pass through three-cells of the form $e(i)$. These come from 2-cells in R and their boundary reads off a word in the edges of R. These words form null-homotopic link diagrams

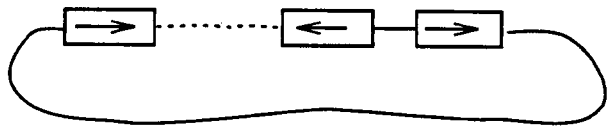

Figure 9.2.5 An edge-word relator diagram.

9.3 The Plane Rack.

Here $R = \mathbb{R}^j$ with rack structure $a^b = 2b - a$. The classifying space $\mathbb{B}R$ is homotopy equivalent to the classifying space of the trivial one-element rack; the rack homomorphism taking the single element to the origin of $\mathbb{R}^j$ and the rack homomorphism taking all elements of $\mathbb{R}^j$ to the single element both give maps between the classifying spaces. These maps give a homotopy equivalence, the composite $\mathbb{B}(*) \longrightarrow \mathbb{B}(R) \longrightarrow \mathbb{B}(*)$ is the identity, and the other composite $\mathbb{B}(R) \longrightarrow \mathbb{B}(*) \longrightarrow \mathbb{B}(R)$ is the last map of the homotopy

$$\begin{array}{ccc} \mathbb{B}\mathbb{R}^j & \longrightarrow & \mathbb{B}\mathbb{R}^j \\ (t_1, .., t_n, a_1, .., a_n) & \mapsto & (t_1, .., t_n, \lambda a_1, .., \lambda a_n) \end{array}$$

This map is welldefined, the identity when $\lambda = 1$ and the required composite when $\lambda = 0$. So

$$\pi_2(\mathbb{B}\mathbb{R}^j) \cong \pi_2(\mathbb{B}(*) \cong \mathbb{Z}$$

Using link diagrams, first we need to give $\mathbb{R}^j$ a CW-structure, split it up into j-cubes and their faces so that the vertices have coordinates of integers and the edges are $\{(m_1, .., m_j + t, .., m_n) : t \in [0, 1]\}$. Check that the 0-skeleton and the 1-skeleton form subracks of R. Then any link diagram has crossings which we can undo. Because the 1-skeleton is connected, we can choose an edge-path between any two vertices. So we can insert specialised edge-labelled points to change any arc-label to any other.

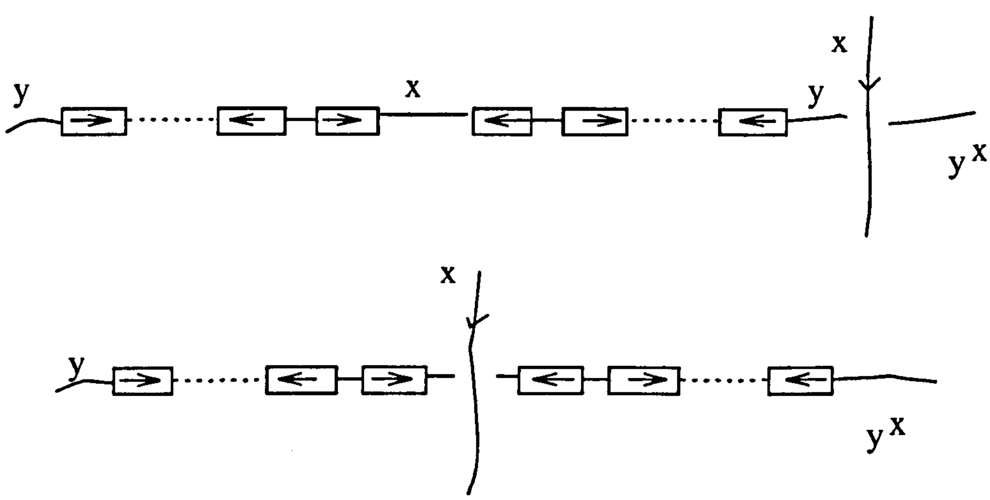

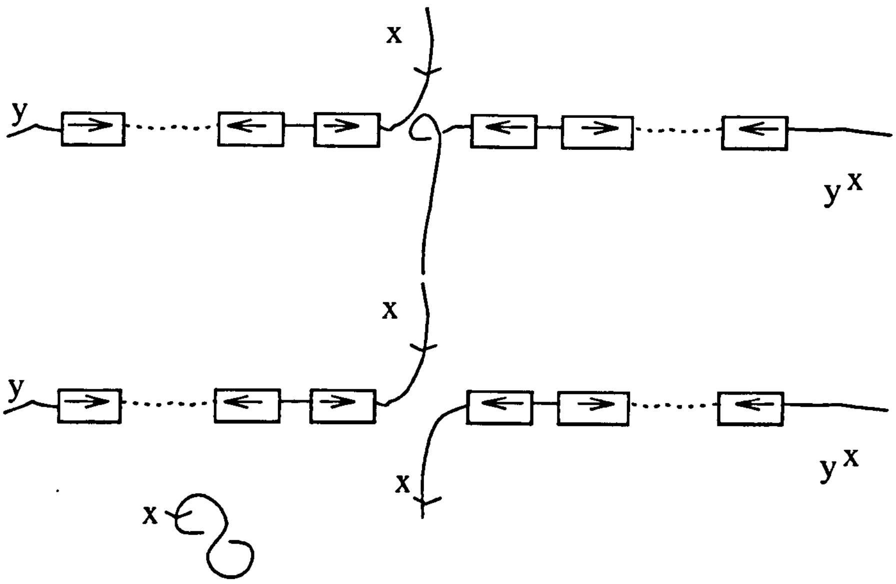

Figure 9.3.1 Undoing crossings in $\pi_2(\mathbb{B}\mathbb{R}^j)$.

The link diagram becomes a sum of unknots with specialised points and figures-of-eight. Any edge-loop in $\mathbb{R}^j$ is null-homotopic through 2-cells so the unknots can be forgotten, leaving us with a single generator $\pi_2(\mathbb{B}\mathbb{R}^j) \cong \mathbb{Z}$ as required.

9.4 The Sphere rack.

Here $R = S^j$ with racks structure $a^b = 2b - a$ along geodesics of the sphere. The sphere has a CW structure with just a basepoint and a j-cell. The vertex is a subrack (the rack is a quandle). If j is greater than 1 then the links representing second homotopy classes have no specialised points, and $\pi_2(\mathbb{B}R) \cong \mathbb{Z}$. If $j = 1$ then the link diagrams have specialised points. There is only one vertex, only one arc-label, so we can undo all the crossings, leaving us with a sum of figures-of-eight and an edge generator.

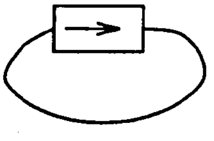

Figure 9.4.1 A generator for $\pi_2(\mathbb{B}S^1)$.

The reflection rack on S^1 has $a^b = 2b - a$. Deduce that $e^0 = -e$ and $0^e = 2e$ The rules of diagram manipulation are as follows

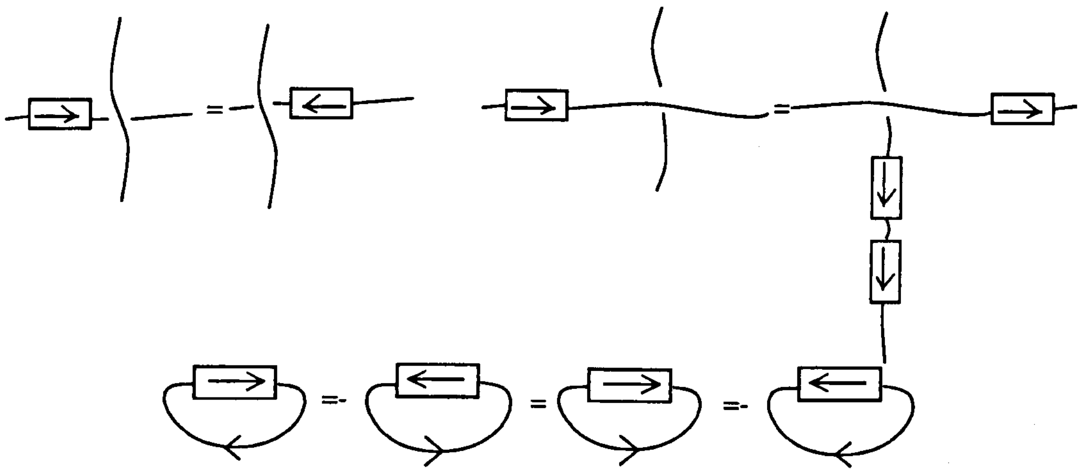

Figure 9.4.2 Relations in $\pi_2(\mathbb{B}S^1)$; the reflection rack.

We can count the number of edge generators in a link diagram by shading the plane in chequerboard fashion and orienting the plane. Each occurence of an edge has orientation which either agrees or disagrees with the orientation of the neighbouring black region.

The trivial rack on S^1 has $a^b = a$ for all a, b in the circle, $e^0 = e$ and $0^e = 2e$. The rules of diagram manipulation are as follows

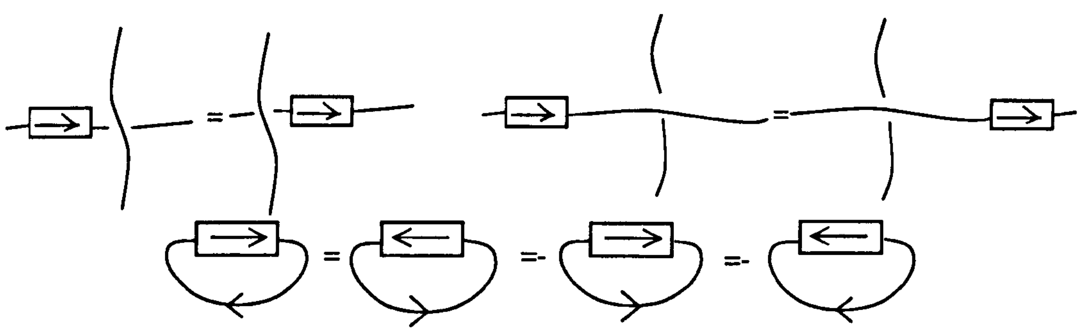

Figure 9.4.3 Relations in $\pi_2(\mathbb{B}S^1)$; the trivial rack.

In a link diagram, the edge orientation either agrees or disagrees with the orientation of the arc. This is how to count the number of edge generators in a diagram.

Both these circle racks have $\pi_2(\mathbb{B}S^1) \cong \mathbb{Z} \oplus \mathbb{Z}$.

9.5 Homotopy invariance of the rack space.

It is clear that some connection between the rack structures is required to ensure homotopy equivalence of the rack spaces. Take the trivial rack on two elements. The first homotopy group of the rack space is free abelian on two generators. The first homotopy group of the rack space of the cyclic rack on two elements, however, is free abelian on only one generator.

If two topological racks are homotopic, with the homotopy respecting the rack structures, then we can construct a map between the classifying spaces. The map preserves the basepoint, and is natural on the 1-cubes. These are indexed by rack elements, and the homotopy associates the elements of one rack with the elements of the other. The boundaries of 2-cubes map to squares which no longer necessarily bound 2-cubes in the second classifying space. But the image squares are homotopic to 2-cube boundaries. This paves the way for an inductive definition of a homotopy equivalence between the two classifying spaces.

Theorem If R is a topological space, with a continuous map $\alpha: I \times R \times R \longrightarrow R$ such that each map

$$\alpha_t: R \times R \longrightarrow R$$

gives R a rack structure, then the classifying spaces $\mathbb{B}(R, \alpha_0)$ and $\mathbb{B}(R, \alpha_1)$ are homotopy equivalent. □

Chapter 10. The third homotopy group

In this chapter we consider the third homotopy group of the classifying space of a rack. As in the geometric approach to the second homotopy group, we use transverse representatives of each homotopy class and consider cell midpoint preimages in the three-sphere. In the two-dimensional case this gave a framed labelled link diagram in the two-sphere. In the three-dimensional case we get framed labelled immersed surfaces in the three-sphere. The worst kind of singularity such a surface will have is a triple-point, the preimage of the centre of a 3-cube in the classifying space. A triple point locally looks like the $x = 0$, $y = 0$ and $z = 0$ planes intersecting at the origin of 3-space. The orientation of cubes in the image gives an order at each intersection, at triple points we can either order the surfaces or order the axes (the three double-point intersection lines through the triple point). In any case, we can manipulate such surfaces using bordism to simplify homotopy representatives. We first calculate the third homotopy group of the trivial rack. This allows us to forget about labels on the surfaces. Next we calculate the third homotopy group of the cyclic racks.

10.1 Transverse representatives of homotopy classes.

A representative $S^3 \longrightarrow \mathbb{B}R$ can be chosen transverse to centres of 1,2 and 3-cubes in $\mathbb{B}R$. The preimages of centres of 3-cubes have cubes around them in S^3, with interiors mapping homeomorphically to a 3-cube in $\mathbb{B}R$. The centres of the faces of these 3-cubes map to centres of 2-cubes. There are 1-manifolds embedded in S^3 which map to centres of 2-cubes, with 2-cube bundles over them;

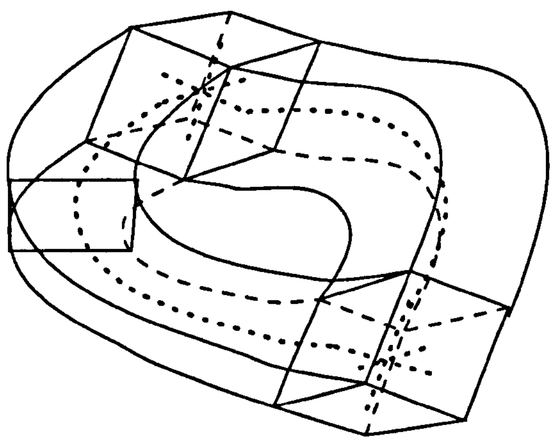

Figure 10.1.1 A transverse preimage for $\pi_3(\mathbb{B}R)$.

There are consistent origins, axis ordering and labels on these preimage cubes. Finally, the 1-cubes have preimages forming 2-manifolds in S^3 filling the gaps. The preimages of the centres of 1, 2 and 3-cubes give an immersed 2-manifold, L, in S^3 with singular set $T \cup D$; T is a 0-manifold of triple points, and D is a 1-manifold of double points. The surface L with these singular points removed is a framed 2-manifold whose components are labelled by R. Each point of D and T has a framed neighbourhood as follows

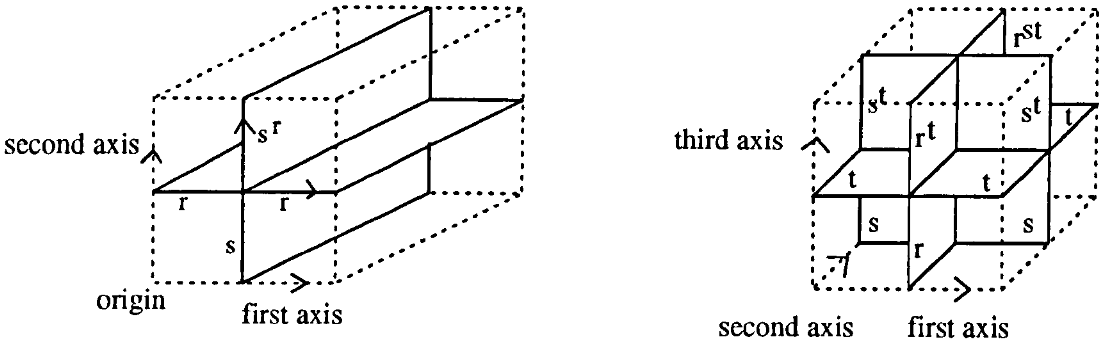

Figure 10.1.2 Singular points in a π_3 representative.

Homotopy between such representatives corresponds to bordism of these immersed surfaces, with regular homotopy. Possible obstructions to apparent simplification occur because of unhelpful axis ordering;

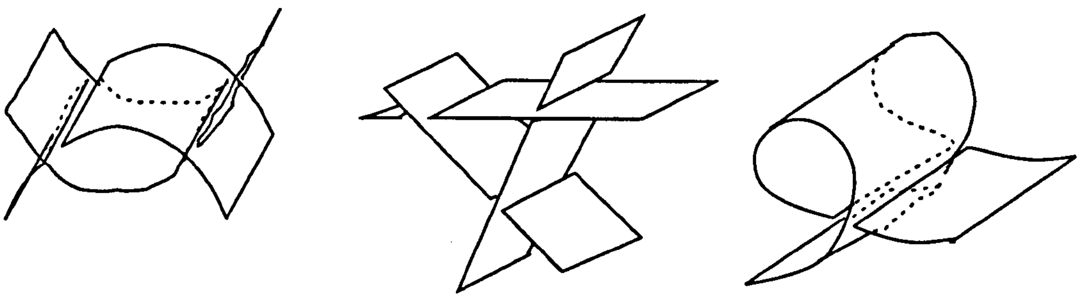

Figure 10.1.3 Obstructions to simplifications of the surface.

Such obstructions are discussed in [HH]. The surface splits S^3 into connected components. The boundary of each component is an oriented surface with double-point singularities forming a graph. Each vertex of the graph (a triple point) has valency 3.

10.2 Calculation of $\pi_3(\mathbb{B}C_1)$; the trivial rack.

Here we can forget about labellings, but still pay attention to the framing and the singular ordering.

In the analysis of π_2 representatives, it was constructive to concentrate on the crossings of the link diagram, and try to isolate them. This was acheived in simple cases by introducing a new link component near a crossing and using bridging moves. We put such new components in two of the four quadrants round a crossing. To apply a similar procedure in the calculation of π_3, we need to choose a suitable surface to introduce, decide where to put it and apply bridging moves to isolate the set of singular points. There a eight quadrants around a triple point, and first we'll specify four of these by shading the complement of the surface $L \subset S^3$ black and white.

Consider a plane at first disjoint from L, moving across L. At any time, the intersection of the plane with the surface forms a link diagram in the plane possibly with singular points (from maxima or minima of the surface) or arcs which cross (at saddle points). The plane can be shaded alternately black and white. As the plane moves across L, we come across birth, death, saddle-points and Reidemeister moves on the intersection, all of which allow a consistent choice of chequerboard shading.

At each doublepoint singularity, the shading of the four quadrants is alternate and is said to agree or disagree with the framing on the surfaces according to the following diagram. The diagram shows sections through the double point line, and the framing of each surface corresponds to the arrows using the orientation convention introduced in chapter 7.

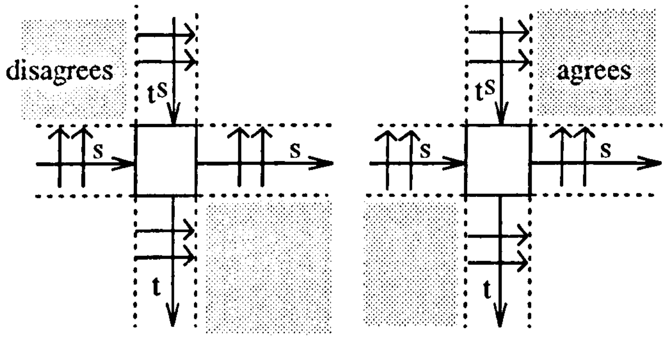

Figure 10.2.1 Chequerboard shading in two dimensions.

At each of the four regions shaded black near a triple point, we have one region in which the shading agrees with all three double-point lines, and three regions in which the shading agrees with one, but disagrees with the remaining two double point lines.

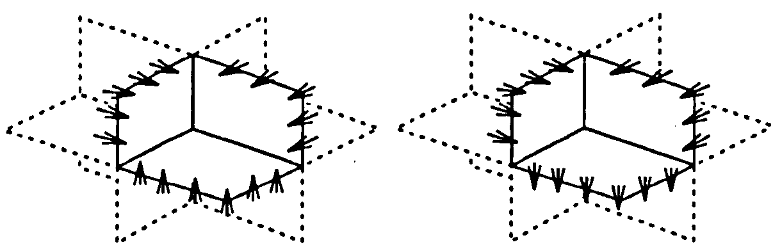

Figure 10.2.2 Chequerboard shading in three dimensions.

Construct a surface to insert near singular points in the components shaded black. If the shading agrees with the double-point framing, we will be able to bridge with an unknot tube (appropriately framed). But if the shading disagrees with the framing, then to bridge with both surfaces we will need a figure-of eight. We have to choose an ordering for the surfaces which intersect at the figure-of-eight. This ordering is determined by the framing near the doublepoint line in the original surface. Put such tubes in two of the four quadrants along double-point lines, and join them up near triple points as shown. The new surface is a high-genus torus with circles of double-point lines.

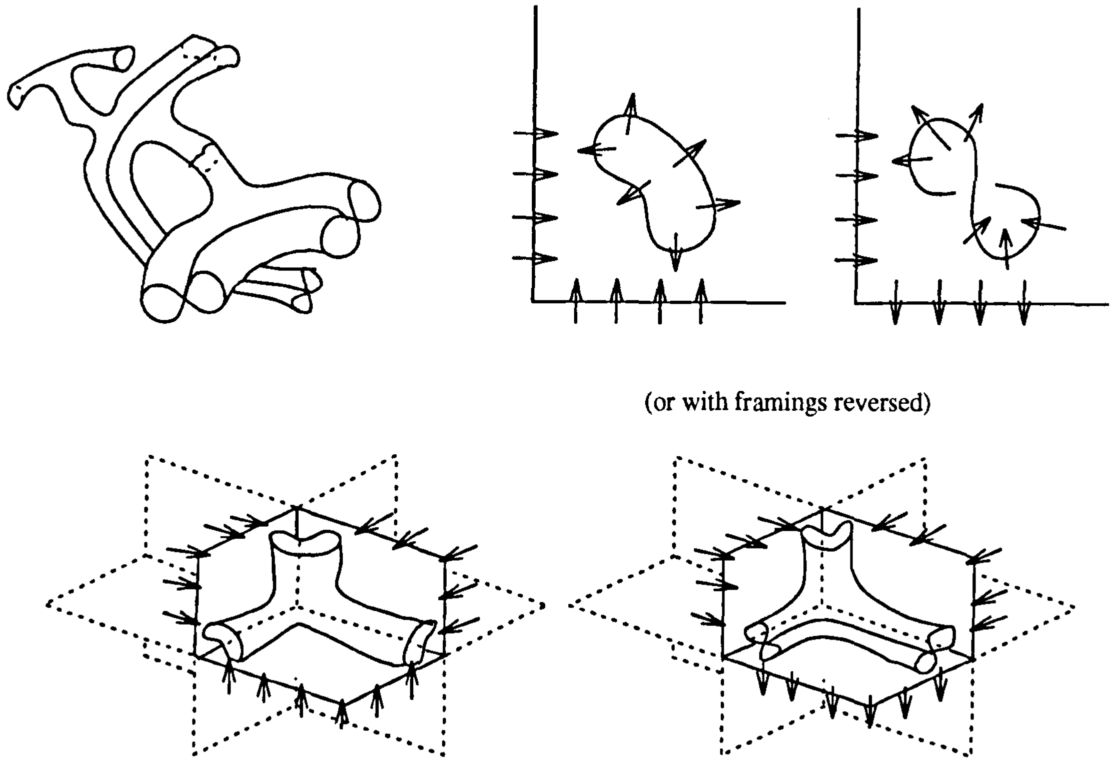

Figure 10.2.3 The triple point with an added surface.

There follow three views of a triple point neighbourhood. The framing is shown by the arrows, and the chequerboard shading has the nearest quadrant black, white and white respectively. If the shading is opposite with respect to the framing, the analysis is similar.

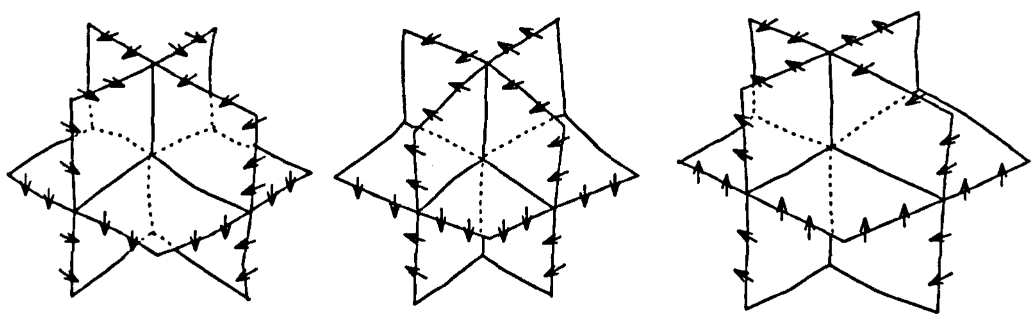

Figure 10.2.4 Three views of a triple point.

Now add the surface along the double-point lines. This added surface will be interpreted in terms of known generators later.

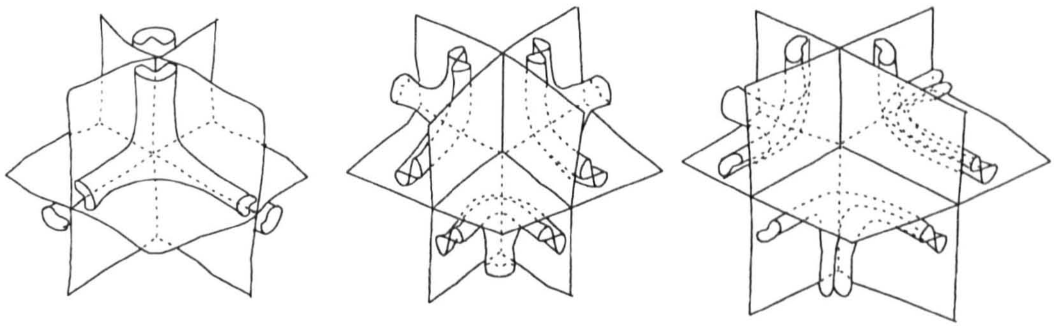

Figure 10.2.5 Three views of the triple point with an added surface.

The framings have been chosen so that we can apply bridging between the new and old surfaces along twelve lines, three in each of the four black-shaded quadrants. After pulling a non-singular surface away from the triplepoint we are left with

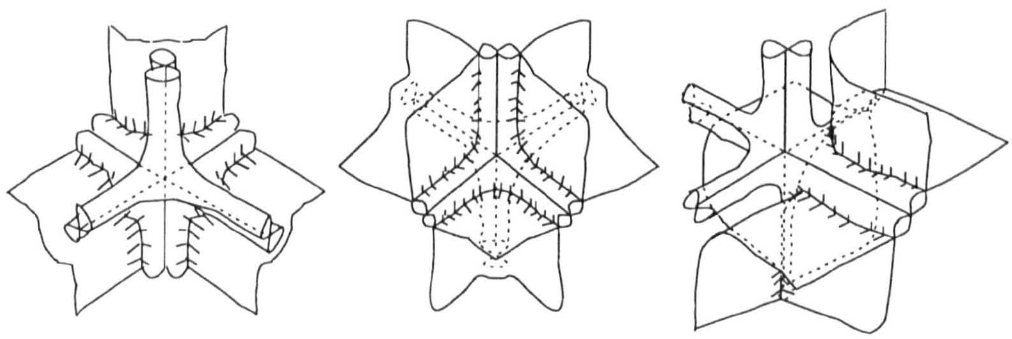

Figure 10.2.6 Three views after one bordism move.

Add another surface in the white-shaded quadrants, this time high genus tori with no self intersection, so nullbordant.

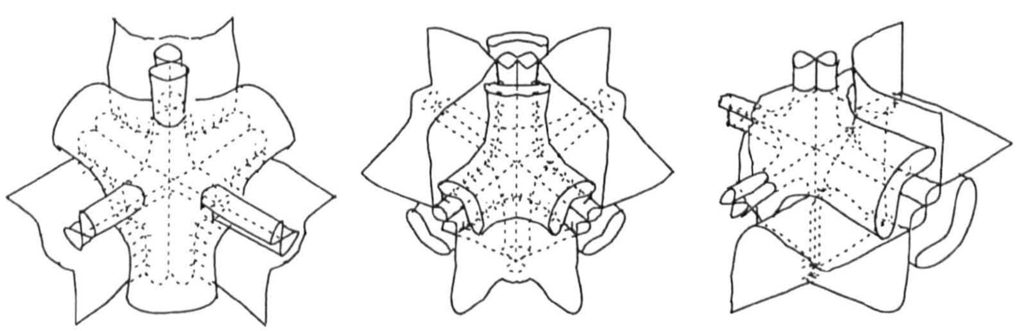

Figure 10.2.7 Three views after adding a second surface.

Apply another bridging move;

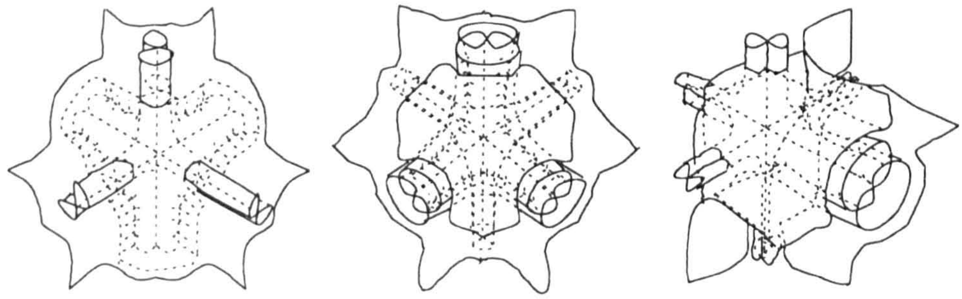

Figure 10.2.8 Three views after a second bordism move.

and remove the nullbordant surfaces (they pass over figure-of-eight tubes)

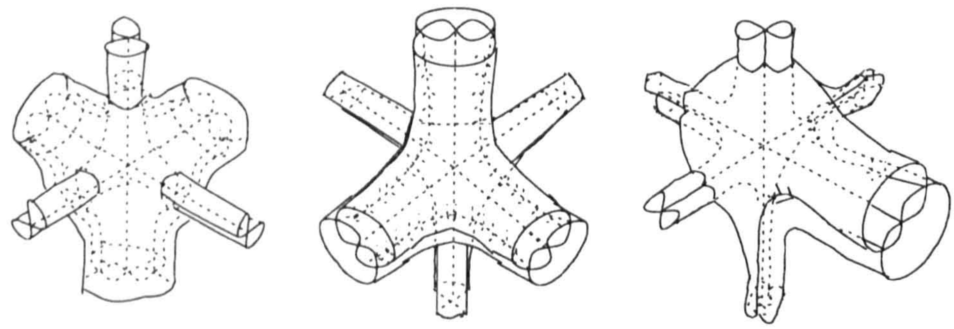

Figure 10.2.9 Three views after removing a null-bordant surface.

Now, remember that at each triple-point the axes have an ordering. Consider the ends of the first and second axes. The ends which are not figures-of-eight can be changed into figures-of-eight, away from the triple points. Then the ordering on the four ends (of the first and second axes) ensures that we can use bordism to join up these tubes.

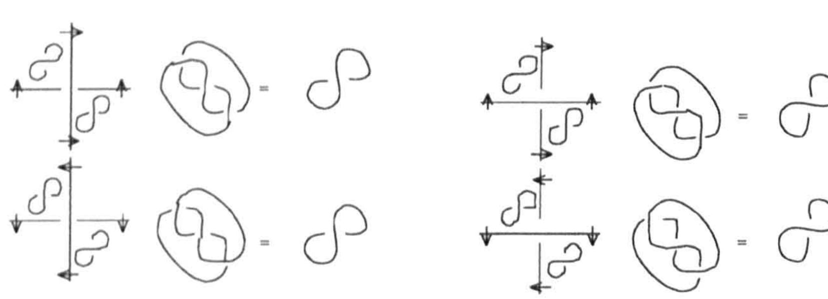

Figure 10.2.10 Each section becomes a figure of eight.

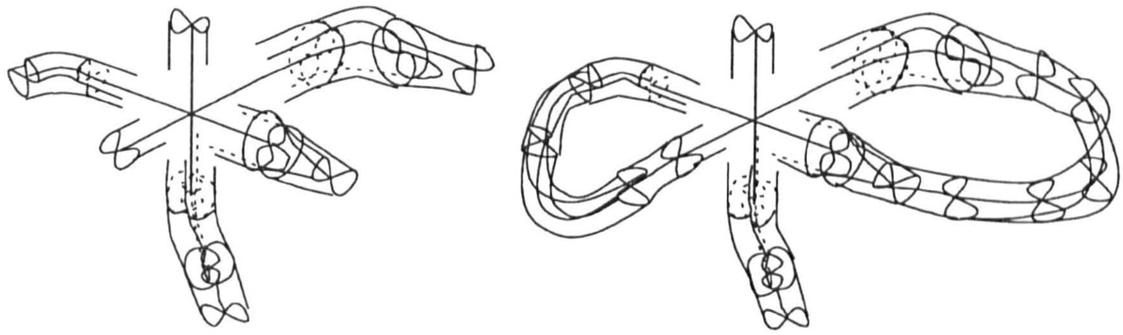

Figure 10.2.11 Bridging off arms from triple points.

Let us look at these last transformations in more detail;

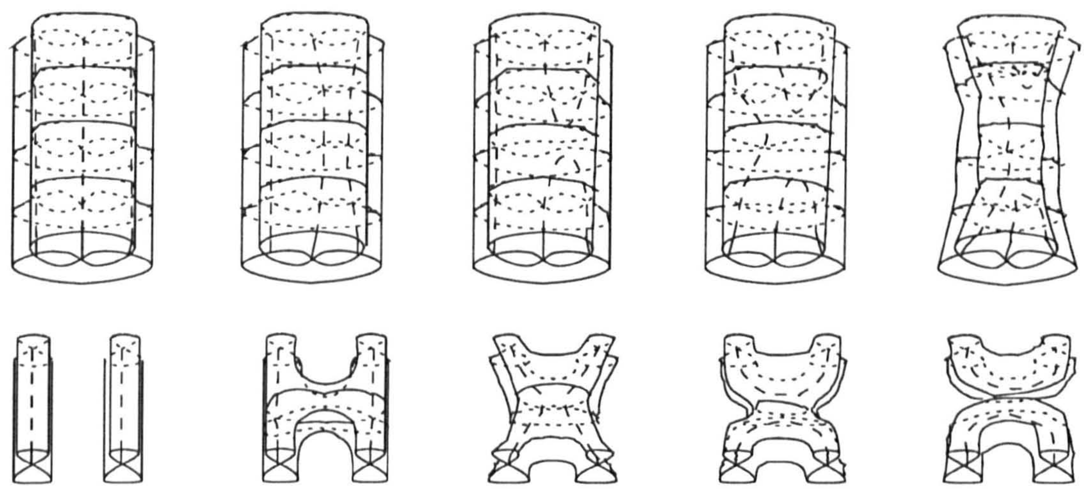

Figure 10.2.12 Bridging between figure of eight tubes.

We can look at what has happened so far again by taking a sequence of sections through the surface near a triplepoint. The triple point gives a sequence

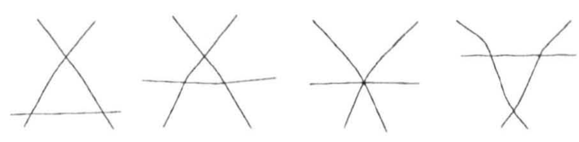

Figure 10.2.13 Sections through a triple point.

After adding the first surface along double-points we get

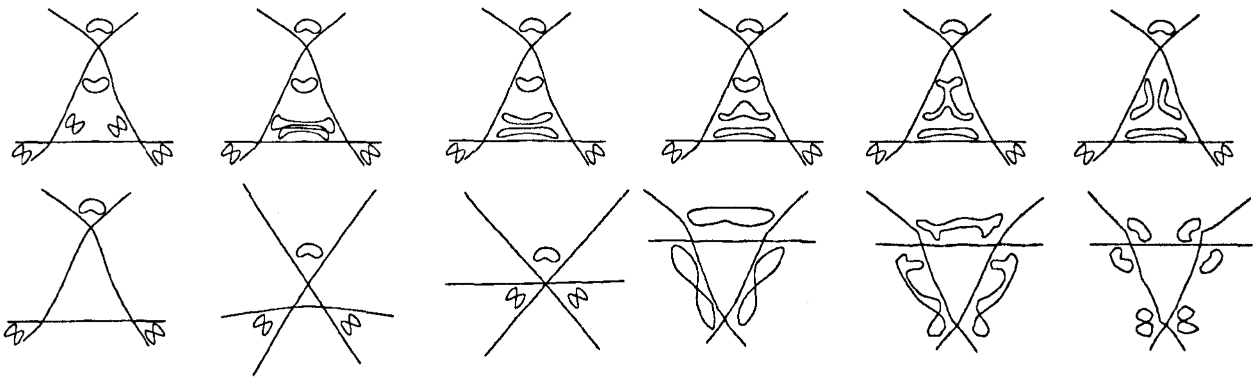

Figure 10.2.14 Sections through a triple point with one surface added.

Now we do a bordism move between the new surface and the old

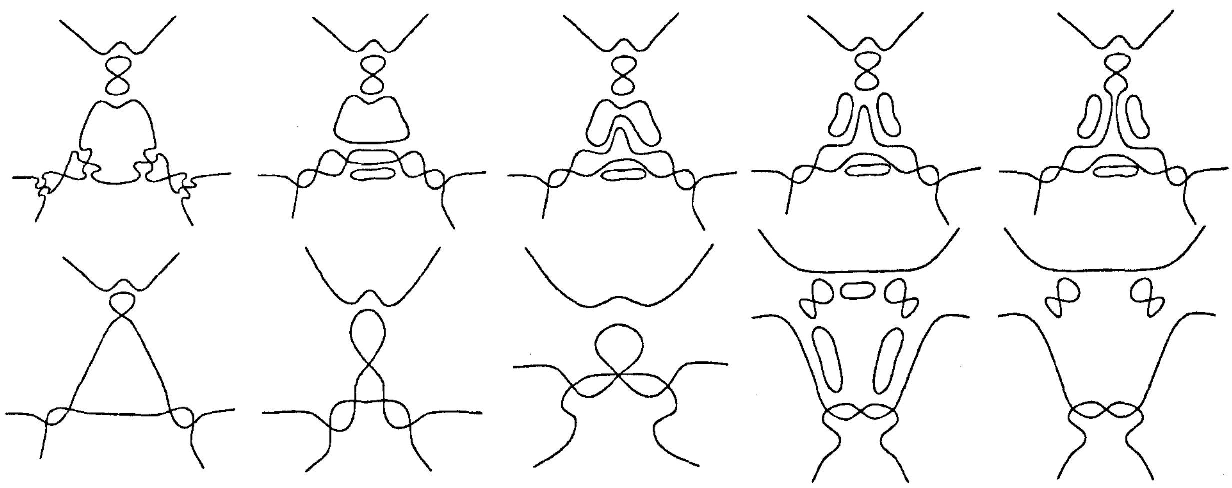

Figure 10.2.15 Sections after one bordism move.

and add another surface, this time a null-bordant surface

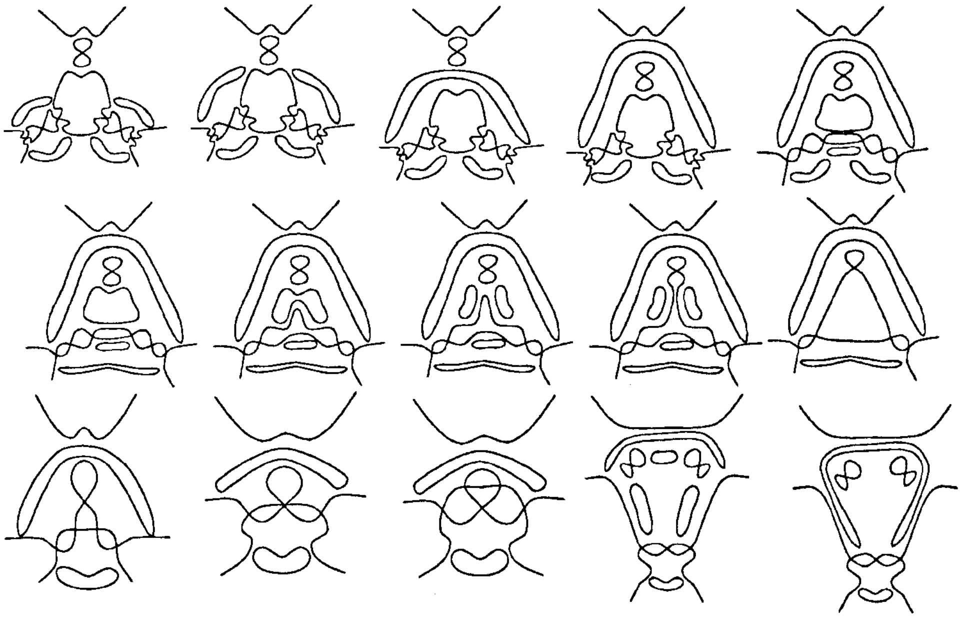

Figure 10.2.16 Sections after adding a second surface.

Another bridging move gives

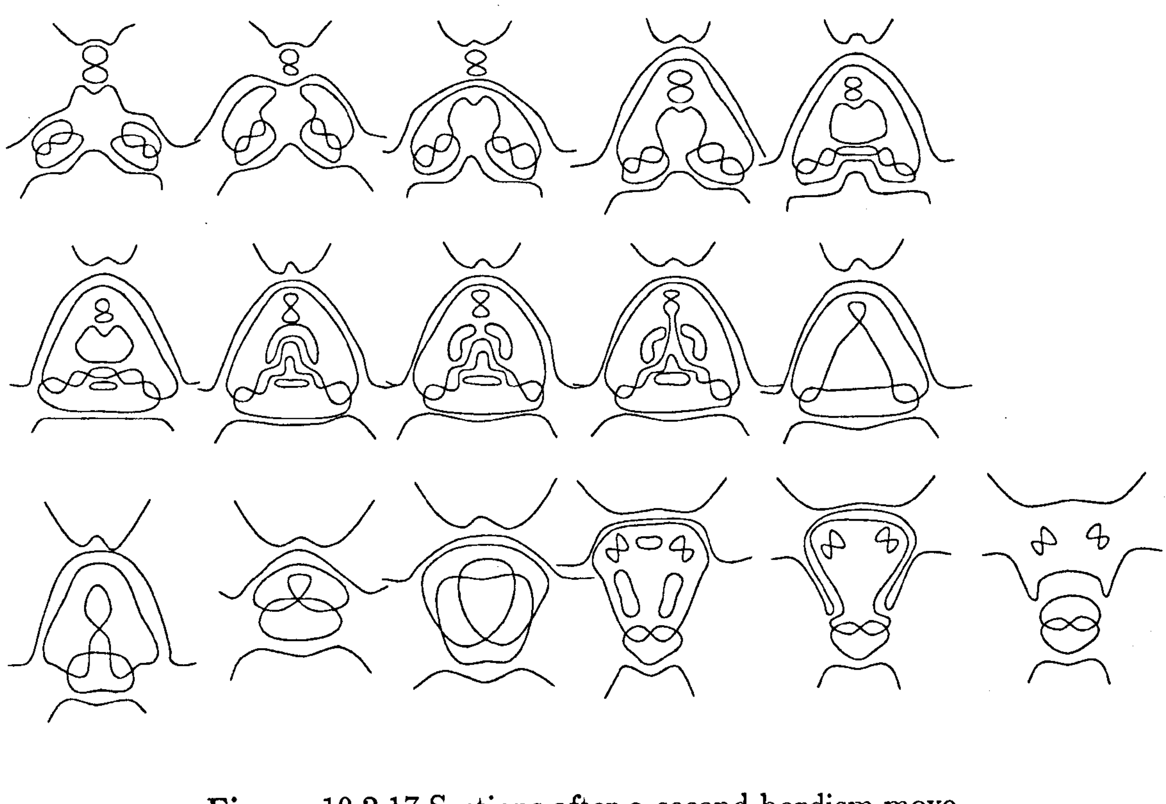

Figure 10.2.17 Sections after a second bordism move.

and finally we remove non-singular (so nullbordant) surfaces in S^3

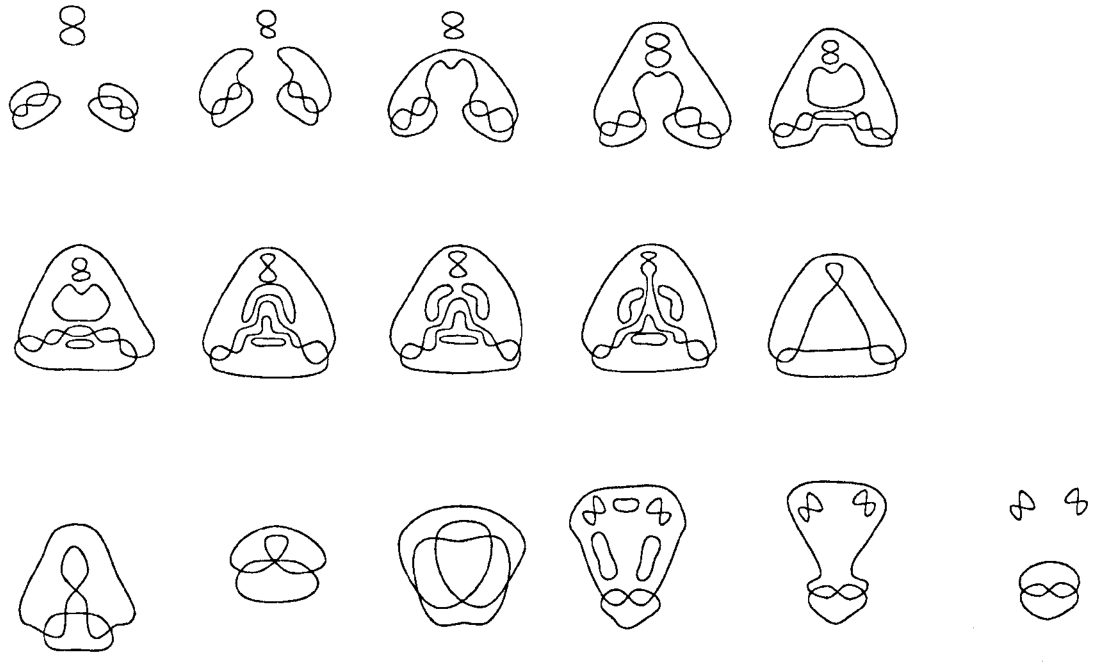

Figure 10.2.18 Sections after removing non-singular surface.

After gluing the ends of the first and second axes, we get another movie

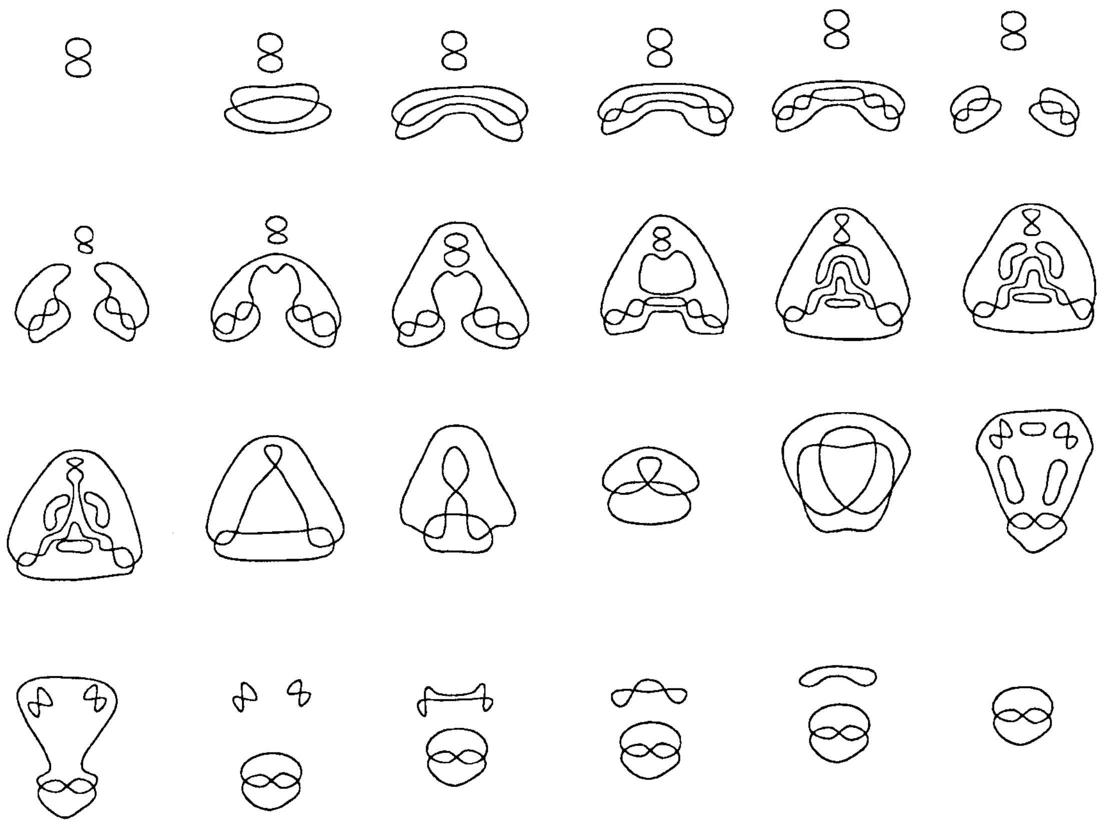

Figure 10.2.19 Sections after bridging between pairs of arms.

On the following pages, first we have a picture of all these sequences of sections running concurrently. The left-hand column is a sequence of sections through a triple point in the surface. The next column of sections includes the first added surface, the next column is the sequence through the surface which remains as a triple point neighbourhood after the first bordism move, and so on. The next page begins with an equivalent movie (equivalent means it's sequence of sections through a bordant surface) to the last one on the first page. The last column of the first page is shown to be equivalent to a simple transition from the figure-of-eight to the non-figure-of-eight.

Each triple point can be split off by inserting this transition and its inverse near the triple point, and applying bridging between the figure-of-eight tubes.

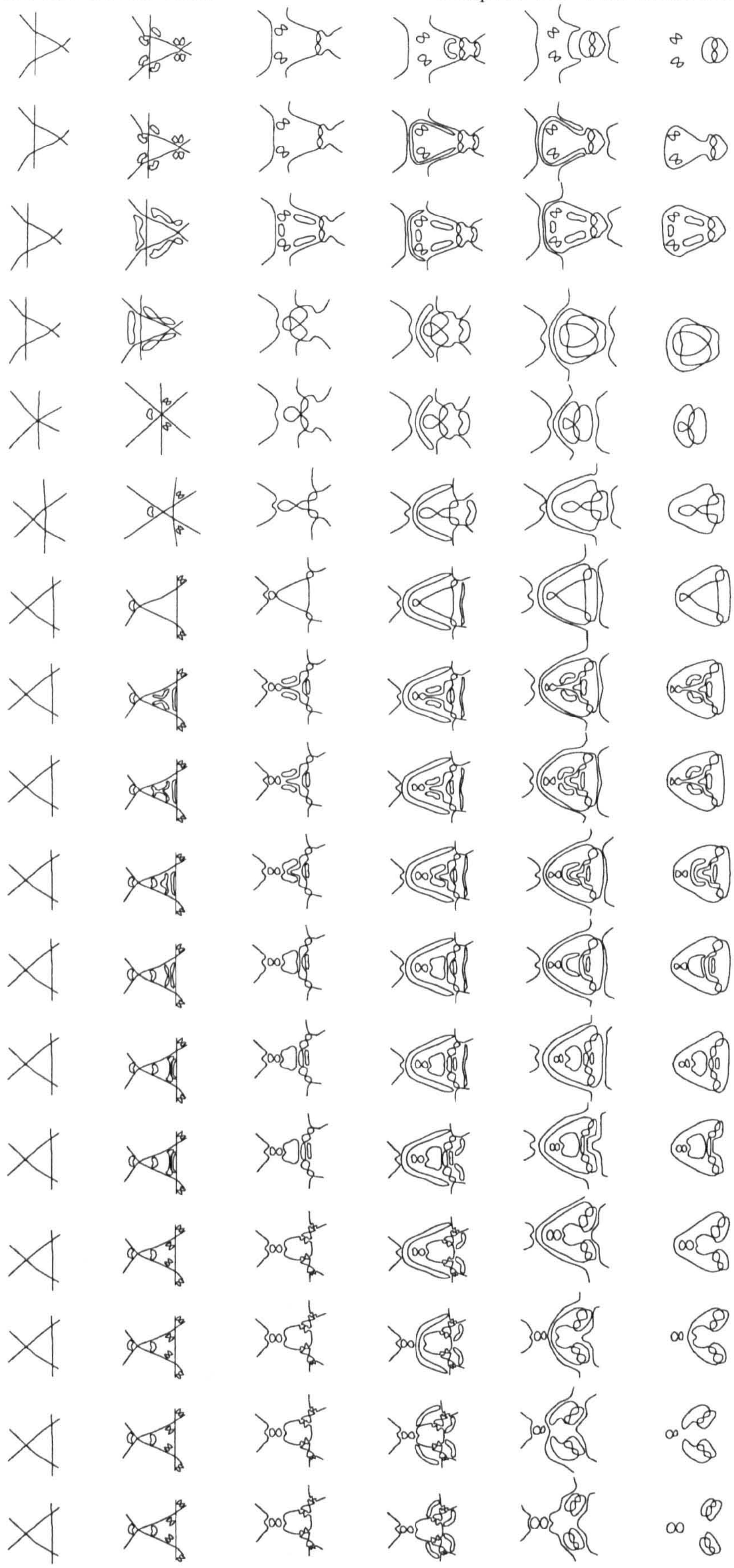

Figure 10.2.20 A summary of the triple point sections.

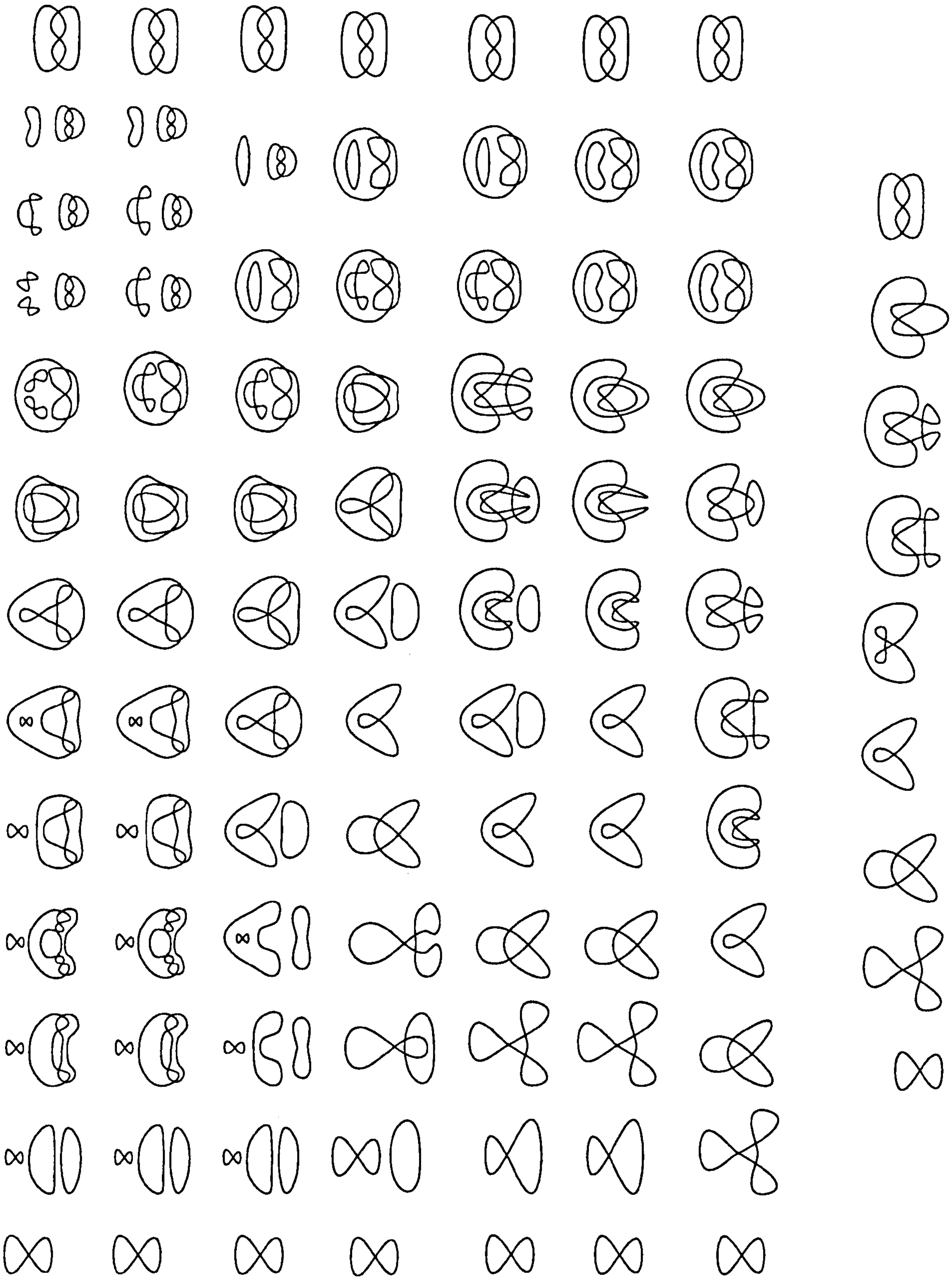

Figure 10.2.21 Equivalence of triple points to a simpler transition.

Every surface has been reduced to double-point neighbourhoods; tubes of figures-of-eight with no further singularities. Using bordism between tubes of figures of eight, we can reduce the surface to a sum of

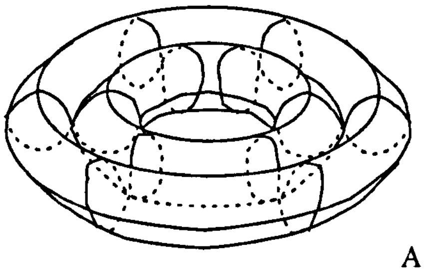

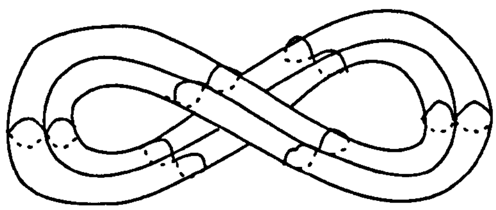

A twisted product of the figure-of-eight and the circle

The product of a figure-of-eight and a circle

Figure 10.2.22 Simplified $\pi_3(\mathbb{B}(*))$ representatives.

The first of these is null-bordant by putting a disc in the middle

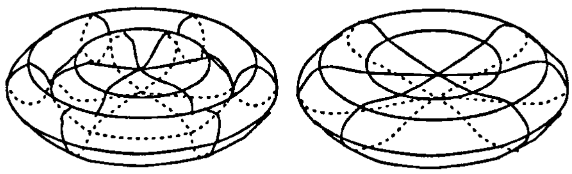

Figure 10.2.23 Null bordism of the product of a circle and a figure of eight.

The second is a generator for $\pi_3(\mathbb{B}(*))$. It is of order 2.

The next figure shows a null-bordism of the sum of two generators. The first pair are both generators. We can reverse the crossing of the second figure-of-eight by passing one surface through another, choose the ordering of new double-point intersections so that one part of the surface (the old over-pass, say) always passes over the other. As the overpass tube first intersects the underpass tube, we introduce an unknot of double points. When this crosses the spine of the figure of eight tube we get two new triple points. Then we pass one spine through the other. Notice that passing a double-point line through another is equivalent to passsing a surface through a triple point which is a homotopy of the three-sphere through a 4-cube in the classifying space.

Rotate the second surface of the second pair through a half-turn around an axis perpendicular to the page to give the third pair.

The surfaces of the third pair have appropriate orientations to enable bordism to occur, giving the remaining moves.

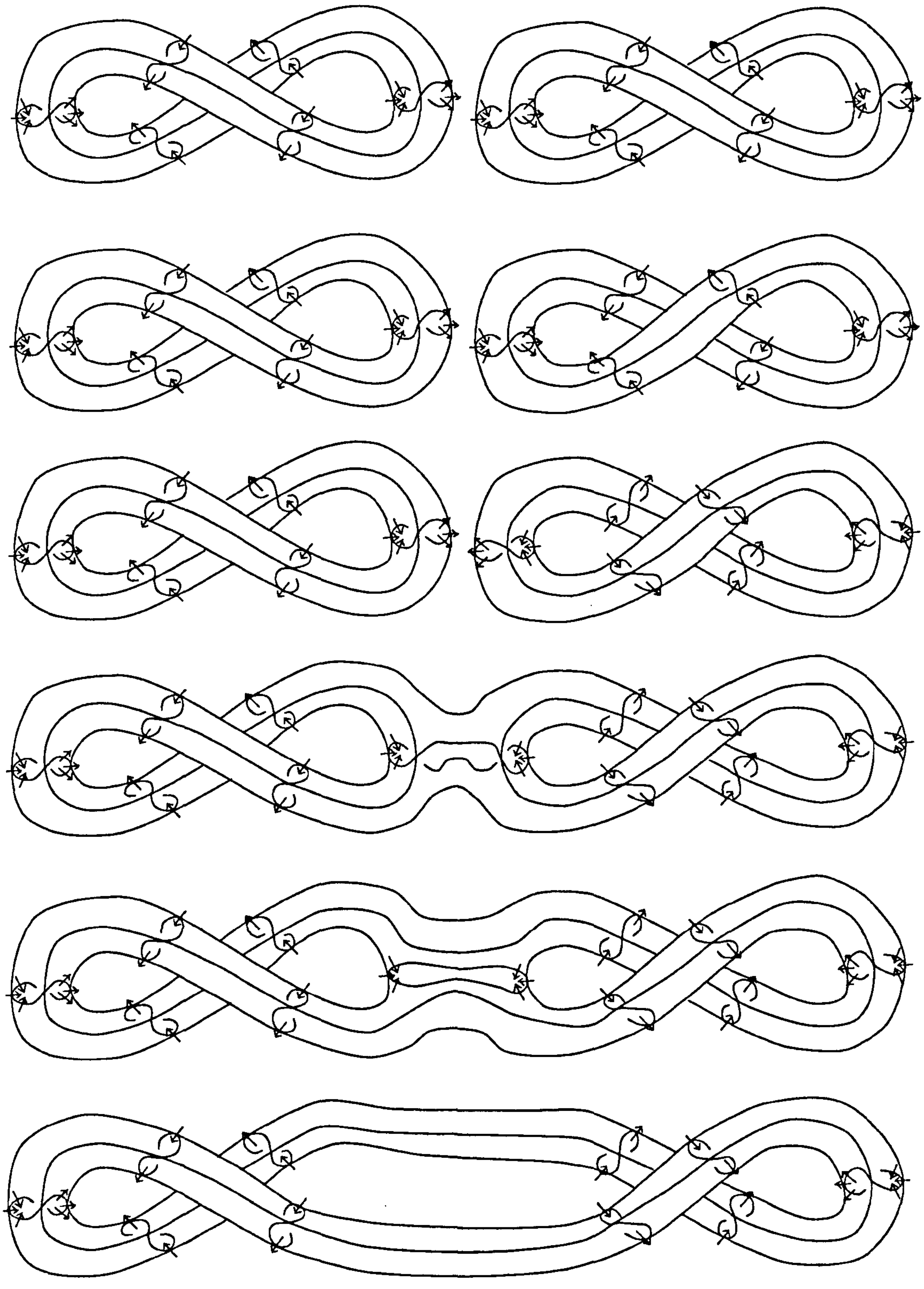

Figure 10.2.24 The generator of $\pi_3(\mathbb{B}(*))$ is of order 2.

To see that this generator is non-zero, take a surface and consider the neighbourhoods of lines of double points. These are framed and oriented, and meet at triple points. Take them apart at triple points, in any one of six ways (see the diagram) and we get a framed link in the three-sphere. The writhe of this link mod 2 is an invariant of the initial surface. The link itself is not, it can depend upon how we took apart the triple points. The writhe has to be reduced mod 2 because we can pass double points through each other in the surface, which corresponds to reversing crossings of the framed link. The generator for the third homotopy group of the trivial rack gives a link with odd writhe. Thus the surface generator is also non-zero.

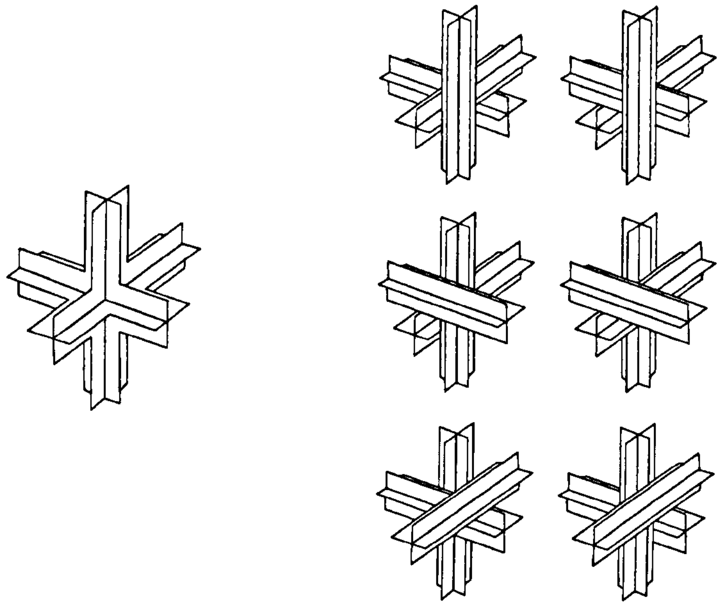

Figure 10.2.25 Pulling apart a triple point in six ways.

Thus

$$\pi_3(\mathbb{B}(*)) \cong \mathbb{Z}_2$$

Work with James bundles [FRS] shows that $\mathbb{B}(*) \cong \Omega S^2$ so

$$\mathbb{Z}_2 \cong \pi_3(\mathbb{B}(*)) \cong \pi_3(\Omega(S^2)) \cong \pi_4(S^2)$$

Here is a sketch-proof

By the Thom-Pontrjagin construction, there is a one-to-one correspondence between elements of $\pi_2(S^4)$ and bordism classes of framed manifolds embedded in S^4. Think of S^4 as the suspension of S^3, and use a bordism on the embedded manifold in S^4 until it becomes a progression of framed links in S^3 with isolated singular points of birth, death and bridging moves. Each framed link in S^3 gives a framed link diagram in S^2 and these diagrams stack up to give a framed immersed surface in S^3, with equivalence by bordism. These surfaces in S^3 are representatives of elements of $\pi_3(\mathbb{B}(*))$ under the same equivalence.

$$\pi_4(S^2) \cong \pi_3(\mathbb{B}(*)) \cong \mathbb{Z}_2$$

10.3 Calculation of $\pi_3(\mathbb{B}C_n)$, the cyclic rack.

We can use the same procedure, with a little care, to show that the third homotopy group of the cyclic rack is also $\mathbb{Z}_2$. Problems arise when we want to attach the tubes to the surface near triple points. Bordism moves are only allowed between surfaces with equal labels. We can, however, change any label on a link arc to any other label by inserting twists. (This was how we calculated the second homotopy group in 7.4). The number of twists to insert is only defined up to a multiple of n (n is the order of the rack). If the racks elements were integers then the number of twists would be absolutely defined as the difference. Choose integer representatives for each label in $\mathbb{Z}/n\mathbb{Z}$. The rack law between these labels only holds when we fall back to $\mathbb{Z}_n$. Consider the ordering of surfaces at intersections to give a 'connectedness' and make each integer choice consistent on a connected component of surface.

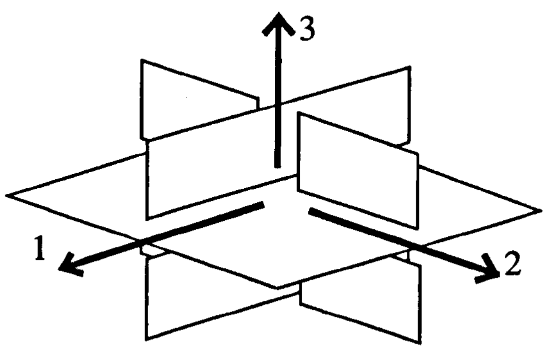

Figure 10.3.1 Connectedness and axis ordering at a triple point.

On each side of all the lines along which we'll do bordism, insert a number of twists, so that bordism always occurs between equally labelled surfaces.

The next figure shows the triple-point bordism with lines drawn where the twists are. The lines of twists never meet, and each line has an integer associated with it, according to the labels either side, and a choice of an element of $n\mathbb{Z}$.

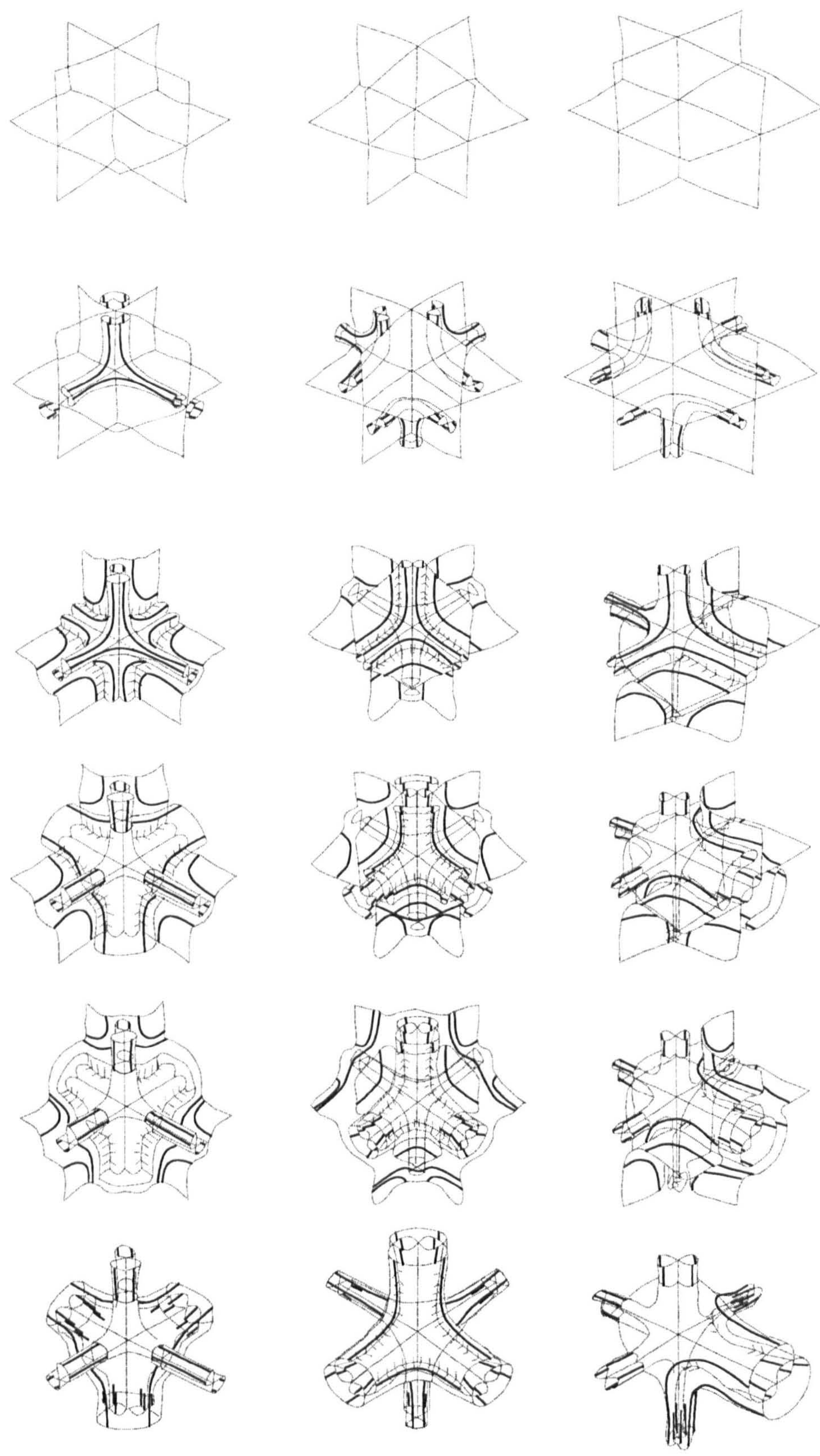

Figure 10.3.2 Addition of twists to find $\pi_3(\mathbb{B}C_n)$.

The calculation carries on in parallel with that of the trivial rack until we have just neighbourhoods of double-point lines joined up at triple points. The arms of each triple point have writhes which may not agree, and this will stop us joining them up and isolating the triple points. The difference in writhe will be a multiple of n, in fact the writhes themselves are all multiples of n.

The writhe contributed by each line of twists is shown here, called $A, B, C, \ldots$.

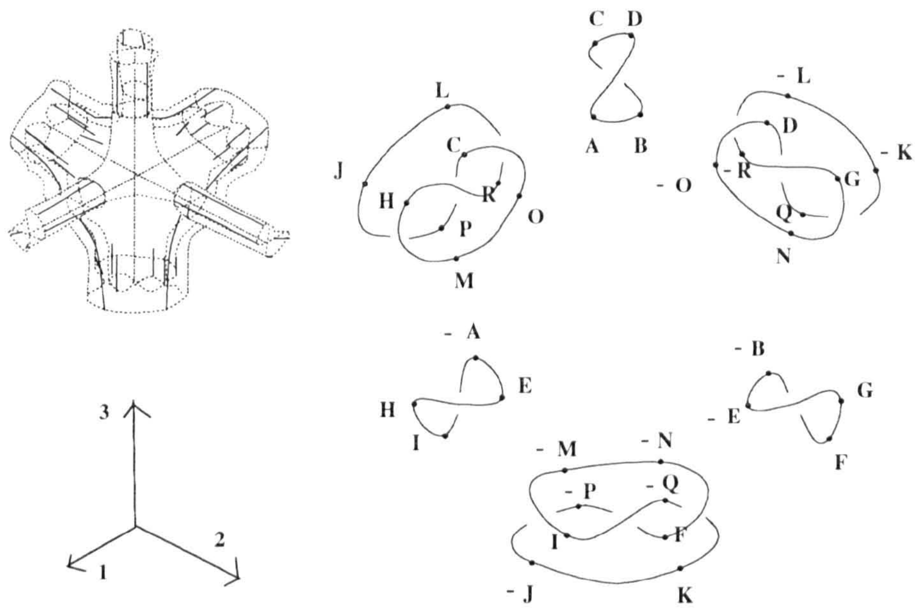

Figure 10.3.3 The writhes on triple-point arms.

We can reduce the number of variables here. First, $J+L$, $L+K$, $K-J$, $M+N$, $N-O$, $O+M$ are all zero. Look at the section, and watch the labels;

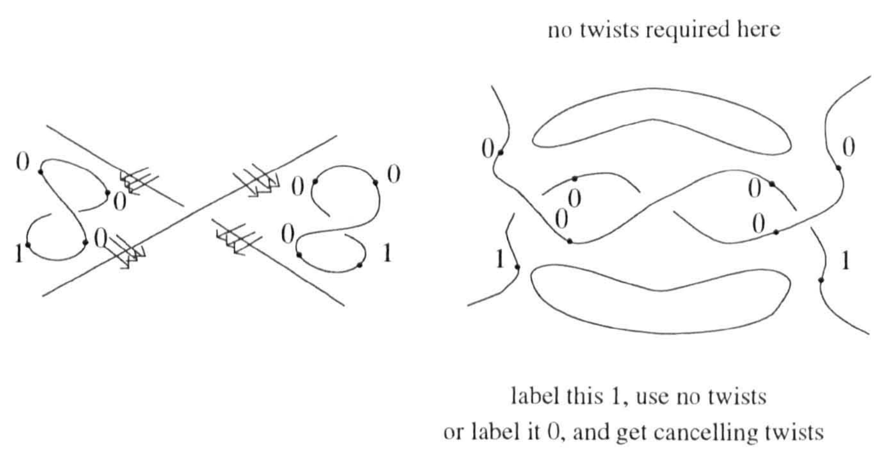

Figure 10.3.4 The number of twists added in detail.

Because of the consistent choice of labelling on the overpassing surface, we see that $H+E=0$, $-E+G=0$, $A+D=0$, $-R+G=0$, $I-Q=0$, and $H+R=0$. Now the twists on the arms from a triple point are as follows;

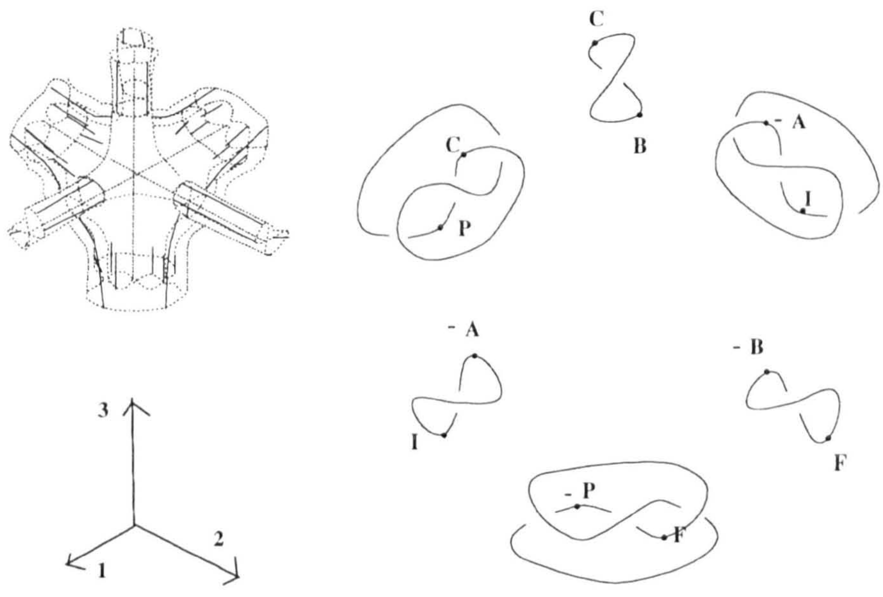

Figure 10.3.5 The writhes on each arm after cancellation.

If we added a multiple of n to C, the labels on the surface, either side of the C twists would stay the same. We're planning to change these variables so that the writhe on each arm totals zero, then we can join the arms together, isolate the triple points as null-bordant surfaces, and end up with sums of generators. But the line of twists may pass near more than one triple point, and we only want to change it locally (the equations to ensure all triple points have zero-writhe arms may be inconsistent). Introduce a null-bordant surface; the product of the circle with the generator of π_2.

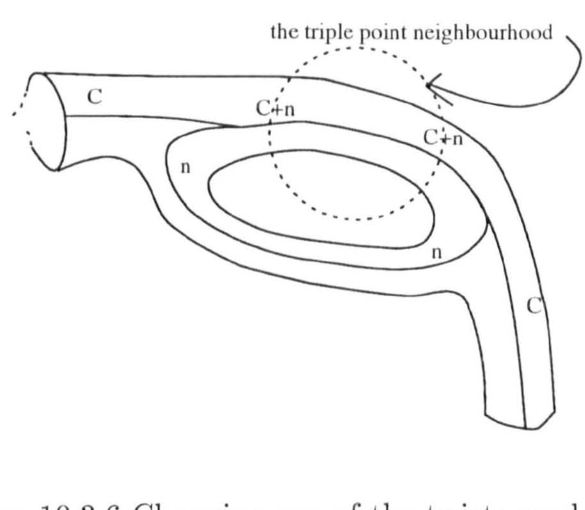

Figure 10.3.6 Changing one of the twists modulo n.

After such adjustments, we can split off the triple points, which look exactly as they did in the calculation for the trivial rack, (so their neighbourhoods are null-bordant) leaving a web of n-twisted tubes.

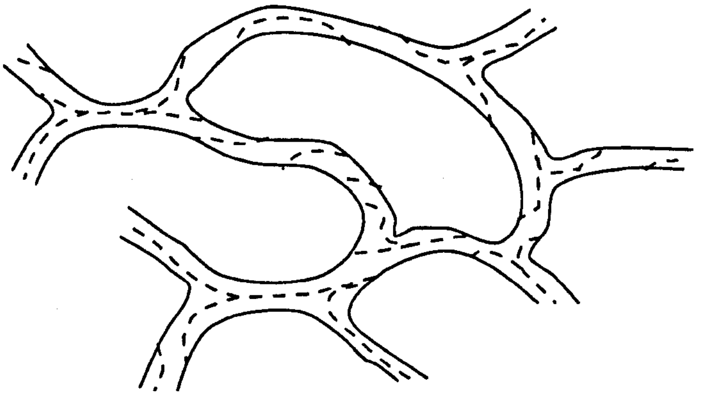

Figure 10.3.7 The simplified $\pi_3(\mathbb{B}C_n)$ representative.

Pull these tubes apart at the Y-shaped junctions (reducing the integral of the writhe squared) until we are left with just sums of a twisted product of the circle with the second homotopy generator. This generates the image of the Hopf map

$$\pi_2(\mathbb{B}C_n) \longrightarrow \pi_3(\mathbb{B}C_n)$$

and it generates $\pi_3(\mathbb{B}C_n) \cong \mathbb{Z}_2$.

References.

[B] **G. E. Bredon,** *Introduction to compact transformation groups,* Academic Press Pure and Applied Math. vol. 46 (1972).

[BD] **S. Buoncristiano, M. Dedo,** *On representing homology classes,* Ricerche Mat. 28, 417–424 (1979).

[BJS] **B. J. Sanderson,** *Topics in topology,* Warwick lectures (1994).

[BRS] **S. Buoncristiano, C. P. Rourke and B. J. Sanderson,** *A geometric approach to homology theory,* London Math. Soc. lecture note series 18 C.U.P. (1976)

[BtD] **T. Brocker, tom Dieck,** *Kobordismentheorie,* Springer Verlag (1985).

[C1] **A. Connes,** *Non-commutative differential geometry,* Publ. Math. I.H.E.S. 62, 257–360 (1985).

[C2] **A. Connes,** *Cohomologie cyclique et foncteurs* Ext^n, C.R. Acad. Sci. Paris 296, 935–958 (1983).

[CW] **C. T. C. Wall,** *Determination of the cobordism ring,* Ann. Math. 72, 293–311 (1960).

[DJ] **D. Joyce,** *A classifying invariant of knots; the knot quandle,* J. of Pure and Applied Algebra 23, 37–65 (1982).

[DR] **D. Rolfson,** *Knots and links,* Publish or perish, math. lecture series 7 (1976).

[EB] **E. Brieskorn,** *Automorphic sets and braids and singularities,* Contemp. Math. 78, 45–115 (1988).

[FR] **R. Fenn and C. P. Rourke,** *Racks and links in codimension two,* J. of Knot Theory and its Ramifications, volume one, No 4, 343–406, World Scientific (1992).

[FRS] **R. Fenn, C. P. Rourke and B. J. Sanderson,** *James bundles, species and the rack space,* preprint, University of Warwick (1992).

[G] **M. J. Greenberg,** *Lectures on algebraic topology,* Benjamin (1967).

[HF] **H. Freundenthal,** *Über die Klassen der Sphärenabbildungen,* Compositio Math. 5, 299–314 (1937).

[HH] **J. Hass, J. Hughes,** *Immersions of surfaces in 3-manifolds,* Topology 24, 97–112 (1985).

[HR] **H. Ryder,** *The structure of racks,* thesis, University of Warwick (1993)

[JDSJ1] **J. D. S. Jones,** *Cyclic homology and equivariant homology,* Invent. math. 87, 403–423 (1987).

[JDSJ2] **J. D. S. Jones,** *The fixed point theorem in equivariant cohomology,* Trans A.M.S. 322, 35–49 (1990)

[K] **L. Kauffman,** *Knots and physics,* World Scientific (1991).

[L] **J-L. Loday** *Cyclic homology,* Springer Verlag 301 (1991).

[LQ] **J-L. Loday and D. Quillen,** *Cyclic homology and the Lie algebra homology of matrices* Comment Math. Helv. 60, 596–591 (1985), summary in C.R Acad. Sci. Paris, Serié I vol. 296, 295–297 (1983).

[M] **J. Milnor,** *Construction of universal bundles, I* Ann. of Math. 63, 272–283 (1956).

[N] **L.Neuwirth,** *Knot groups,* Princeton University Press (1965).

[S1] **G. Segal,** *Classifying spaces and spectral sequences,* I.H.E.S. 34, 105–112 (1968).

[S2] **G. Segal,** *Categories and cohomology theories,* Topology 13, 293–312 (1974).

[SM] **S. Matveev,** *Distributive groupoids in knot theory,* Math. USSR Sbornik. 119, 28–88 (1982).

[SW] **S. Winker,** *Quandles, knot invariants and the n-fold branched cover,* thesis, University of Chicago (1984).

[T] **Thom,** *Quelques propriétés globales des variétés différentiables,* Comment. Math. Helv. 28, 17–86 (1954).

[WGS] **Warwick graduate school,** *Guide to examinations for higher degrees by research,* Sept. 1993.